

2021-07

A Comprehensive Review of Dehumidifiers and Regenerators for Liquid Desiccant Air Conditioning System

A, Gurubalan

Elsevier

A. Gurubalan, Carey J. Simonson, (2021). A comprehensive review of dehumidifiers and regenerators for liquid desiccant air conditioning system, *Energy Conversion and Management*, 240, 114234. <https://doi.org/10.1016/j.enconman.2021.114234>.

<https://hdl.handle.net/10388/14941>

<https://doi.org/10.1016/j.enconman.2021.114234>.

This is an Accepted Manuscript of an article published by Elsevier in *Energy Conversion and Management* on July 15, 2021, available at: <https://doi.org/10.1016/j.enconman.2021.114234>

Downloaded from HARVEST, University of Saskatchewan's Repository for Research

A Comprehensive Review of Dehumidifiers and Regenerators for Liquid Desiccant Air Conditioning System

A. Gurubalan*, Carey J Simonson

Department of Mechanical Engineering

University of Saskatchewan, Saskatchewan, Canada - S7N0W5

*Corresponding author Email: gurumariner60@gmail.com

Abstract

Liquid desiccant air conditioning systems (LDAS) are an energy-efficient and eco-friendly alternative to conventional air conditioning systems. The performance of a LDAS significantly depends on its simultaneous heat and mass transfer components, namely dehumidifier and regenerator. These components are referred to as liquid desiccant energy exchangers (LDEEs) since the working fluids (air and desiccant) exchange both heat and moisture. There has been a lot of research on LDEEs over the last two decades to improve their performance, thereby enhancing the efficiency of the LDAS. The main objective of this comprehensive review paper is to summarize the developments of LDEEs. The desiccant material, and design, operating, and performance parameters of LDEEs are explained in detail. Even though a lot of research has been done on LDEEs, they are not much utilized in the practical heating, ventilation, and air conditioning (HVAC) systems. To address this issue, future research should prioritize its focus on (i) practical problems of LDEEs such as cross contamination, and leakage and blockage of the membrane, (ii) long term performance study in the practical systems, (iii) noncorrosive and inexpensive solution, (iv) compatible material for efficient heat and mass transfer, and (v) generalized design and performance control methodology. The discussions presented in this communication will be useful to ascertain the crucial research gaps that need to be addressed by future research studies.

Keywords: Liquid desiccant system, Dehumidifier, Regenerator, Humidity control, Hybrid air conditioning system

Nomenclature

A	Area (m^2)
C	Heat capacity rate (kW/K)
C_p	Specific heat capacity (kJ/kg.K)
Cr	Capacitance ratio
h	Enthalpy (kJ/kg)

h_c	Convective heat transfer coefficient (kW/m ² .K)
h_{fg}	Latent enthalpy of condensation (kJ/kg)
h_m	Convective mass transfer coefficient (kg/m ² .s)
m	Mass flow rate (kg/s)
m^*	Mass flow rate ratio
p	Pressure (Pa)
Q	Heat transfer (kW)
R_h	Overall heat transfer resistance (m ² .s/ kg)
R_m	Overall mass transfer resistance (m ² .K/ kW)
T	Temperature (°C)
U_h	Overall heat transfer coefficient (kW/m ² .K)
U_m	Overall mass transfer coefficient (kg/m ² .s)
W	Specific humidity (kg _w /kg _{da})
X	Concentration

Greek symbols

ε	Effectiveness
η	Efficiency

Subscripts

a	Air
act	Actual
c	Contact material
cw	Cooling water
e	Effective
h	Enthalpy
in	Inlet
min	Minimum
out	Outlet
r	Regeneration
s	Solution
S	Sensible
t	Total
v	Water vapor

W Latent

Abbreviations

AC	Air conditioning
ACF	All counterflow
A-LAMEE	Adiabatic liquid to air membrane energy exchanger
A-LDEE	Adiabatic liquid desiccant energy exchanger
APF	All parallel flow
BA-LDEE	Bubble absorption liquid desiccant energy exchanger
CaCl ₂	Calcium chloride
CACS	Conventional air conditioning systems
CC	Cooling capacity
CFC	Chlorofluorocarbon
CFD	Computational fluid dynamics
CO ₂	Carbon di oxide
COP	Coefficient of performance
CWA	Cooling water and air in counterflow
CWD	Cooling water and desiccant in counterflow
DP	Dehumidification perfectness
DTRC	Desiccant temperature change rate
E-LDEE	Electrodialysis based liquid desiccant energy exchanger
FF-LDEE	Falling film liquid desiccant energy exchanger
HCFC	Hydrochlorofluorocarbon
HFC	Hydrofluorocarbon
HG-LDEE	Hyper gravity liquid desiccant energy exchanger
IAQ	Indoor air quality
I-LAMEE	Internally cooled or heated liquid to air membrane energy exchanger
I-LDEE	Internally cooled or heated liquid desiccant energy exchanger
LAMEE	Liquid to air membrane energy exchanger
LDAS	Liquid desiccant air conditioning systems
LDEE	Liquid desiccant energy exchanger
LDS	Liquid desiccant system
LiBr	Lithium bromide

LiCl	Lithium chloride
MD	Membrane distillation
MD-LDEE	Membrane distillation based liquid desiccant energy exchanger
MFR	Moisture flux rate
MI-LDEE	Modified internally cooled or heated liquid desiccant energy exchanger
MRR	Moisture removal rate
NTU _h	Number of heat transfer units
NTU _m	Number of mass transfer units
ORO	Osmotically assisted Reverse osmosis
PB-LDEE	Packed bed liquid desiccant energy exchanger
Re	Reynolds number
RO	Reverse osmosis
RO-LDEE	Reverse osmosis based liquid desiccant energy exchanger
SHR	Sensible heat ratio
SC-LDEE	Solar collector based liquid desiccant energy exchanger
TEG	Triethylene glycol
U-LDEE	Ultrasound based liquid desiccant energy exchanger
V-LDEE	Vacuum liquid desiccant energy exchanger

1. Introduction

Energy systems, both present and future, have the dual challenge [1] of having to meet the constantly increasing energy demands with minimum CO₂ emissions. Several noteworthy steps are being taken to reduce CO₂ emissions from the energy systems of all sectors [1]. In the building sector, the reduction measures taken are the judicious combination of retrofitting existing buildings and strict regulations for new buildings and electric appliances. It is anticipated that the carbon reduction measures (i.e., low carbon scenario) will reduce the annual energy demand growth from 1.1% to 0.7% in the time frame of 2017 to 2040, as shown in Fig.1 [2]. It is also observed from the figure that the energy demand growth of the building sector is higher than that of the industrial sector [2]. It is expected that air conditioning (AC) systems will consume a maximum proportion of the overall electricity used in buildings and will account for 30% of the total global electricity demand in 2050 [2]. The increase in living standards, rapid urbanization, and greater affordability has led to a surge in the use of AC

systems in the building sector. Climate changes have also played a significant role in expanding the use of AC systems [2].

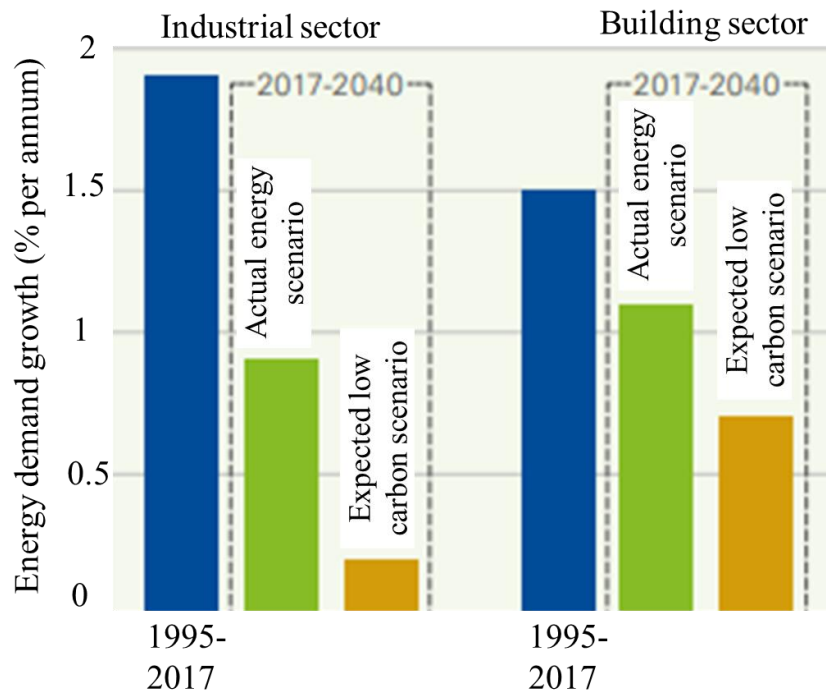


Fig.1: Annual energy demand growth of industrial and building sectors [1]

According to the International Energy Outlook, the global cooling energy demand may increase from 850 to 3350 GW, which can double the CO₂ emissions in the time frame of 2016 to 2050 [2]. Therefore, it is essential to use an energy-efficient and eco-friendly AC system to meet the increased energy demand with reduced emissions. However, most conventional AC systems (CACS) belong to the vapour compression type, which is energy inefficient [3]. This is due to its method of humidity control. In CACS, the air is cooled down to its dew point temperature to condense the water vapor in it. Consequently, the air is reheated to its supply temperature before it enters the air conditioning room. Hence, the air is overcooled for the humidity control and subsequently reheated for the temperature control. This makes CACS energy inefficient. Moreover, the water condensed from the air during its humidity control facilitates the growth of microorganisms and thereby affects the indoor air quality of the air conditioning room [4]. Besides, the water condensate can re-evaporate into the supply air, which leads to an undesirable humidity in the air conditioning room [5]. Moreover, the conventional chlorofluorocarbon and hydrochlorofluorocarbon refrigerants of CACS must be eliminated due to high global warming and ozone depleting potentials. However, CACS have limitations in the elimination of such refrigerants. This is because, the flammable nature of the alternative

low global warming potential refrigerants, and the newly introduced ones are more expensive. On the other hand, due to the transcritical cycle properties, complete redesign of the current system is required to utilize the natural refrigerant [6].

Desiccant dehumidification is one of the promising alternatives to CACS for humidity control. It is the process of removing the water vapour from the air using a desiccant material, which is hygroscopic [7]. Based on the material type, desiccants can be broadly classified as liquid and solid types. Liquid desiccants are preferred over the solid desiccants due to their advantages, listed as follows [7-9].

- i. Lesser pressure drop on the airside
- ii. Lesser regeneration temperature
- iii. Higher energy storage
- iv. Higher moisture holding capacity
- v. More flexibility in utilizing the heat source for regeneration
- vi. Can be regenerated during the availability of heat source and stored for further use
- vii. Ability to filter microbial contamination (bacteria, viruses and moulds)
- viii. Appropriate for combined cooling and dehumidification process
- ix. Small and compact system

A liquid desiccant system (LDS) utilizes low-grade energy sources such as waste gas or solar energy for its desiccant regeneration. Therefore, it is more environmentally friendly when compared to CACS. LDS mostly combines with a sensible cooling system (for the temperature control of air) to achieve complete air conditioning [10]. Such a combination of LDS and sensible cooling systems is referred to as a hybrid liquid desiccant air conditioning system (LDAS). The most used sensible cooling systems are vapour compression, vapour absorption, and evaporative cooling systems. The vapour compression assisted LDAS is most promising since it is suitable for almost all climatic conditions and also easy to control [7,11]. Here, the vapor compression systems are only utilized to control the temperature of desiccant which in turn controls the temperature and humidity of air. Hence, the supply air is not cooled down to its dewpoint temperature and thus, there is no need of air reheating. Hence, LDAS with vapor compression system is energy efficient when compared to vapor compression based CACS. The comparison between CACS and LDAS is presented in Table-1 [7, 8, 12].

Figure 2 shows the schematic of the LDAS. The basic principle of the LDAS is to transfer the required amount of heat and moisture from supply air to the exhaust air using the liquid

desiccant. The LDAS system has two circuits, namely air and desiccant circuits. The sequential operations in the air circuit are explained as follows [13].

Table-1: Comparison between CACS and LDAS [7, 8, 12]

Parameter	CACS	LDAS
Indoor air quality	Average	High
Energy source	Electricity or natural gas	Waste heat, solar or any other low-grade heat
Humidity control	Average	Accurate
Operational cost	High	Saves 40 – 50 %
Energy storage capacity	Low	High
Working fluid	HFC, CFC, HCFC	LiCl, LiBr, CaCl ₂ , TEG
Effect on environment	Harmful	Comparatively ecofriendly
System installation	Average	Slightly complicated

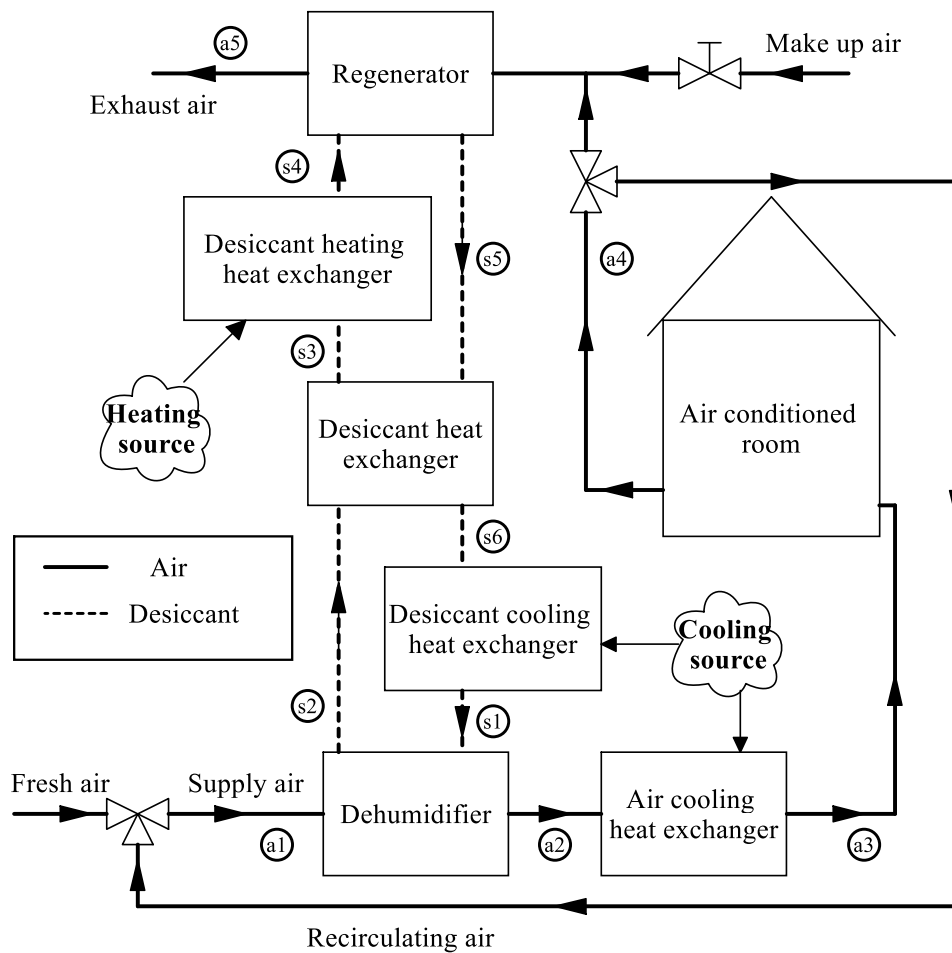


Fig.2: Schematic of LDAS [7]

- (i) The high humid and temperature supply air (state a1) is cooled (depending upon the temperature of liquid desiccant) and dehumidified simultaneously (state a2) in the dehumidifier.
- (ii) The temperature of supply air is further adjusted (state a3) to the required supply condition in air cooling heat exchanger and supplied to the air conditioning room.
- (iii) The temperature and specific humidity of the supply air increase (state a4) while removing the sensible and latent loads of the air conditioning room.
- (iv) The exhaust air enters into the regenerator where it gets heated and humidified (state a5) before it is released into the ambient.

On the other hand, the corresponding cycle of desiccant takes the following path.

- (i) The cooled and concentrated desiccant (state s1) enters the dehumidifier to remove the excess heat and moisture from the supply air and gets warmed and diluted while it leaves (state s2).
- (ii) The diluted desiccant is heated up (state s3) in desiccant heat exchanger by absorbing the heat from the hot concentrated desiccant from the regenerator.
- (iii) The temperature of diluted desiccant is further raised (state s4) to the required level in desiccant heating heat exchanger.
- (iv) The diluted desiccant enters the regenerator, where it becomes concentrated (state s5) by releasing its water vapor into the exhaust air.
- (v) The hot concentrated desiccant from the regenerator is cooled (state s6) in desiccant heat exchanger by the dilute desiccant (state s2) from the dehumidifier.
- (vi) The concentrated desiccant is further cooled down to the required level (state s1) in desiccant cooling heat exchanger and enters the dehumidifier to repeat the cycle.

The process of air and desiccant in the LDAS is summarized in Table-2 [13]. Figure 3 shows the typical operating conditions of air and desiccant in the LDAS for the hot and humid climatic conditions prevailing in the city of Chennai, India [13]. Numerous experimental and numerical studies of LDAS are reported in literature. To gain a better understanding of the performance of LDAS, few experimental studies are discussed as follows. Alizadeh [14] tested the solar powered LDAS for a building of 120 m² in the tropical climate of Queensland, Australia. Aqueous solution of lithium chloride (LiCl) was used as a desiccant. The results showed that the electrical coefficient of performance (COP) of LDAS was 6 and significantly higher than CACS. Yamaguchi et al. [15] analyzed the performance of vapor compression based LDAS where the dehumidifier and regenerator are combined with the evaporator and condenser,

respectively. LiCl and R407C were used as desiccant and refrigerant, respectively. It was found that the system could dehumidify 5.9 g_w/kg_{da} for the summer climatic conditions of Tokyo, Japan. Moreover, the thermal COP of the system was reported as 2.7. In addition, the performance study revealed that COP of the system could be enhanced by improving the isentropic efficiency of compressor and temperature efficiency of the desiccant heat exchanger.

Table-2: Process of air and desiccant in LDAS [13]

Stream	State points	Process	Place	Temperature	Specific humidity	Concentration
Air	a ₁ -a ₂	Cooling and dehumidification	Dehumidifier	Decreases	Decreases	-
	a ₂ -a ₃	Sensible cooling	Air cooling heat exchanger	Decreases	-	-
	a ₃ -a ₄	Heating and humidification	Air conditioning room	Increases	Increases	-
	a ₄ -a ₅	Heating and humidification	Regenerator	Increases	Increases	-
Desiccant	s ₁ -s ₂	Heating and diluting	Dehumidifier	Increases	-	Decreases
	s ₂ -s ₃	Sensible heating	Desiccant heat exchanger	Increases	-	-
	s ₃ -s ₄	Sensible heating	Desiccant heating heat exchanger	Increases	-	-
	s ₄ -s ₅	Cooling and concentrating	Regenerator	Decreases	-	Increases
	s ₅ -s ₆	Sensible cooling	Desiccant cooling heat exchanger	Decreases	-	-

Zhao et al. [16] compared the performance of LDAS with CACS for the climatic conditions of Shenzhen, China. The results of the study showed that the energy consumption of LDAS was 32.2 kWh/(m²yr) whereas CACS consumed around 49 kWh/(m²yr). Similar comparison study by Bassuoni [17] reported that COP of LDAS was 54% higher than that of CACS and the maximum overall energy saving was 46%. Longo and Gasparella [18] conducted a similar comparison study for three years in a flower greenhouse. Aqueous solution of LiCl, potassium formate and lithium bromide were used as desiccant in 2010, 2011 and 2012, respectively. The energy savings of greenhouse with LDAS was 9.6%, 11.7% and 15.1% in 2010, 2011 and 2012, respectively. In addition to the performance, Guan et al. [19] compared the effects of LDAS

and CACS on the indoor air quality of the air conditioning room. The COP of LDAS and CACS was in the range of 3.5-4.5 and 1.8-2.3, respectively. Moreover, LDAS performed better with respect to the filtration efficiency of particulate matter.

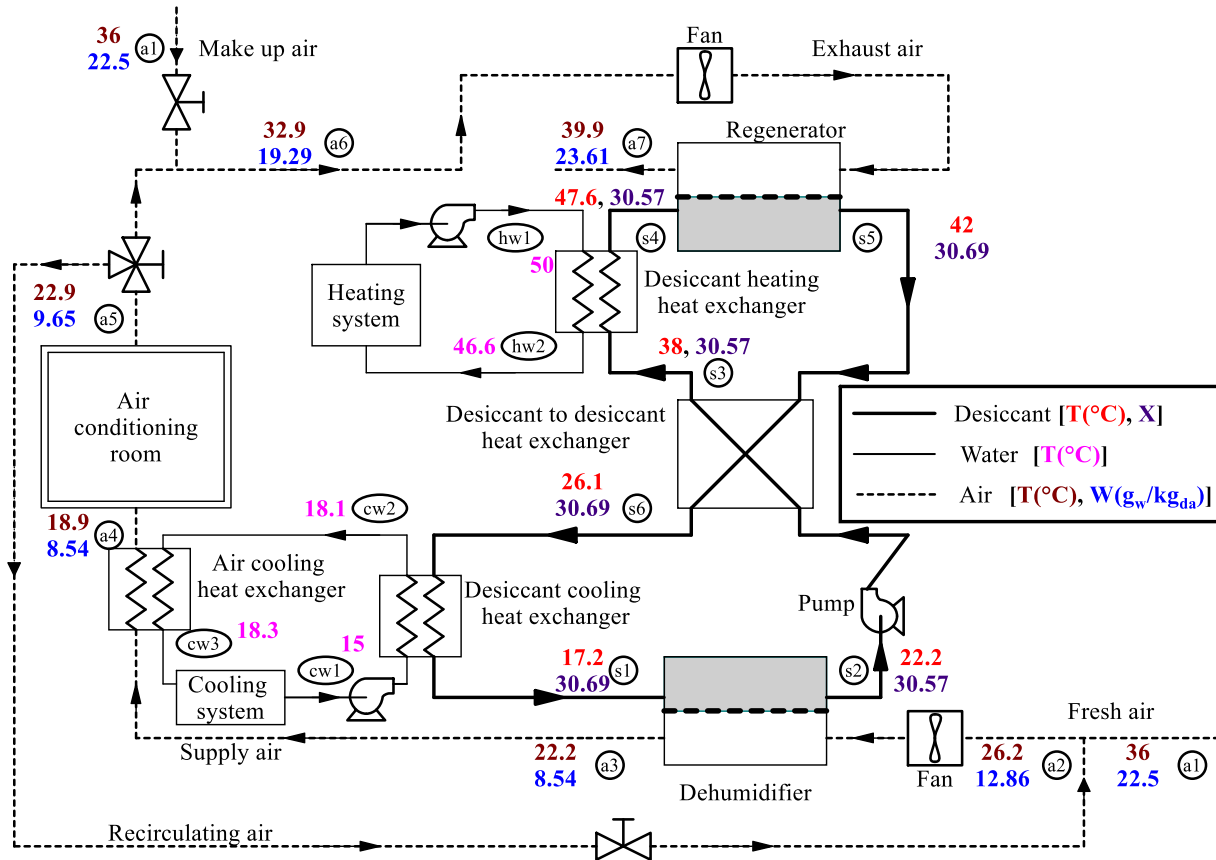


Fig.3: Typical operating conditions of air and desiccant in membrane based LDAS for the hot and humid climatic conditions [13]

In LDAS, the air exchanges both heat and moisture with the desiccant in both the dehumidifier and regenerator. Therefore, these components are referred to as liquid desiccant energy exchangers (LDEEs). The performance of the LDAS significantly depends on the efficiency of such LDEEs [10]. Even though literature focused on LDEEs is voluminous, the present study selectively reviews some important investigations, which gives a summary of developments in LDEEs so far.

The main objective of this review is to present an up-to-date comprehensive overview for the development of LDEEs. The review starts with the working principle of LDEEs. Then, it explains the desiccant material, and design, operating, and performance parameters of LDEEs. Further, the operation, flow configuration, merits, and demerits of various types of LDEEs are discussed in detail. Moreover, the mathematical models used for the performance evaluation

of LDEEs are explained. The present review will be valuable in determining the research gaps and discerning promising pathways for future research in the design and operation of LDEEs.

2. Liquid Desiccant Energy Exchangers

The performance of the LDAS depends on the efficiency of two LDEEs, namely dehumidifier and regenerator, as mentioned earlier in Section 1 [10]. The former is responsible for removing the required heat and moisture from the supply air, whereas the latter reactivates the desiccant for the continuous operation of the LDAS [11]. In the dehumidifier, the vapour pressure in the air is higher than that of the desiccant. Consequently, the vapour diffuses through the air-desiccant interface and gets absorbed into the desiccant. The heat of absorption (the latent heat of condensation and heat of mixing) is released during this absorption process. On the other hand, the vapour pressure of desiccant is higher than that of the air in the regenerator, and hence, the water vapour is transferred from desiccant to air. Therefore, the working principle of both dehumidifier and regenerator is the same except for the direction of water vapour.

2.1 Desired characteristics

The desired characteristics to develop an energy-efficient LDEE are listed as follows [8].

- i. High rates of heat and mass transfer
- ii. Large contact area per unit volume
- iii. Less pressure drop of air
- iv. Made of material which is compatible with desiccant and cost effective

2.2 Heat and mass transfer processes

Figure 4 shows the equivalent circuit for the heat and mass transfer processes of the LDEE. As shown, the processes are interrelated in both LDEEs (dehumidifier and regenerator). In LDEEs, the heat transfer process between the air and desiccant influences the temperature of the desiccant, which affects the mass transfer process. This is because the mass transfer potential depends on the vapour pressure of desiccant, which depends on its temperature. On the other hand, due to the heat of absorption, the mass transfer process also influences the temperature of the desiccant and hence, it affects the heat transfer potential between the air and desiccant. Thus, the mass transfer process influences the heat transfer process and vice versa [13, 20, 21]. The mass transfer process of LDEE is directly proportional to the mass transfer potential (i.e., the difference between the vapour pressure of air and that at the air-desiccant interface) and inversely proportional to its mass transfer resistance [20, 21]. Hence,

$$m_v \propto \left(\frac{W_a - W_s}{R_m} \right) \quad (1)$$

Where, m_v is the mass of water vapour transferred from air to desiccant, W_a is the specific humidity of air and W_s is the equivalent specific humidity of desiccant (i.e., specific humidity of air in equilibrium with the desiccant at the air-desiccant interface). The overall mass transfer resistance (R_m) is defined as follows [20-22].

$$R_m = \left(\frac{1}{h_{m,a}} + R_{m,c} \right) \quad (2)$$

Where, $R_{m,c}$ is the mass transfer resistance of the contact material between the air and desiccant, and $h_{m,a}$ is the convective mass transfer coefficient of air.

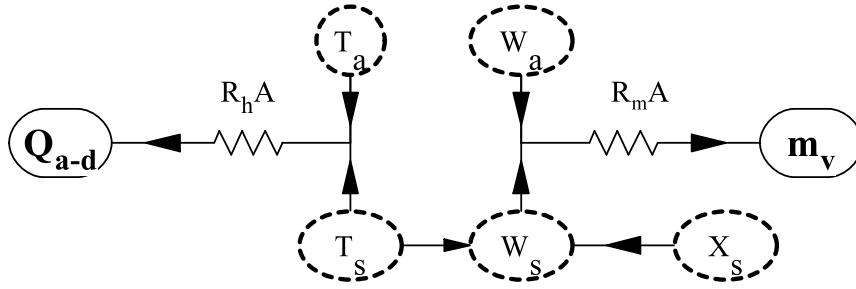


Fig.4: Equivalent circuit for the heat and mass transfer processes of LDEE

Similarly, the heat transfer process of LDEE is directly proportional to the heat transfer potential (i.e., the difference between the temperature of air and that at the air-desiccant interface) and inversely proportional to its heat transfer resistance. The overall heat transfer resistance (R_H) of LDEE is as follows [13, 20-22].

$$R_h = \left(\frac{1}{h_{c,a}} + R_{h,c} + \frac{1}{h_{c,s}} \right) \quad (3)$$

Where, $R_{h,c}$ is the heat transfer resistance of the contact material, and $h_{c,a}$ and $h_{c,s}$ are the convective heat transfer coefficient of air and desiccant, respectively.

3. Liquid Desiccant Materials

Liquid desiccant materials attract water vapour due to their hygroscopic nature. In most cases, the desiccant is a mixture of salt and water [7]. When the desiccant salt is dissolved in water

(solvent), it decreases the vapour pressure of the solution to lower than that of the pure solvent. The vapour pressure decrement depends on concentration and temperature [7]. Equivalent specific humidity of desiccant is a measure of its vapour pressure at the given temperature [13]. Figure 5 compares the effect of temperature on the equivalent specific humidity of water and LiCl desiccant at two different concentrations. As shown, the equivalent specific humidity of LiCl desiccant solution is lower than that of water. Moreover, it decreases when the concentration is increased (at a given temperature), whereas it increases when the temperature is increased (at a given concentration). Figure 6 compares the specific humidity of air with that (equivalent) of LiCl desiccant. As shown, the specific humidity of air is higher than that of desiccant, which is the driving potential in LDEE for the dehumidification process and vice versa for the regeneration process [20]. Figure 7 shows the processes of desiccant in the LDAS.

3.1 Types of materials

LDS was initially developed with glycol-based desiccant solutions [12]. However, as glycol solutions are very volatile and highly viscous, they increase the economic penalty and environmental impacts of LDEE [23]. This resulted in a number of research studies on halide salt-based desiccant solutions, which are less volatile and less viscous than glycol solutions. However, the corrosive nature of salt desiccants restricts their application. In addition, halide salts are relatively costlier than glycol solutions [8]. Consequently, most of the desiccant research has focussed on weak organic acids, which are comparatively cheap as well as non-volatile and less viscous. However, their mass transfer performance is lower than that of salt-based desiccants [24]. Currently, ionic liquids are considered as a good alternative to salt-based desiccants due to their lower vapour pressure, lower regeneration temperature and non-corrosiveness [25].

The most common desiccants of all types (i.e., glycol based, halide salt based, weak organic acids and ionic liquid) studied so far are Calcium chloride, Diethyleneglycol, Dipropylene glycol, Lithium bromide, Lithium chloride, Lithium iodide, Magnesium chloride, Potassium acetate, Potassium fluoride, Potassium formate, Propyleneglycol, Sodium acetate, Sodium formate, Sodium lactate, Tetra-ethyleneglycol, Triethylene glycol, Zinc chloride and 1-Ethyl-3-methylimidazolium acetate [12, 7, 24-27]. There are very limited studies on the performance comparison of desiccant solutions. Mostly the comparison studies are focussed only on the halide salt-based desiccants. The comparison studies [4, 7, 18, 28] revealed that the desiccant with low vapor pressure performs better.

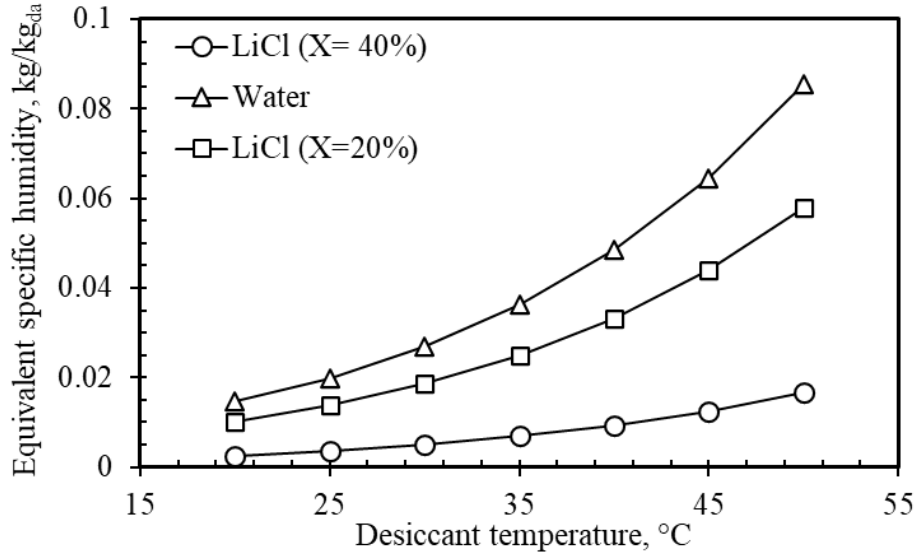


Fig.5: Comparison of equivalent specific humidity of water and LiCl desiccant

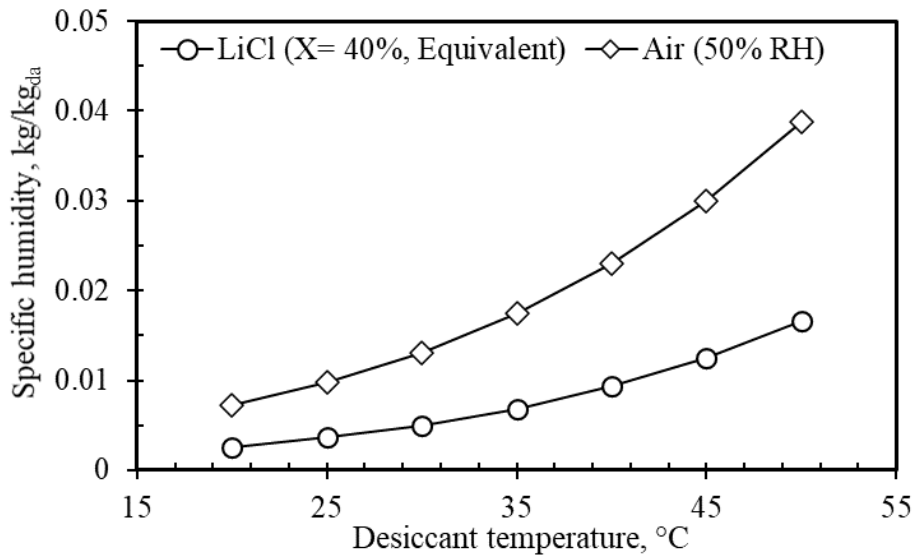


Fig.6: Comparison of specific humidity of air and LiCl desiccant

3.2 Properties

The properties of the desiccants that influence the performance as well as operating and initial costs of LDEEs are listed in Table-3 [28]. The desirable properties of desiccant materials are as follows [7- 10].

- i. High density
- ii. High heat transfer
- iii. Large saturation absorption capacity
- iv. Low cost
- v. Low crystallization point

- vi. Low regeneration temperature
- vii. Low vapour pressure
- viii. Low viscosity
- ix. Non-corrosive
- x. Non-flammable
- xi. Non-toxic
- xii. Non-volatile
- xiii. Odourless
- xiv. Stable

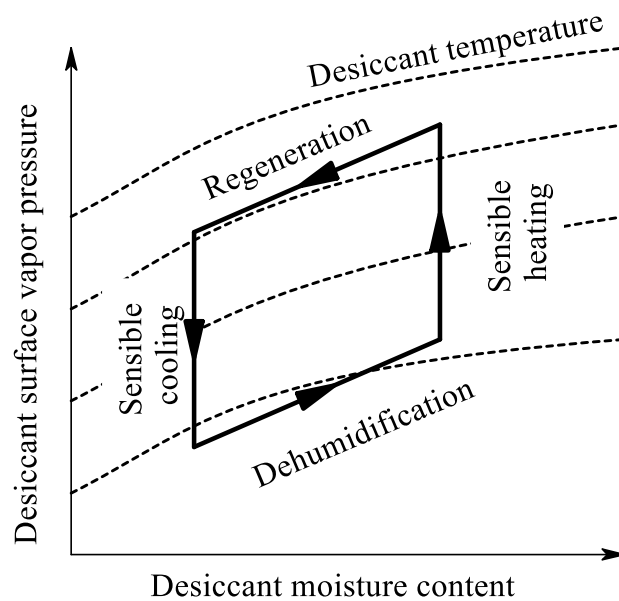


Fig.7: Liquid desiccant processes in LDAS [7]

Table-3: Properties of desiccant materials [28]

Classification	Property
Absorption properties	Equivalent specific humidity
	Heat of absorption
	Diffusion coefficient
	Energy storage capacity
Transport properties	Specific heat capacity
	Viscosity
	Density
	Thermal conductivity
	Surface tension
Economic and environmental properties	Cost
	Safety
	Material compatibility

The effects of desiccant properties are interrelated, and thus, selecting an appropriate desiccant for the given operating conditions is critical. Studak and Peterson [29] developed a marking criterion (figure of merit) for selecting a suitable desiccant. Table-4 lists the figure of merits for the characteristics and properties of the desiccant. The pure desiccants developed so far do not have all the desired properties which are listed above. Therefore, the desiccants are mixed in different proportions to achieve the desired properties. Most of the earlier works on mixed desiccants were focussed on lowering the vapour pressure, regeneration temperature and cost [24, 26]. The performance influencing properties of desiccants can also be modified by the addition of additives [30]. The addition of copper [31, 32], iron [33], silver [34], aluminium oxide [35], ferric oxide [35], zinc ferrite [35] nanoparticles and carbon nanotubes [36] to the desiccant significantly improves its thermal conductivity, which in turn improves the performance of the LDEE. Surfactant-based additives also enhance the performance of the LDEE by improving the wettability of desiccants on its contact surface [30]. The most used surfactants are polyether-modified siloxane [37], triton X-100 [38], 1-octanol [39] and 2-ethyl-1-hexanol [40]. However, these surfactants are poisonous and odorous. To mitigate these problems, Wen et al. [41] proposed a new surfactant, Polyvinyl Pyrrolidone (0.4%), which improved the moisture removal rate of LDEE by 22%. The surfactant, hydroxyethyl urea not only increases the wettability but also reduces the corrosive nature of LiCl desiccant [42].

Table-4: Weighing factors and figures of merits for desiccant selection [29]

Characteristics	Weighing factor	Figure of merit
Safety	1	Lethal dose (LD50)
Corrosion	0.8	Corrosion rate
Mass transfer potential	0.8	Equivalent vapor pressure
Heat of absorption	0.6	Energy/ kg of absorbed water
Cost of desiccant	0.5	Cost/100 kg of solution
Heat transfer potential	0.5	Thermal conductivity
Parasitic power losses	0.3	Viscosity

4. Performance Parameters

The parameters used to evaluate the performance of the LDEE for its dehumidification and regeneration processes are discussed as follows.

4.1 Performance parameters for dehumidification process in adiabatic LDEE

4.1.1 Moisture removal rate (MRR)

It is the total amount of moisture transferred from the supply air to the desiccant. It is given as follows [7].

$$MRR = m_a \times (W_{a,in} - W_{a,out}) \quad (4)$$

Where, m_a is the mass flow rate, and $W_{a,in}$ and $W_{a,out}$ are the inlet and outlet specific humidity of air, respectively.

4.1.2 Latent effectiveness (\mathcal{E}_W)

It is the ratio of actual moisture transfer from the supply air to the desiccant to the maximum possible moisture transfer that can take place. It is calculated as [7]

$$\mathcal{E}_W = \frac{W_{a,in} - W_{a,out}}{W_{a,in} - \{W_{s,in} @ X_{s,in}, T_{s,in}\}} \quad (5)$$

Where, $W_{s,in}$ is the inlet equivalent specific humidity of desiccant, which is calculated as a function of its inlet temperature ($T_{s,in}$) and concentration ($X_{s,in}$) [43].

4.1.3 Sensible effectiveness (\mathcal{E}_S)

It is the ratio of actual sensible heat transfer from the supply air to the desiccant to the maximum possible sensible heat transfer that can take place [7]. It is given as follows.

$$\mathcal{E}_S = \frac{T_{a,in} - T_{a,out}}{T_{a,in} - T_{s,in}} \quad (6)$$

Where, $T_{a,in}$ and $T_{a,out}$ are the inlet and outlet temperature of the air, respectively. In hot and humid conditions, the inlet temperature of desiccant is lower than that of air in adiabatic LDEE (A-LDEE). Consequently, the desiccant absorbs both the heat and moisture from the air. However, in certain operating conditions, the air may be heated due to the heat of absorption released during dehumidification processes. Therefore, sensible effectiveness can be less than zero [44,45].

4.1.4 Enthalpy effectiveness (\mathcal{E}_h)

Air exchanges both heat and moisture with the desiccant in the LDEE, as mentioned earlier in Section 1. Therefore, the changes in the air conditions can be quantified using its enthalpy. Enthalpy effectiveness is extensively used in the performance evaluation of direct contact LDEE [46]. It is the ratio of actual enthalpy transfer from the supply air to the desiccant to the maximum possible enthalpy transfer that can take place. It is calculated as,

$$\mathcal{E}_h = \frac{h_{a,in} - h_{a,out}}{h_{a,in} - h_{s,in}} \quad (7)$$

Where, $h_{a,in}$ and $h_{a,out}$ are the inlet and outlet enthalpy of air, respectively and $h_{s,in}$ is the inlet enthalpy of desiccant.

4.1.5 Total effectiveness (ϵ_t)

It is the ratio of actual energy transfer from the supply air to the desiccant to the maximum possible energy transfer that can take place [22]. Thus,

$$\epsilon_t = \frac{\epsilon_S + (H^* \times \epsilon_W)}{1 + H^*} \quad (8)$$

Where, H^* is the operating factor of the dehumidifier [47]. It is the ratio of latent to sensible energy difference across the LDEE. It can be observed from Eqn. (8) that the total effectiveness is essentially a weighted average of the sensible and latent effectiveness. When H^* tends to ∞ , the total effectiveness is close to latent effectiveness (i.e., dominant moisture transfer). Similarly, when H^* tends to 0, the total effectiveness is close to sensible effectiveness (i.e., negligible moisture transfer) [47]. The total effectiveness is extensively used in the performance evaluation of Liquid-to-Air Membrane Energy Exchanger (LAMEE) [48].

4.1.6 Mass transfer coefficient (h_m)

It is defined as the ratio of the moisture removal rate per unit area [49]. It is given as follows,

$$h_m = \frac{MRR}{A \times (W_{a,in} - \{W_{s,in} @ X_{s,in}, T_{s,in}\})} \quad (9)$$

Where, A is the contact area between the air and desiccant.

4.1.7 Cooling Capacity of Air (CC_a)

It is the amount of cooling energy transferred from the supply air to the desiccant [50]. It is given as follows,

$$CC_a = m_a \times (h_{a,in} - h_{a,out}) \quad (10)$$

4.1.8 Sensible heat ratio (SHR)

The heat transfer process in the LDEE depends not only on the inlet temperature of air and desiccant but also on the heat of absorption. As a result, the sensible heat transfer process is not necessarily equal to the mass transfer process in the LDEE. Therefore, SHR was introduced as a performance parameter to find out the most influenced process in the LDEE [51]. SHR is defined as the ratio between the sensible and total heat transfer from the supply air to the desiccant. It is calculated as,

$$SHR = \frac{m_a \times C_{p,a} \times (T_{a,in} - T_{a,out})}{CC_a} \quad (11)$$

Where, $C_{p,a}$ is the specific heat capacity of air.

4.1.9 Moisture flux rate (MFR)

It is defined as the ratio of moisture removal rate to the overall mass transfer conductance [20]. It is used to evaluate the LDEE based on the inlet conditions of the streams. Moreover, it is independent of the size of the LDEE, and thus, it makes the evaluation more general. MFR is calculated as follows,

$$MFR = \frac{MRR}{A \times U_m} \quad (12)$$

Where, U_m is the overall mass transfer coefficient of the LDEE.

4.1.10 Desiccant temperature change rate (DTRC)

If the desiccant heats up more during the dehumidification process, the required heating of desiccant for its regeneration process decreases. Similarly, if the desiccant cools down more during the regeneration process, then the required cooling of desiccant for its dehumidification process decreases. Therefore, DTRC is defined to evaluate the temperature change of desiccant (i.e., desiccant's sensible performance) in the LDEE [52]. It is calculated as follows,

$$DTRC = \frac{T_{s,in} - T_{s,out}}{T_{s,in}} \quad (13)$$

Where, $T_{s,out}$ is the outlet temperature of the desiccant.

4.1.11 Dehumidification perfectness (DP)

The conventional sensible or latent effectiveness definition is applicable only for the counterflow arrangement where the outlet of supply air is located exactly at the same place as the inlet of desiccant. However, such a flow operating condition is not valid for the parallel or crossflow configurations of the LDEE. Therefore, Yang et al. [53] introduced a new parameter, "dehumidification perfectness", to evaluate the performance of the LDEE in parallel or crossflow arrangement. DP is calculated as follows,

$$DP = \frac{W_{a,in} - W_{a,out,act}}{W_{a,in} - W_{a,out,ideal}} \quad (14)$$

Where, $W_{a,out,act}$ and $W_{a,out,ideal}$ are outlet specific humidity of air at actual and ideal conditions, respectively [53].

4.2 Performance parameters for dehumidification processes in internally cooled or heated LDEE

Most of the performance parameters for A-LDEE discussed so far are applicable to internally cooled or heated LDEE (I-LDEE), except for few effectiveness parameters. The definitions of such effectiveness are discussed as follows.

4.2.1 Sensible effectiveness (\mathcal{E}_S)

The sensible effectiveness of I-LDEE is derived based on the definitions of three fluid heat exchangers. The typical operating conditions of the LDEE under hot and humid climatic conditions (i.e., the air is cooled and dehumidified by the desiccant) are: (i) heat capacity rate of air is higher than that of the desiccant and cooling streams and (ii) the inlet temperature of cooling stream is lower than that of air and desiccant [54]. Then, the sensible effectiveness can be calculated using the following equation,

$$\mathcal{E}_S = \frac{T_{a,in} - T_{a,out}}{T_{a,in} - T_{cw,in}} \quad (15)$$

Where, $T_{cw,in}$ is the inlet temperature of cooling water.

4.2.2 Latent effectiveness (\mathcal{E}_W)

The definition of latent effectiveness is similar for both A-LDEE and I-LDEE. However, due to the cooling of desiccant by the cooling stream, the equivalent specific humidity of desiccant is calculated based on the temperature of the cooling stream [54]. The latent effectiveness equation is given as follows,

$$\mathcal{E}_W = \frac{W_{a,in} - W_{a,out}}{W_{a,in} - \{W_{s,in} @ X_{s,in}, T_{cw,in}\}} \quad (16)$$

Similarly, the inlet temperature of cooling water should be used instead of the inlet temperature of desiccant in the equations of enthalpy effectiveness [Eqn. (7)] and mass transfer coefficient [Eqn. (9)] for its application in I-LDEE.

4.3 Performance parameters for regeneration processes in A-LDEE

Even though dehumidification parameters discussed so far are mostly focused on the airside parameters; theoretically, they are valid for the regeneration process as well. However, the main focus of the regeneration process is on desiccant side parameters. Therefore, similar performance parameters are developed using desiccant parameters and they are listed as follows [55].

4.3.1 Moisture removal rate: $MRR = m_s \times (X_{s,in} - X_{s,out})$ (17)

Where, $X_{s,out}$ is the outlet concentration of desiccant.

4.3.2 Sensible effectiveness:

$$\mathcal{E}_S = \frac{\{m_s \times C_{p,s} \times (T_{s,out} - T_{s,in})\} - \{m_{salt} \times h_{fg} \times (X_{s,out} - X_{s,in})\}}{m_a \times C_{p,a} \times (T_{a,in} - T_{s,in})} \quad (18)$$

Where, m_{salt} and $C_{p,\text{salt}}$ are the mass flow rate and specific heat capacity of salt, respectively; m_s and $C_{p,s}$ are mass flow rate and specific heat capacity of desiccant, respectively, and h_{fg} is the enthalpy of absorption.

$$\mathbf{4.3.3 Latent effectiveness:} \quad \varepsilon_{\text{W}} = \frac{m_{\text{salt}} \times C_{p,\text{salt}} \times (X_{\text{s,out}} - X_{\text{s,in}})}{m_{\text{a}} \times (W_{\text{a,in}} - \{W_{\text{s,in}} @ X_{\text{s,in}}, T_{\text{cw,in}}\})} \quad (19)$$

4.3.4 Total effectiveness:

$$\varepsilon_{\text{t}} = \frac{m_{\text{s}} \times C_{p,s} \times (T_{\text{s,out}} - T_{\text{s,in}})}{\left[m_{\text{a}} \times C_{p,a} \times (T_{\text{a,in}} - T_{\text{s,in}}) \right] + \left[m_{\text{a}} \times h_{\text{fg}} \times (W_{\text{a,in}} - \{W_{\text{s,in}} @ X_{\text{s,in}}, T_{\text{cw,in}}\}) \right]} \quad (20)$$

4.3.5 Regeneration efficiency (η_{r})

It is defined as the actual latent energy from the desiccant to air during the regeneration process, to the heat energy supplied (Q_{r}) to the desiccant [56]. It is used to evaluate the energy utilization efficiency of the desiccant and is calculated as follows,

$$\eta_{\text{r}} = \frac{MRR \times h_{\text{fg}}}{Q_{\text{r}}} \quad (21)$$

5. Design Parameters

In addition to operating parameters, the heat and mass transfer performance of the LDEE significantly depends on the design parameters, which are discussed as follows [54, 57].

5.1 Mass flow rate ratio (m^*)

It is the ratio of the mass flow rate of air to desiccant and is calculated as follows,

$$m^* = \frac{m_{\text{s}}}{m_{\text{a}}} \quad (22)$$

Where, m_{a} and m_{s} are the mass flow rate of air and desiccant, respectively. The performance of the A-LDEE increases when the mass flow rate ratio is decreased.

5.2 Capacitance ratio (Cr)

It is the ratio of heat capacity rate of desiccant to air in the A-LDEE. It is given as,

$$Cr_{\text{s/a}} = \frac{C_{\text{s}}}{C_{\text{a}}} = \frac{m_{\text{s}} \times C_{p,s}}{m_{\text{a}} \times C_{p,a}} \quad (23)$$

Where, C_{s} and C_{a} are the heat capacity rate of desiccant and air, respectively. The performance of the A-LDEE increases with an increase in the capacitance ratio. Due to the additional stream

in the I-LDEE, there are additional capacitance ratios for the dehumidification process, which are listed as follows.

$$Cr_{a/cw} = \frac{C_a}{C_{cw}} = \frac{m_a \times C_{p,a}}{m_{cw} \times C_{p,cw}} \quad (24)$$

$$Cr_{s/cw} = \frac{C_s}{C_{cw}} = \frac{m_s \times C_{p,s}}{m_{cw} \times C_{p,cw}} \quad (25)$$

Where, C_{cw} , m_{cw} and $C_{p,cw}$ are the heat capacity rate, mass flow rate and specific heat capacity of the cooling stream, respectively. Similarly, there are additional capacitance ratios (with respect to hot stream) in I-LDEE for the regeneration process.

5.3 Number of heat transfer units

The number of heat transfer units denotes the heat transfer capability of the LDEE. It is given as,

$$NTU_h = \frac{U_h \times A}{C_{\min,s/a}} \quad (26)$$

Where, U_h is the overall heat transfer coefficient and $C_{\min,s/a}$ is the minimum heat capacitance rate between the air and desiccant. The performance of the LDEE increases with an increase in NTU_h .

5.4 Number of mass transfer units

The number of mass transfer units signifies the mass transfer capability of the LDEE. It is calculated as,

$$NTU_m = \frac{U_m \times A}{m_{\min,s/a}} \quad (27)$$

Where, $m_{\min,s/a}$ is the minimum mass flow rate between the air and desiccant. The performance of the LDEE increases with an increase in NTU_m .

5.5 Effective capacitance ratio (Cr_e)

To adopt the standard effectiveness-NTU (ϵ -NTU) equations of heat exchangers to LDEE for its sensible effectiveness, Kamali [58] proposed an effective capacitance ratio (Cr_e) which is the ratio between the temperature change of desiccant and air in the LDEE.

$$Cr_e = \frac{T_{s,out} - T_{s,in}}{T_{a,out} - T_{a,in}} \quad (28)$$

5.6 Effective mass flow rate ratio (m_e^*)

To adopt the standard ε -NTU equations of heat exchangers to LDEE for its latent effectiveness, Kamali [58] proposed an effective mass flow rate ratio (m_e^*) which is the ratio between the specific humidity change of desiccant and air in the LDEE.

$$m_e^* = \frac{W_{s,out} - W_{s,in}}{W_{a,out} - W_{a,in}} \quad (29)$$

Where, $W_{s,out}$ is the outlet equivalent specific humidity of the desiccant.

6. Operating Parameters

The air and desiccant are the two main streams in A-LDEE. The parameters of air are mass flow rate, and inlet temperature and specific humidity. The mass flow rate of air depends on the application of the LDAS. The other parameters, namely, the temperature and specific humidity, depend on the climatic conditions of the application. The climatic design data of ASHRAE lists the design values of temperature and specific humidity for various climatic conditions [59]. Since the air parameters depend on the application and climatic conditions, the desiccant parameters are used to improve or control the performance of the LDEE. The parameters of the desiccant are mass flow rate, and inlet temperature and concentration. Table-5 lists the desired characteristics and optimum range of the desiccant parameters [7]. The operating parameters of the cooling or heating stream (i.e., temperature and mass flow rate) are used to maintain the desired desiccant conditions in the I-LDEE.

Table-5: Desired conditions of desiccant parameters in the LDEE [7]

Parameters	Desired condition for maximum MRR	Effects	Optimum range
Mass flow rate	High	Needs more pumping power and large storage tanks	1.5-3 times and 0.5-1 time the mass flow rate of air for the A-LDEE and I-LDEE, respectively
Temperature	Low	Needs more cooling energy	20-25°C and 45-55°C at the inlet of the A-LDEE for dehumidification and regeneration processes, respectively
Concentration	High	Needs more regeneration energy	Depends on the type of desiccant and varies between 0.3-0.5 for the desiccants of salt solution type

7. LDEE Classifications

The performance of the LDAS significantly depends on the efficiency of the LDEEs [9], as mentioned earlier in Section 1. Besides the humidity control in comfort air conditioning, LDAS has a wide variety of applications such as humidity control in textile mills, drying of natural gas, gas absorption, and crop drying [60]. Thus, LDEEs are developed in different approaches in terms of applications and also based on flow configuration, contact between the air and desiccant, etc. Figure 8 shows the broad classifications of LDEEs. The operation, flow configuration, merits, and demerits of various types of LDEEs are discussed in detail as follows.

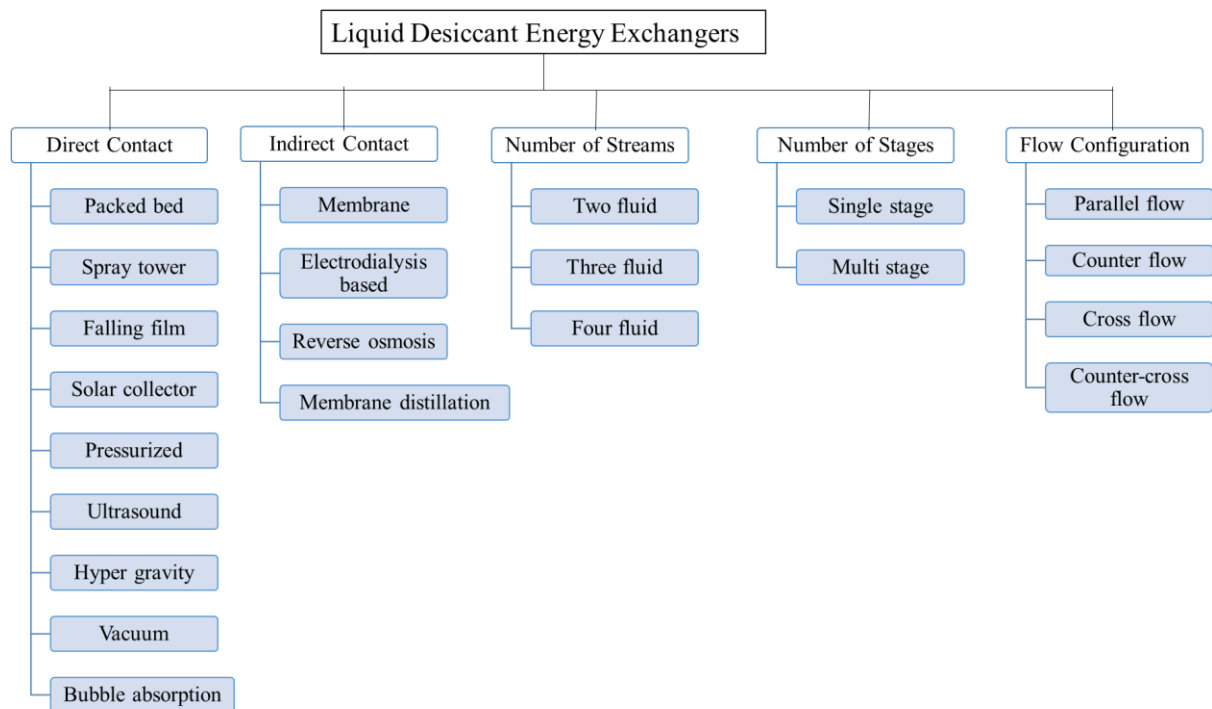


Fig.8: Classification of LDEEs

7.1 Direct contact LDEE

The air and desiccant streams are in direct contact with each other during the heat and mass transfer processes in the direct contact LDEE. Most of the previous works on LDEEs have concentrated on direct contact type due to its high effectiveness, simple structure and easy arrangement [24]. As a result, different types of direct contact LDEEs have been developed so far, as shown in Fig.8, and such types are discussed as follows.

7.1.1 Packed bed LDEE

Air exchanges its heat and moisture with the desiccant in the presence of packing fills in the packed bed LDEE (PB-LDEE). PB-LDEE has a higher heat and mass transfer performance

when compared to most other of the direct contact LDEEs, and thus, it is the most studied direct contact type in literature [7]. In addition to air conditioning, the packed bed is widely used for gas separation and absorption in chemical industries. Hence, its desirable design characteristics are well established, and they are listed as follows [61].

- i. Should operate in the loading region (a region where the gas flow rate does not influence the liquid holdup), which assures a surface area to achieve maximum mass transfer performance
- ii. Packing size should not be greater than 1/8 of the column diameter
- iii. Should have an efficient liquid distribution

Figure 9 lists the stepwise procedure for the preliminary design of PB-LDEE [62]. In PB-LDEE, the packing fills provide contact area for the heat and mass transfer processes between the air and desiccant. Therefore, the selection and arrangement of such fills play a significant role in the design and performance of the PB-LDEE.

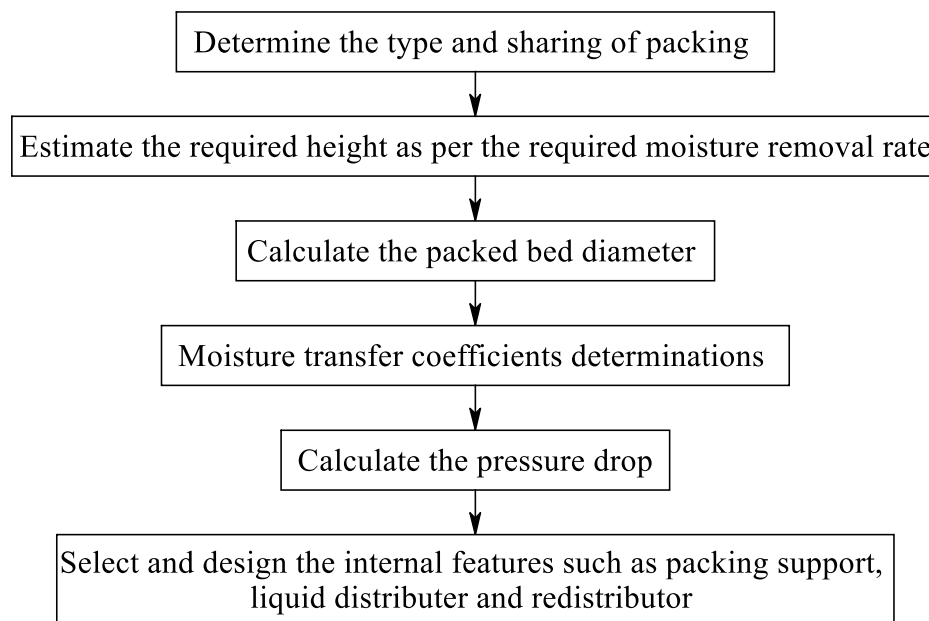


Fig.9: Flow chart for the stepwise procedure for the preliminary design of PB-LDEE [61, 62]

The desirable requirements of the packing fill are [12,63]:

- i. Maximize the contact areas between the air and desiccant to improve the performance
- ii. Maximize the void space per unit volume which decreases resistance to airflow
- iii. Minimize friction to reduce the pressure drop
- iv. Minimize cost
- v. Promote the uniform distribution and flow of streams throughout the packed bed

- vi. Should be chemically inert and capable of structurally withstanding the air velocity
- vii. Provision to arrange with optimum spacing (6-8 mm) between its layers

Packing fills are broadly classified as structured and random types. In the former, the fills are in fixed geometric form, whereas, in the latter, they are in an irregular geometric shape, which are randomly arranged in the PB-LDEE, as shown in Fig.10 [8]. Figure 11 shows the photographic views of various structured and random packing fills [64] and the comparison between these packing fills is presented in Table-6 [63]. Packing fills such as raschig rings, intalox saddles, and berl saddles are widely used for random packing. The commonly used structured fills are cellulose rigid media pads, wood grids, expanded metal lash packing, and double spiral rings [26]. Of late, ceramic and plastic fills are being extensively used to mitigate the corrosion of liquid desiccants. Even though plastic fills are lightweight and inexpensive, they are not suitable for the regeneration process due to the higher temperature of desiccant [26]. The wettability of liquid desiccant over the packing fills considerably influences the performance of the PB-LDEE. Therefore, several studies have focused on improving the wetting area by providing a coating to the surface of the packing fills. Notably, the coating made of titanium oxide doubles the moisture removal rate of the LDEE [27].

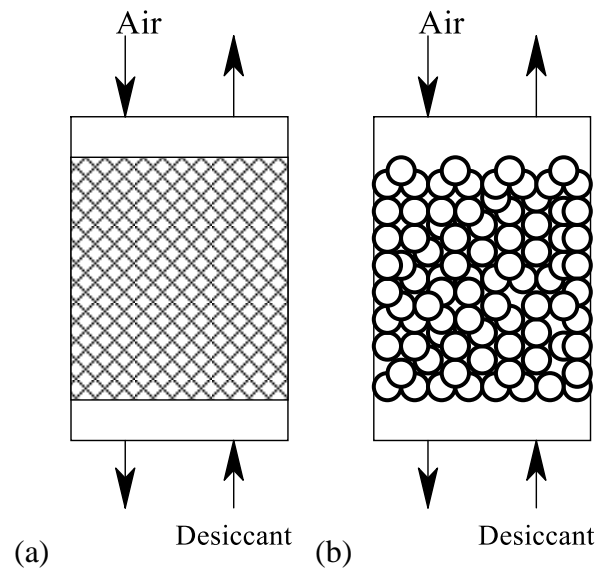


Fig.10: Schematic of PB-LDEE with (a) structured and (b) random packing fills

PB-LDEE with random fills has not only higher mass transfer performance but also higher pressure drop in the airstream [65]. Moreover, the random fills require a higher desiccant flow rate to achieve good wetting characteristics [66]. Furthermore, the performance, pressure drop and wetting characteristics depend on the type and arrangement of fills [8]. Hence, nowadays,

the configurations of the fills are efficiently developed (Fig.12) to (i) increase the contact area for the given volume, (ii) improve the wettability of desiccant and (iii) decrease the pressure drop [66].

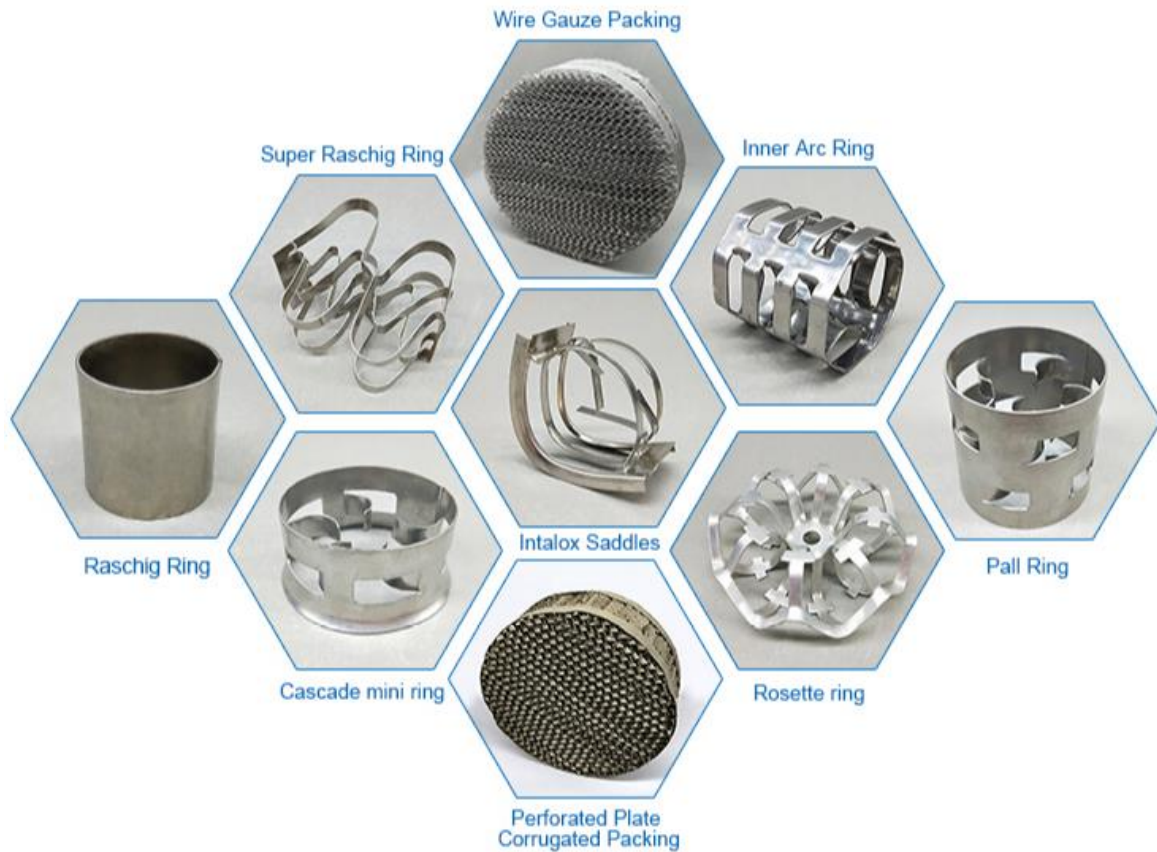


Fig.11: Photographic views of structured and random packings [64]

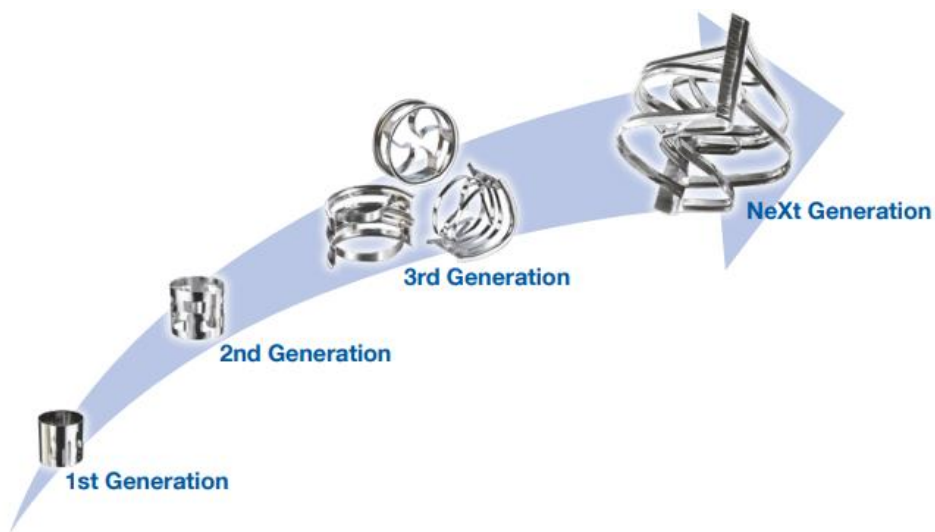


Fig.12: Development of random packings for gas absorption [66]

Table-6: Comparison between structured and random packings [63]

Structured packing	Random packing
Uniform flow channel	Non-uniform flow due to irregular packing structure
Expensive	Inexpensive
Lesser airside pressure drop	Higher airside pressure drop due to irregular packing shape
Higher surface area	Lesser surface area due to its arrangement
Difficult to transport without damage	Easy to transport and store

The air and desiccant are in direct contact in the PB-LDEE, as mentioned earlier. As a result, the air carries tiny droplets of desiccant (desiccant carryover) to the air conditioning space. This deteriorates the indoor air quality, which can be hazardous to the health of the occupants. Moreover, the desiccant carryover corrodes not only the air handling equipment and ducts but also the equipment and instruments in the air conditioning space. Even though PB-LDEE offers high heat and mass transfer performance, the issues due to desiccant carryover restrict its applications in various sectors, including comfort air conditioning [7]. These desiccant carryover issues are relatively predominant in PB-LDEE with random fills since it requires a higher desiccant flow rate to achieve a wetting area equal to that of structured fills [27]. Several types of innovative filters have been developed to reduce the desiccant carryover by air. However, they significantly increase the pressure drop of air, and consequently increase the running cost of the LDAS.

7.1.2 Spray tower LDEE

Spray tower is an alternative design to PB-LDEE in terms of simpler construction, lesser cost, and more compactness [24]. In the spray tower LDEE, the desiccant is finely atomized and sprayed to improve the contact area between the air and desiccant [27]. In addition to LDAS, the spray tower design is widely used in the closed sorption systems (i.e., absorption refrigeration systems) [67, 68]. Hence, the research findings from such systems are generally applicable to the LDAS. The droplet size plays a significant role in the performance of the spray tower LDEE [10]. It depends not only on the desiccant properties but also on the design of the desiccant spray system. The droplet speed also influences the performance of the spray tower LDEE. An increase in the speed increases its Reynolds number and decreases its residence time in the LDEE. The former increases the mass transfer rate due to droplet circulation, whereas the latter reduces the transfer rate owing to less contact time between the air and desiccant. These counteracting factors should be considered while designing the spray

system to have a net positive effect on the performance of the LDEE [67]. The pressure drop of air in the spray tower LDEE is lesser than that of PB-LDEE due to the absence of packing fills. Moreover, the former type requires a lower desiccant flow due to its high contact area [69]. However, due to the fine sprayed droplets, the possibility of desiccant carryover with the air is more predominant in spray tower LDEE [10]. The lesser the droplet size, the more the probability of desiccant carryover [70]. Therefore, the droplet size determines not only the performance of the LDEE but also the amount of desiccant carryover. A new design for spray tower LDEE was proposed by Kumar et al. [70] to avoid the desiccant carryover. The proposed tower was divided into main and zero carryover sections, as shown in Fig.13. The air from the main section was rested in the enlarged free space before it was exhausted from the tower. The velocity of the air was reduced (1 to 0.75 m/s) in the zero carryover section. This reduced the uplifting drag force on the desiccant droplets, and consequently, the droplets fell back to the main section. Therefore, the desiccant carryover was avoided in the proposed tower design without any additional pressure drop in the air stream. Moreover, the restriction in the droplet size due to desiccant carryover was evaded in the proposed tower design [70].

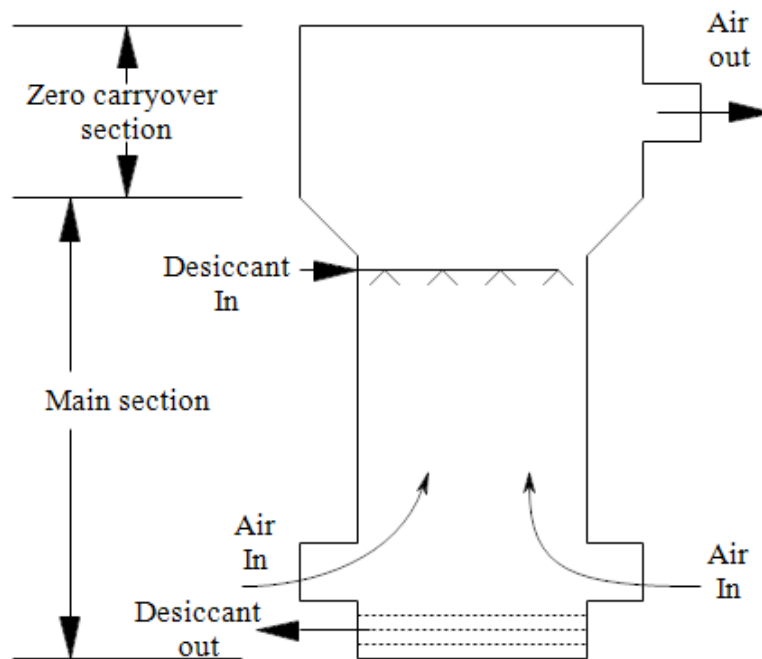


Fig.13: Innovative zero carryover spray tower LDEE [70]

7.1.3 Falling film LDEE

In the falling film LDEE (FF-LDEE), the desiccant flows by gravity as a continuous thin film over the surface of tubes or plates, which can be arranged either horizontally or vertically, as

shown in Fig.14. Besides the operating conditions and contact area, the performance of the FF-LDEE depends on film thickness, desiccant wettability, and its geometry [24,71, 72].

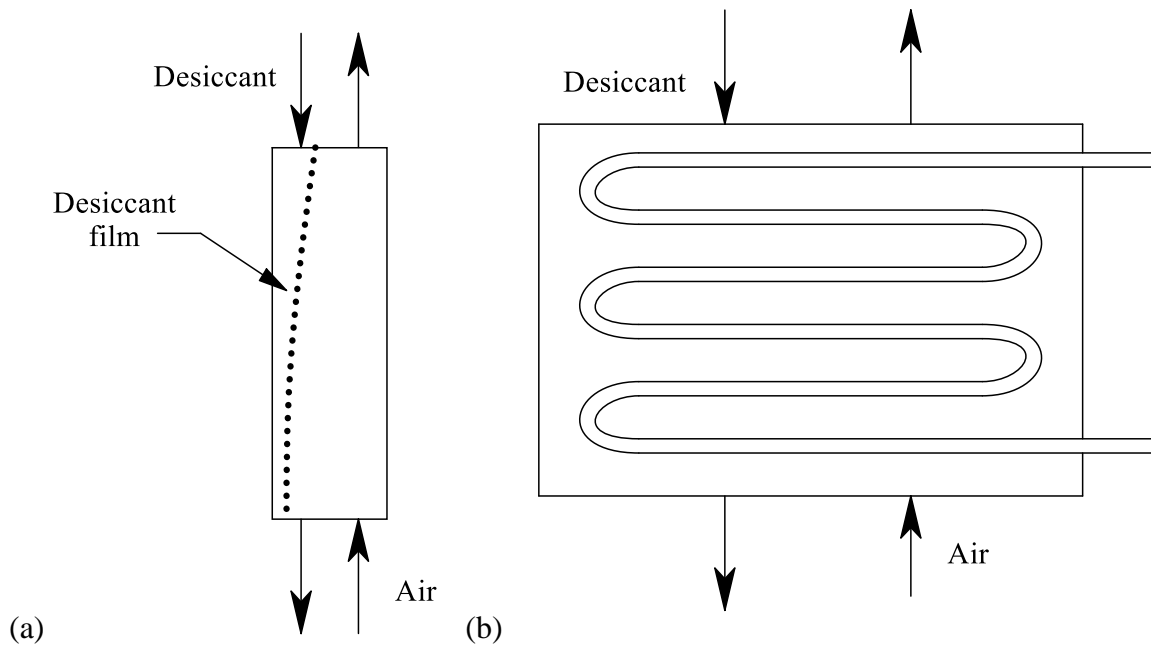


Fig.14: Schematic of (a) plate and (b) shell and tube type FF-LDEE

The advantages of the FF-LDEE are (i) lower pressure drop than PB-LDEE, (ii) good performance even at low desiccant and airflow rates, (iii) suitable to provide additional cooling or heating streams, (iv) stable flow and (v) constant contact area [24,69,72]. Moreover, the risk of desiccant carryover is lesser than in the spray tower LDEE [11]. The constraints of falling film configuration are the difficulty in maintaining the required film thickness throughout the LDEE [73] and higher construction costs [24]. The corrosive nature of the liquid desiccant has promoted the utilization of plastic materials in the LDEE. However, such materials' wettability and thermal conductivity are lower compared to conventional materials such as stainless steel, copper, aluminium, etc. [74]. Therefore, the surface coating of material becomes essential to improve either the wettability of alternative material (i.e., plastic) or the corrosion resistance of the conventional materials [74, 75].

The performance of the FF-LDEE can be improved by altering the plate structures. An earlier study showed that LDEE with curved fin has a 10% better performance than that with straight fins. With both surface treatment using titanium oxide and curved fins, the performance can be improved by 47% [76]. In FF-LDEE, the air comes into contacts with the desiccant at the film surface. Thus, most part of the desiccant film (area underneath the film) do not comes into contacts with the air. To utilize the unused desiccant in the film, Islam et al. [77] proposed a

film inverting configuration, as depicted in Fig.15. As shown, the baffles are used to invert the film, and thus, the inner part of the film comes into contacts with air. This improves the heat and mass transfer performance of the LDEE. The falling film configuration is extensively used in closed absorption systems. In such systems, various surface modifications such as scratched surfaces (to increase the surface roughness), curvature tubes, fluted tubes, micro-finned tubes, corrugated plates, and finned plates have been employed to improve the performance [78]. These modifications can be directly or indirectly applied to the FF-LDEE to improve its performance.

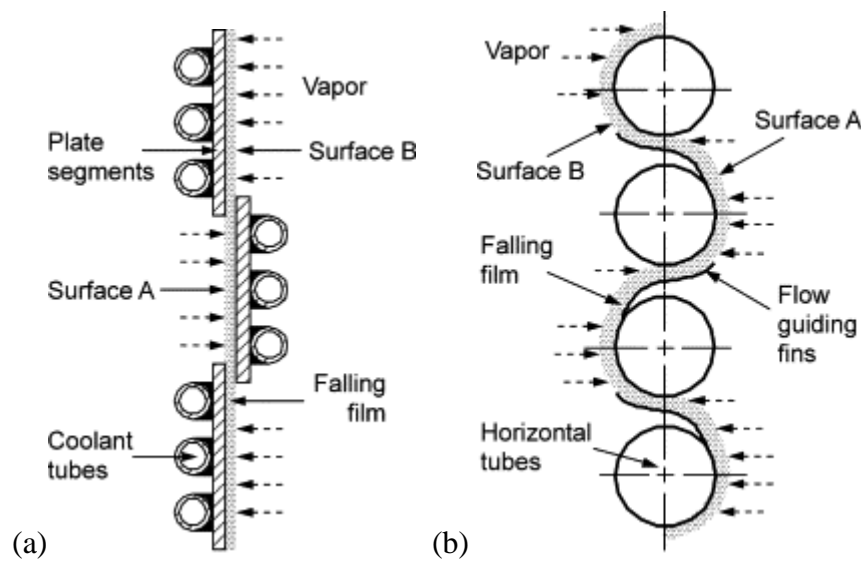


Fig.15: Film inverting configurations of (a) plate and (b) shell and tube types FF-LDEE [77]

7.1.4 Solar collector based LDEE

One of the main advantages of using the LDAS is the utilization of low-grade energy sources for the regeneration of its desiccant [69]. Most of the earlier studies have focused on solar energy utilization (as a low-grade energy source) due to the relative coincidence of peak cooling load and solar insolation [10]. Solar energy can be used either directly or indirectly to regenerate the desiccant. In the indirect type, a heat transfer fluid collects the heat energy in a solar collector. Subsequently, the fluid either preheats the desiccant in a heat exchanger before it reaches the LDEE or heats the desiccant simultaneously during its regeneration process in the LDEE. However, in the direct type, the desiccant itself circulates in the solar collector to collect the heat energy for its regeneration [12]. Therefore, the direct type combines the effects of photothermal transformation and regeneration of the desiccant [79]. Hence, it is more efficient than the indirect type in terms of solar utilization ratio [40] and is referred to as solar collector based LDEE (SC-LDEE), which was first developed by Kakabaev et al. [41] in 1969.

Due to the direct utilization of solar energy, the performance of SC-LDEE is better than that of conventional regeneration techniques, as shown in Fig.16 [24]. Unlike all other LDEEs discussed so far, SC-LDEE is only used as a regenerator in the LDAS.

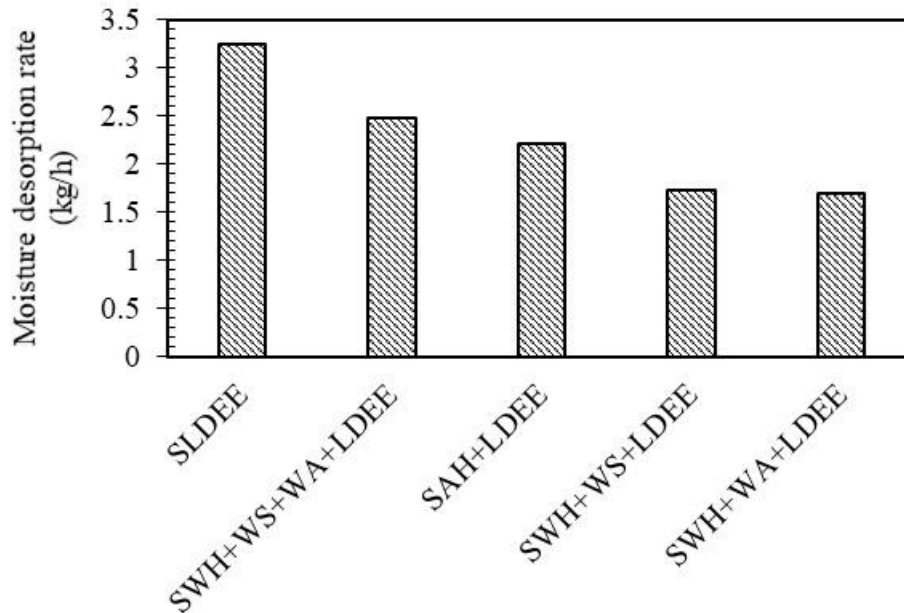


Fig.16: Comparison between SC-LDEE and conventional LDEE regeneration types [24]

SC-LDEE simplifies and reduces the initial and running costs of the LDAS due to the absence of a separate desiccant regeneration chamber [24]. The geometry of the SC-LDEE is similar to that of the FF-LDEE. Therefore, the research outcomes of the FF-LDEE in terms of wettability, film thickness, inclination, and flow configuration are expected to be applicable for the SC-LDEE [10]. SC-LDEE is broadly classified as open, closed, and connective types, which are discussed as follows.

7.1.4.1 Open type SC-LDEE

The open type SC-LDEE is the simplest one (Fig. 17(a)) in which the desiccant flows over the surface of the collector, and consequently, gets heated up. As a result, the vapour pressure of the desiccant increases more than that of the ambient air, and hence, the desiccant gets concentrated by releasing its vapour to the ambient air. Adverse climatic conditions, such as gales and rain, can affect the performance of the open type SC-LDEE. The efficiency of the open type SC-LDEE is comparatively lower due to its heat loss to the ambient [12].

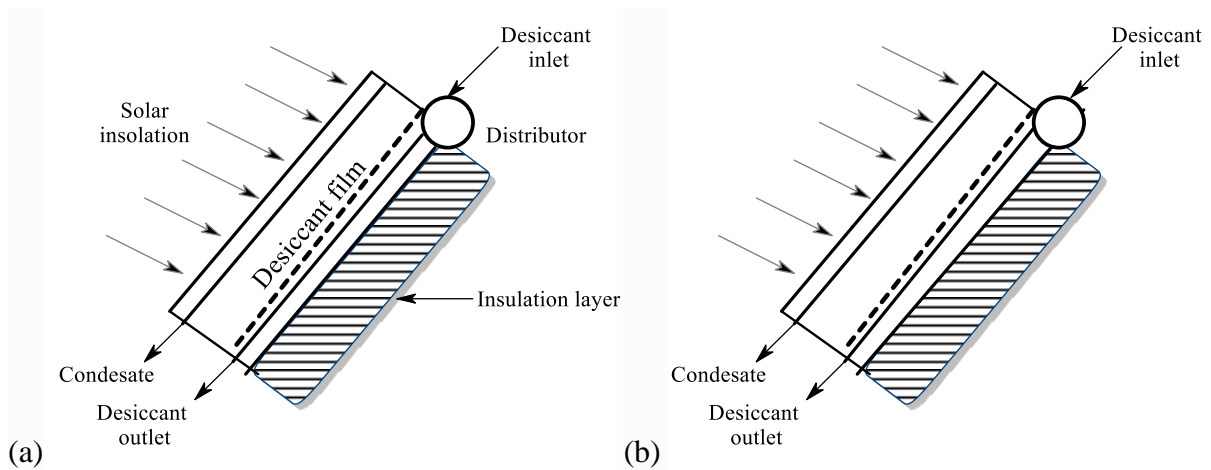


Fig.17: Schematic diagram of (a) open and (b) closed type SC-LDEE

7.1.4.2 Closed type SC-LDEE

The configuration of the closed type SC-LDEE is similar to that of the open type except for the addition of a top glass cover, as shown in Fig. 17(b). As a result, the influences of weather conditions and ambient heat losses are significantly reduced. As depicted in Fig. 17(b), the vapour evaporated from the desiccant is condensed underneath the top glass cover. In a single-stage, the latent heat of condensation is wasted since it is rejected to the ambient air. To utilize the latent heat, a multi-stage design was proposed and found to be more efficient than the single-stage [24]. The condensate increases the vapour pressure of ambient air, which in turn decreases the performance of the closed type SC-LDEE [12]. The operation of the solar still is similar to that of the closed type SC-LDEE. Therefore, the research findings of the solar still can be used to design an efficient closed type SC-LDEE [24]. To employ the advantages of both open and closed types, Gadhidasan and Al-Farayedhi [82] proposed a partly closed type, which is shown in Fig.18.

7.1.4.3 Convective type SC-LDEE

The air is ventilated in the convective type SC-LDEE by providing openings at both ends, as shown in Fig.19. The ventilation can be natural or forced by an external device [83, 84]. In the naturally ventilated type, the length of the collector plate is limited by the randomness of the wind flow direction. This may create a stagnant air pocket in the desiccant film, which in turn reduces the performance [10]. Yang et al. [85, 86] proposed a double glass forced convective SC-LDEE, which was more efficient than that of other SC-LDEEs discussed so far.

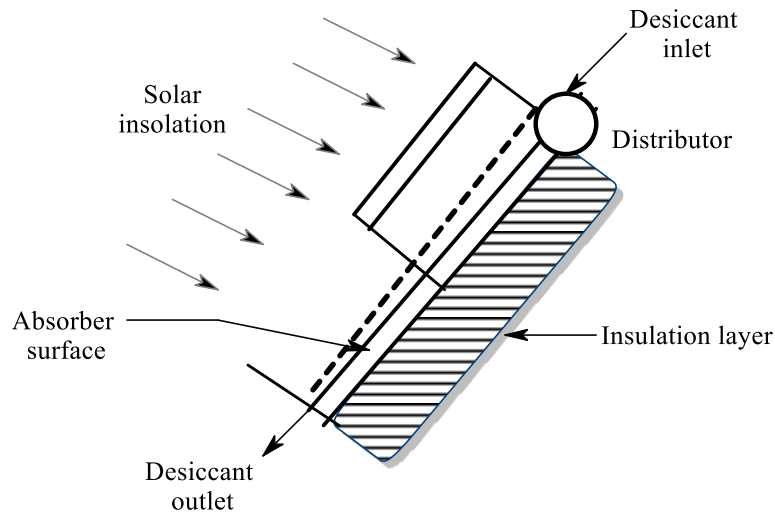


Fig.18: Schematic diagram of partly closed type SC-LDEE

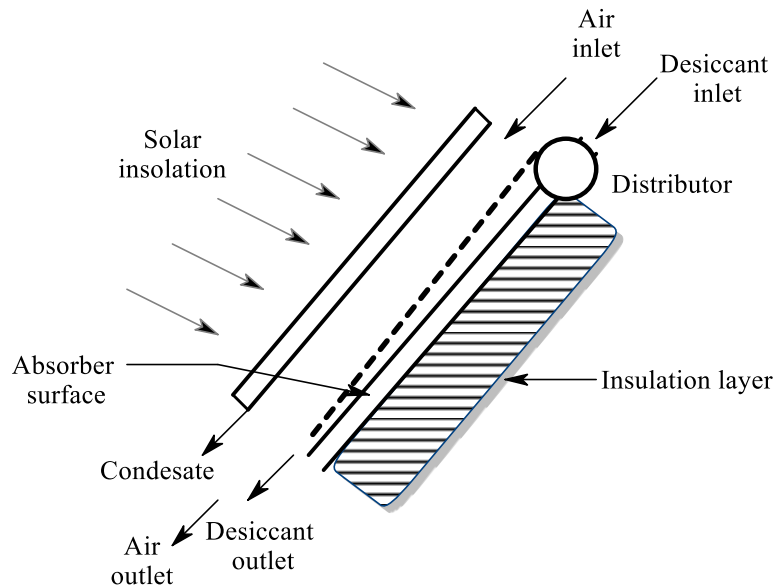


Fig.19: Schematic diagram of convective type SC-LDEE

7.1.5 Pressurized LDEE

The dehumidification of compressed air is essential in various applications such as pharmaceutical manufacturing, food production, electrolytic plant, clean-room, pneumatic system of aircraft, refinery, and plasma preparation [87, 88]. Yin et al. [89] proposed a liquid desiccant based compressed air dryer (pressurized LDEE) as an alternative to the conventional system, which is based on either condensation or solid desiccant type. Figure 20 shows the schematic of the compressed air-drying system with pressurized LDEE. The system has air and desiccant circuits. The sequential operations in the process air circuit are (i) the pressure of air

is increased by the compressor, (ii) the temperature of the air is reduced by the desiccant in the heat exchanger, (iii) air is further cooled down to its dew point temperature in the air cooler, and consequently, it is dehumidified initially, (iv) air is further dehumidified in the pressurized LDEE by the desiccant and (v) the pressure of air is reduced to atmospheric level by the throttling valve before it is exhausted. The pressurized LDEE was applied only for the dehumidification processes in the proposed system. The corresponding variations in the total and vapour pressures and specific humidity of the air in the proposed system are shown in Fig.21.

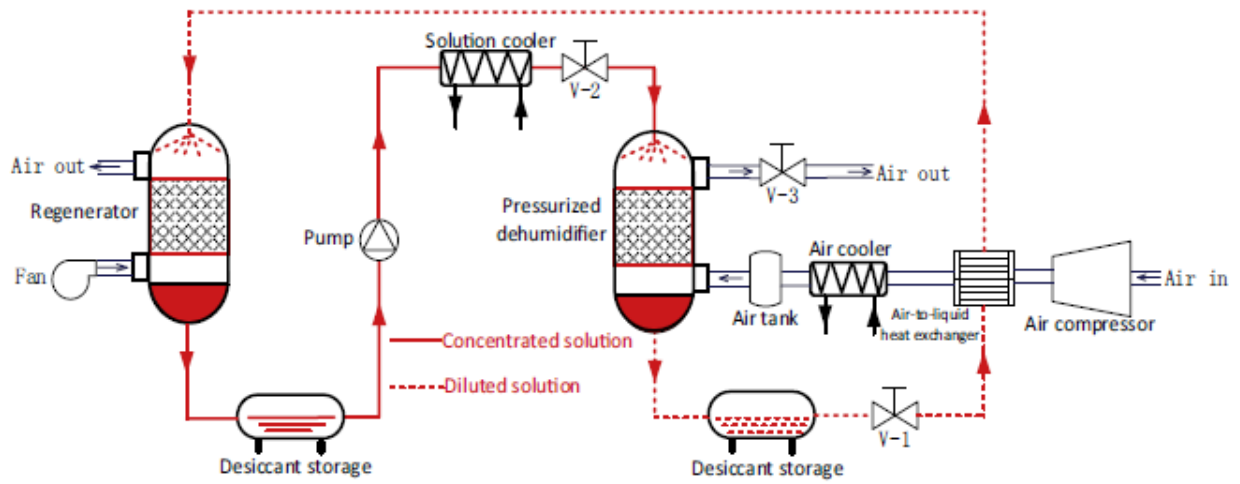


Fig.20: Schematic of pressurized LDEE based compressed air-drying system [89]

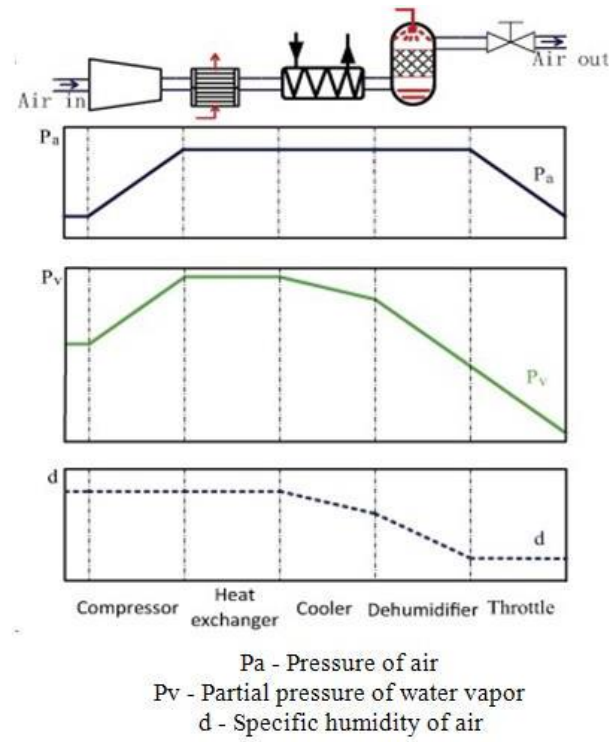


Fig.21: Schematic of variations in the air properties in the proposed system [89]

In contrast to the other types, the pressurized LDEE operates at a higher pressure. Therefore, the dehumidification performance of the pressurized LDEE is also better than that of the other types of LDEEs. Consequently, the air can be dried to a lower specific humidity ($<1 \text{ g}_w/\text{kg}_{da}$). In the proposed system (Fig.20), the air was dried up to $0.9 \text{ g}_w/\text{kg}_{da}$ at an operating pressure of 0.5 MPa. In addition, the effectiveness was around 0.9 for most of the operating conditions [89]. It is expected that the energy consumption of LDAS would increase due to the addition of the compressor. However, the increase in the moisture removal rate and internal desiccant heating by the hot compressed air can make the performance of LDAS with pressurized LDEE comparable to or better than that with other types of LDEEs.

7.1.6 Ultrasound based LDEE

The performance of the LDEE mainly depends on the contact area between the air and desiccant, as discussed earlier. Therefore, to improve the contact area, the desiccant is finely atomized ($\approx 50 \text{ }\mu\text{m}$ diameter) using a transducer in the ultrasound-based LDEE (U-LDEE), as shown in Fig.22. Even though ultrasound technology is now widely used in many applications, it was introduced to the LDEE only a decade ago by Wang et al. [90] in 2010. It is essential to design and operate the U-LDEE at the optimum desiccant droplet size to achieve maximum mass transfer performance [91].



Fig.22: Desiccant droplets generated in U-LDEE [92]

U-LDEE not only requires a lower desiccant flow rate (40-75%) and regeneration temperature (around 4.5°C) but also consumes less energy (60%) than PB-LDEE [91-93]. During the heat and mass transfer processes, the desiccant droplets can easily drift and adhere to the wall of U-LDEE. Then, the desiccant droplets group together and form a film on the wall. This reduces

the contact area between the air and desiccant and thereby deteriorates the performance of the U-LDEE [94]. To mitigate this issue, Yang et al. [90] proposed a design methodology to calculate the minimum height of the U-LDEE using the criterion “droplet suspension rate” which is defined as the ratio of the mass proportion of droplets that remain suspended (are not attached to the wall) to the entire droplets generated by the transducer during a specific period. An efficient design based on this design methodology can improve the effectiveness of the U-LDEE by 45% [90]. However, similar to spray tower LDEE, the possibility of desiccant carryover with the air is more predominant in U-LDEE due to fine droplets of desiccant [30].

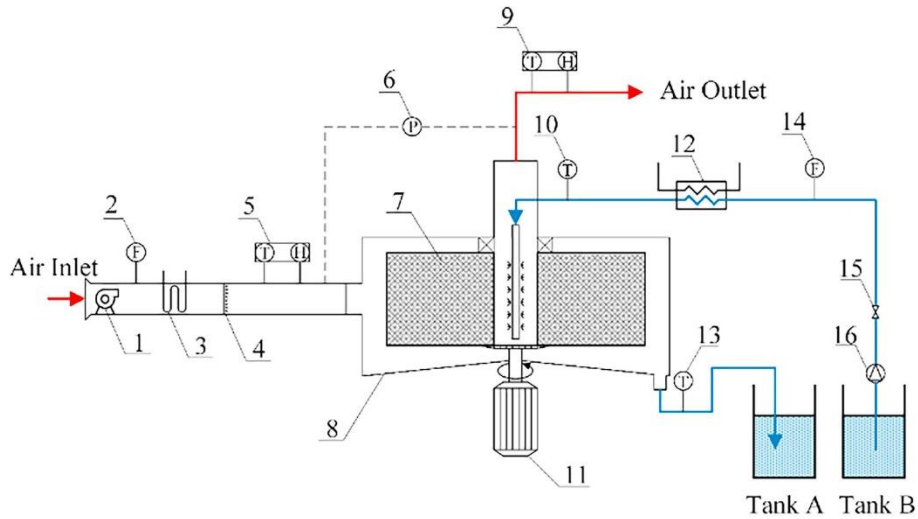
7.1.7 Hypergravity LDEE

The rotating packed bed system operates based on hypergravity technology. It employs a rotating packing to create a centrifugal force which is significantly stronger than that of the gravity force. The created centrifugal force enhances the heat and mass transfer coefficients of gas and liquid streams [95]. The rotating packed bed was introduced by Ramshaw and Mallinson [96] and is widely used in many applications such as absorption, stripping, adsorption, distillation, desorption, nanoparticles production and reactive crystallization [97-99]. Gu and Zhang [100] applied the rotating packed bed technology to LDEE, which is referred to as hypergravity LDEE (HG-LDEE). Due to the rotating packed bed, the desiccant is converted to thin films and fine droplets to improve the contact area in the HG-LDEE. Figure 23 shows the schematic of a testbed of HG-LDEE. The performance of the HG-LDEE is better than that of the PB-LDEE due to its increased contact area and intensive mixing of water vapour in the desiccant or air [100]. Moreover, HG-LDEE has a self-cleaning mechanism due to its rotation. Furthermore, the centrifugal force separates the desiccant droplet from the air stream, and hence, there is no desiccant carryover in the HG-LDEE [101]. A detailed CFD study for determining the thermal characteristics of the HG-LDEE was carried out by Saurabh and Murthy [101].

7.1.8 Vacuum LDEE

The regeneration temperature in the LDAS depends on the dehumidification load and effectiveness of the LDEE, and the availability of the cooling energy source [10]. It varies between 50-80°C for halide salt-based desiccants [102]. To reduce the regeneration temperature, Gao et al. [103] proposed a flash evaporation technique for the regeneration process in the LDEE. When the desiccant is introduced into vacuum conditions, the water component in the desiccant gets superheated and consequently evaporates at a lower

temperature. This is similar to flash evaporation in ice making, seawater desalination, biopharmaceuticals, etc. [103]. Figure 24 shows the schematic of the LDEE with flash evaporation technology, which is referred to as vacuum LDEE (V-LDEE) [104]. Similar to SC-LDEE, V-LDEE is only used for the regeneration process in LDAS. As shown in Fig.24, the desiccant is heated in the generator section using the heating source at vacuum pressure. Consequently, the water is evaporates from the desiccant and condenses in the condenser section using the cooling source.



Schematic diagram of the rotating packed bed (RPB) dehumidifier for liquid desiccant. Components: (1)Fan; (2)Airflow meter;(3)Heat Exchanger;(4)Humidifier; (5)Integrated temperature and humidity sensor; (6)Differential pressure gauge; (7)RPB; (8)RPB shell; (9)Integrated temperature and humidity sensor; (10)PT100; (11)Motor; (12)Heat Exchanger; (13)PT100; (14)Liquid flow meter; (15)Valve; (16)Pump.

Fig.23: Schematic of a test bed of HG-LDEE [100]

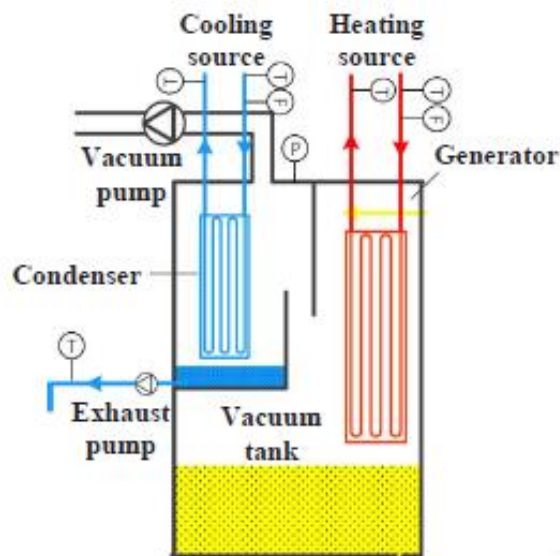


Fig.24: Schematic of V-LDEE [104]

Figure 25 shows the regeneration temperature of LiBr desiccant at vacuum pressure. Due to the low regeneration temperature, V-LDEE reduces the energy consumption of the LDAS by 40%. In addition, V-LDEE improves the potential of the LDAS to utilize low-grade energy sources [102]. Moreover, the problem of desiccant carryover is avoided in the V-LDEE as there is no requirement of regenerative air. Table-7 shows the differences between PB-LDEE and V-LDEE [102].

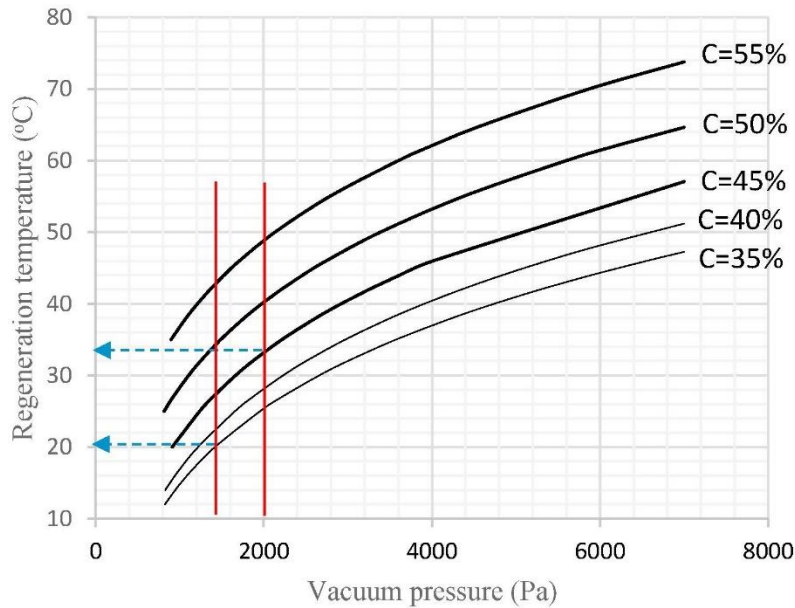


Fig.25: Regeneration temperature of LiBr desiccant at vacuum pressure [102]

Table-7: Comparison between PB-LDEE and V-LDEE [102]

PB-LDEE	V-LDEE
Works at atmospheric pressure	Works at vacuum pressure
Requires regenerative air to remove water vapour	No need of regenerative air
Mass transfer due to vapour pressure difference	Boiling of water vapour due to vacuum pressure
Regeneration can increase only by increasing the temperature of hot source	Regeneration can increase by increasing temperature of the hot source or reducing the vacuum pressure
Fan is required	Vacuum pump is required

7.1.9 Bubble absorption LDEE

Kabeel [105] introduced the bubble absorption technique for the LDEE. The air was injected into the liquid desiccant storage tank instead of being passed over the surface of the flowing desiccant, as shown in Fig.26. The mass transfer performance of bubble absorption LDEE (BA-LDEE) is better than that of the PB-LDEE. It was found that the dehumidification and

regeneration effectiveness of the BA-LDEE were 0.87 and 0.92, respectively [105]. An investigation by Saikiran and Benny [106] revealed that the mass transfer performance was independent of bubble size. The bubble absorption technology is well established in the closed sorption system as an alternative to the falling film type. Therefore, the performance enhancement techniques of bubble absorption developed so far in such an application can be utilized while designing a BA-LDEE for LDAS. Figure 27 summarizes such enhancement techniques [107]. Table-8 compares the characteristics of falling film and bubble type absorption processes [107].

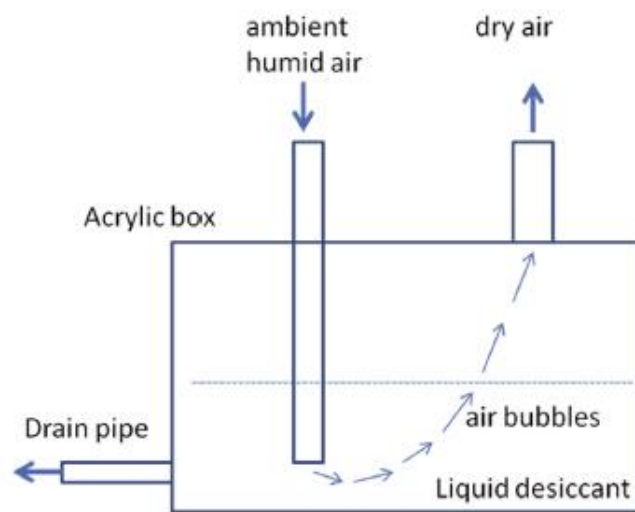


Fig.26: Schematic of BA-LDEE [106]

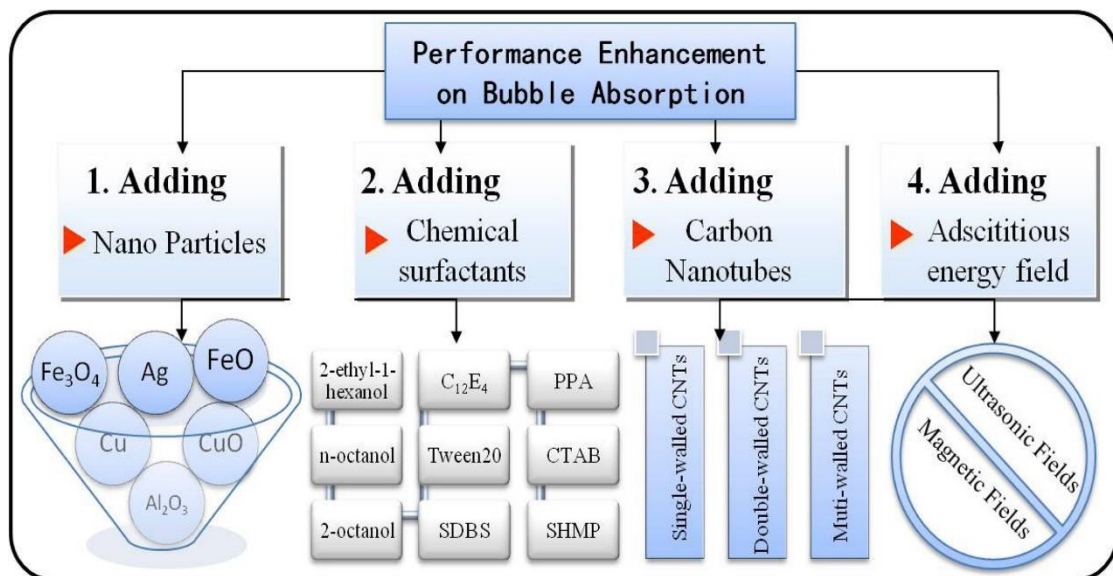


Fig.27: Summary of performance enhancement techniques for bubble absorption [107]

Table-8: Comparison between falling film and bubble absorption processes [107]

Characteristics	Falling film absorption	Bubble absorption
Distributor	Needs liquid distributor	Needs vapour distributor
Flow regime	Separated two-phase flow	Non-separated two-phase flow
Interface and mixing	Poor	Good
Wettability	Has wettability issues	Good wettability
Heat transfer coefficient	High heat transfer coefficient and stability	Low heat transfer coefficient
Increase in the gas flow rate	Improves the performance	Deteriorates the performance

7.2 Indirect contact LDEE

Most of the direct contact LDEEs restrict the application of LDAS in various residential and industrial sectors due to its desiccant carryover problems [5]. To mitigate this issue, indirect contact LDEEs have recently been developed with the aid of membrane-based technologies. The developments in various types of indirect contact LDEEs are discussed as follows.

7.2.1 Membrane-based LDEE

In the membrane-based LDEE, there is an intermediate membrane between the air and desiccant to avoid direct contact. It is commonly referred to as LAMEE (liquid to air membrane energy exchanger) [48]. The membrane is selected in such a way that it allows only the water vapour to pass through but not the desiccant [108]. Therefore, the desiccant carryover issues are avoided in the LAMEE. Moreover, the pressure drop of air and transient response delay time in LAMEE are lesser than those of the PB-LDEE [7]. The performance of the LAMEE significantly depends on the properties of the intermediate membrane. Ideally, the membrane should have high liquid penetration pressure for desiccants, modulus of elasticity, porosity, selectivity, temperature and chemical stability, durability and fouling resistance [109]. On the other hand, the membrane should have low water vapour diffusion resistance, tortuosity factor and be less expensive [109]. Among the desired properties, the permeability and selectivity of the membrane play significant roles in the performance of the LAMEE. The membranes are mostly made up of polymer-based organic materials [110]. Ideally, the membrane in the LAMEE should be permeable only to water vapour. However, the other components of air, particularly nitrogen, can also diffuse through the membrane. The selectivity of water vapour with respect to nitrogen for various polymeric membranes was summarized by Metz et al. [111] and is shown in Fig. 28.

The selectivity of the membrane with respect to volatile organic compounds also plays a significant role in terms of indoor air quality (IAQ). This has been improved by coating techniques [110]. The silver cation coating on the membrane can improve IAQ by preventing airborne bacterial microorganisms [112]. In most simple membranes, the permeability and selectivity are incompatible with each other. Composite membranes can mitigate such incompatibility, and hence, such membranes are now utilized in LAMEE. The additional support layer increases the mechanical strength of the composite membrane [110]. According to the configuration, LAMEE can be broadly classified as flat plate and hollow fiber types [11], which are discussed below.

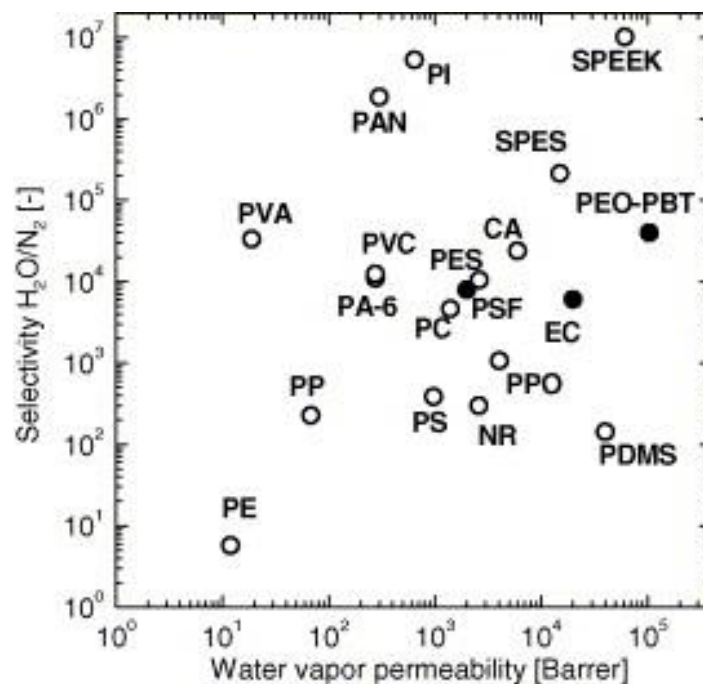


Fig.28: Water vapour permeability and water vapour/N₂ selectivity for various polymers at 30°C [111]

7.2.1.1 Flat plate LAMEE

The configuration of the flat plate LAMEE is similar to that of the plate heat exchanger, as shown in Fig.29 (a). However, instead of plates, flat membranes are used to separate the air and desiccant channels. The flat plate type is simpler to construct and has a lesser pressure drop of air than the hollow fiber type [110]. In addition to operating conditions and membrane properties, the performance of the flat plate LAMEE depends on the spacing of air and desiccant channels. The decrease in the flow spacing increases the performance as well as the pressure drop. Therefore, the optimum air and desiccant channel gaps are 5-6 mm and 1-2 mm, respectively [113]. The membrane in the LAMEE can deflect from its position due to the

pressure difference between the air and desiccant streams. Such membrane deflection not only decreases the performance but also increases the pressure drop of air. This can be mitigated by using a membrane with high elastic modulus, pre-stressed membrane, support grid and insert, and membrane support layer [114, 115]. The inserts (i.e., air screen) are mostly placed on the airside, and thus, they disturb the airflow in the LAMEE. This, in turn, increases not only the convective coefficient but also the pressure drop of air. It was reported that the insert could improve the airside Nusselt number from 8.4 to 11.2 (at $Re=620$), which in turn increases the sensible, latent and total effectiveness by 4% [22].

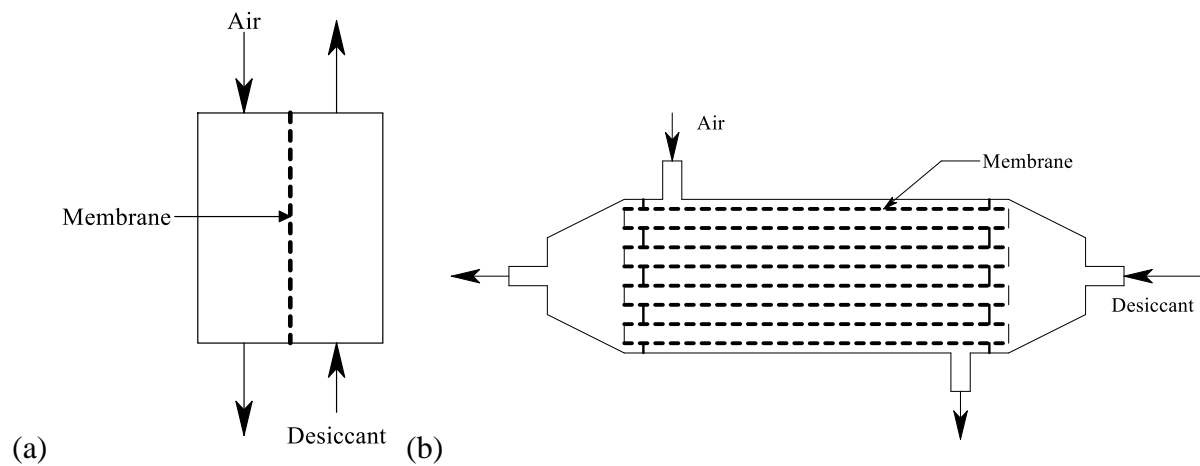


Fig.29: Schematic of (a) flat plate and (b) hollow fiber LAMEEs

7.2.1.2 Hollow fiber LAMEE

The schematic of the hollow fiber LAMEE is analogous to that of shell and tube heat exchanger, as shown in Fig.29 (b). However, the tubes are made up of membranes. Mostly, the desiccant flows in the tube, and air flows over the tubes [116]. The packing density of the hollow fiber type is higher than that of flat plate type [30]. The heat and mass transfer performance and the pressure drop of the staggered arrangement are higher than those of the inline arrangement of membrane tubes [117]. When compared to straight tubes, the curved tubes increase not only the performance but also the pressure drop of air [118]. Compared to single-channel hollow fiber, the multi-channel design has a higher contact area per unit volume and shear strength in both radial and axial directions [119]. To utilize these advantages, Bettahalli et al. [120] introduced a triple bore (a multi-channel design) hollow fiber LAMEE for the dehumidification process.

The intermediate membrane between the air and desiccant not only avoids the desiccant carryover but also increases the heat and mass transfer resistances of LAMEE. Ge et al. [109]

found that the mass transfer performance of PB-LDEE was 16% higher than that of LAMEE under the same contact area, whereas LAMEE showed 13–20% better performance than PB-LDEE under equal pressure drop conditions. It is expected that the pore of the membrane may be wetted by the desiccant, which can lead to leakage of desiccant into the airside after a long period of operation [30]. Moreover, the desiccant flow distribution in the membrane tubes of hollow fiber type [121] and channels of flat plate type is critical, as it can significantly influence the heat and mass transfer performance of the LAMEE [30].

The intermediate membrane increases the heat and mass transfer resistances of LAMEE, as mentioned earlier. This is majorly because of the boundary layer at the membrane-air interface. It is possible to reduce the resistance of the membrane by breaking the boundary layer. Hence, Gurubalan et al. [122] investigated the influence of ultrasound (which can break the boundary layer by its vibration) on the mass transfer performance of LAMEE. It was found that the vibration due to ultrasound enhances the performance of LAMEE by 1.5 times.

7.2.2 Electrodialysis based LDEE

The thermal energy requirement of the LDAS to regenerate its desiccant is quite large [30]. Moreover, in most cases, the regeneration process depends on the availability of low-grade energy sources, which in turn depends on weather conditions or industrial processes. The energy-saving potential of the LDAS is comparatively higher in hot and humid climatic conditions. On the other hand, the high humid regenerative air increases the regeneration temperature of desiccant, which decreases COP of the LDAS [123]. To mitigate this, a new type of regeneration process was developed based on electrodialysis technology, which works on electrical energy instead of thermal energy. Thus, this technology reduces the dependence of LDAS on low-grade energy sources [30].

The electrodialysis method works based on the transport of ions through selective membranes under the influence of an electrical field [124]. This method has been widely used in applications such as desalination, purification, effluent treatment, recycling of industrial process streams and salt production [123]. Li and Zhang [123] introduced this method in 2009 to regenerate the liquid desiccant. Electro-osmosis, osmosis, ion migration and diffusion are the four major mass transfer mechanisms in the electrodialysis assisted LDEE (E-LDEE). Electro-osmosis and osmosis are responsible for water transport, whereas the ion migration and diffusion govern transport of the ions through the membrane [125]. The schematic of the E-LDEE is shown in Fig.30. Similar to SC-LDEE, E-LDEE is only used for the regeneration

process. As shown in Fig.30, the cation and anion exchange membranes are placed alternatively between the cathode and anode in each stack [126].

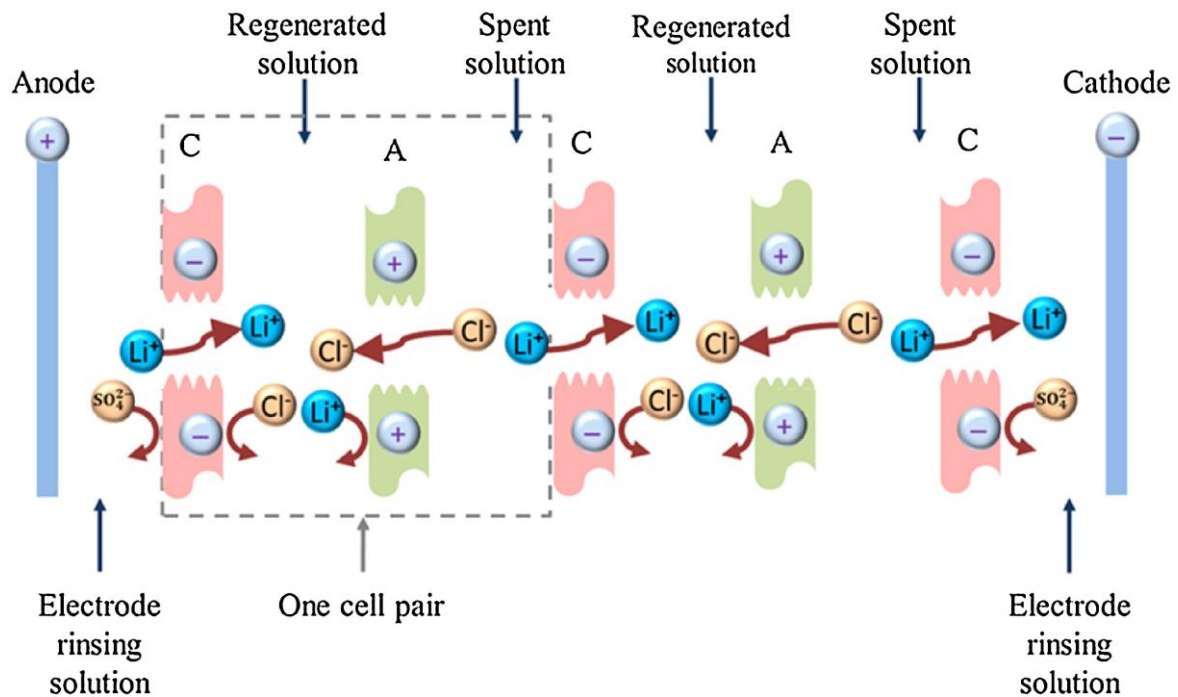


Fig.30: Schematic of E-LDEE for LiCl regeneration with Li_2SO_4 as rinsing solution [126]

When an electrolyte solution passes through the cell and potential difference is applied between electrodes, the cations move towards the cathode through the cation exchange membrane, whereas anions move towards the anode through the anion exchange membrane. The cations and anions cannot migrate through the anion and cation exchange membranes, respectively. This movement concentrates and dilutes the desiccant in the concentrate and dilute cells, respectively [123]. Since there is no requirement of regenerative air, the desiccant carryover is avoided in the E-LDEE. Li and Zhang [123] compared the performance of the E-LDEE and SC-LDEE. The performance of the former was low due to the low efficiency of the solar photovoltaic panels ($\approx 10\%$). Besides, the optimum concentration range of commonly used desiccants in E-LDEE is much lower when compared to its working concentration [30]. Therefore, more research must be done on E-LDEE to enable its application in the LDAS.

7.2.3 Reverse osmosis LDEE

Osmosis is a process in which the solvent is transported through the membrane due to the difference in trans-membrane concentration [127]. In contrast, pressure is applied to transfer the solvent in the reverse osmosis (RO) processes, as shown in Fig.31 [128]. RO process is extensively used in the application of seawater desalination [129]. Al-Farayedhi [127]

introduced the RO process for desiccant regeneration. When high pressure is applied to the diluted desiccant, the water molecules from the high-pressure side (desiccant side) migrate towards the low-pressure side (water side) through the semipermeable membrane. Consequently, the concentration of the desiccant increases since the salt ions cannot be transferred through the membrane. Unlike RO process in desalination, the membrane for the desiccant regeneration in RO based LDEE (RO-LDEE) should have high salt rejection with acceptable water permeability [128].

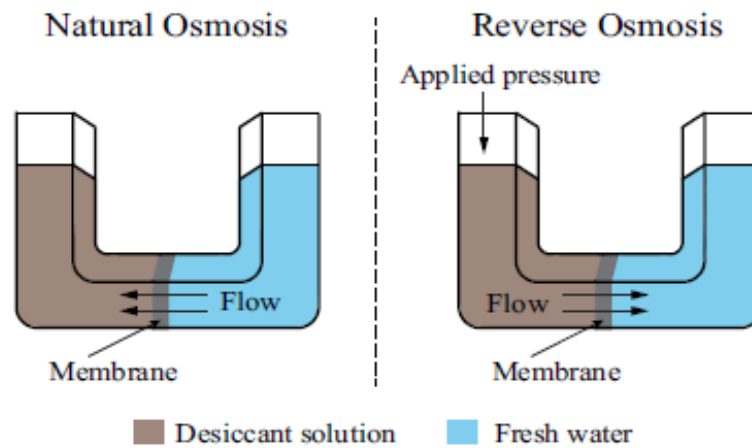


Fig.31: Schematic of natural osmosis and RO processes [128]

To improve the salt rejection, several techniques have been employed for RO membranes such as fabrication of membrane with fluorinated silica nanoparticles [130] and heat treatment [131]. The membranes modified with these techniques are more suitable for RO-LDEE. The operating pressure of the RO-LDEE is significantly higher than that of RO processes in desalination. For example, LiCl desiccant's osmotic pressure at 25% concentration is around 180 bar [127]. Such a high-pressure requirement restricts the application of the RO-LDEE. An osmotically assisted RO (ORO) process is an alternative option to the conventional RO processes to reduce the osmotic pressure in desalination applications [132]. Figure 32 shows the ORO process for regenerating liquid desiccant [128]. However, ORO process has not been studied so far for desiccant regeneration.

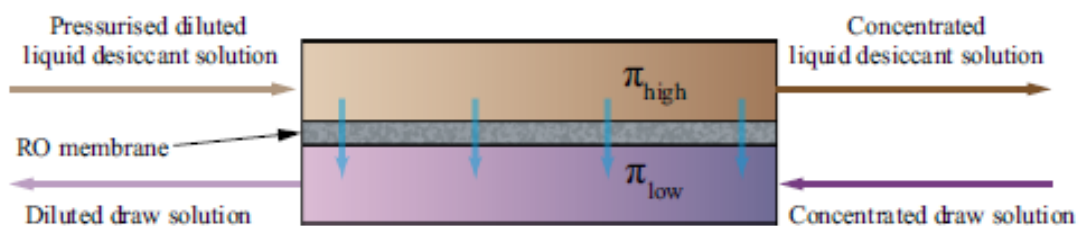


Fig.32: Schematic of ORO process [128]

7.2.4 Membrane distillation LDEE

Membrane distillation (MD) is a hybrid separation process based on thermal distillation and membrane separation [128, 132]. Unlike RO process, the water is hydraulically separated from the desiccant in MD process. In addition, MD process is independent of the osmotic pressure of desiccant [128]. The thermal energy requirement for MD process can be obtained from low-grade energy sources. The water vapor pressure difference across the membrane is the driving force for the regeneration process in MD based LDEE (MD-LDEE). Various configurations of MD-LDEE are shown in Fig.33.

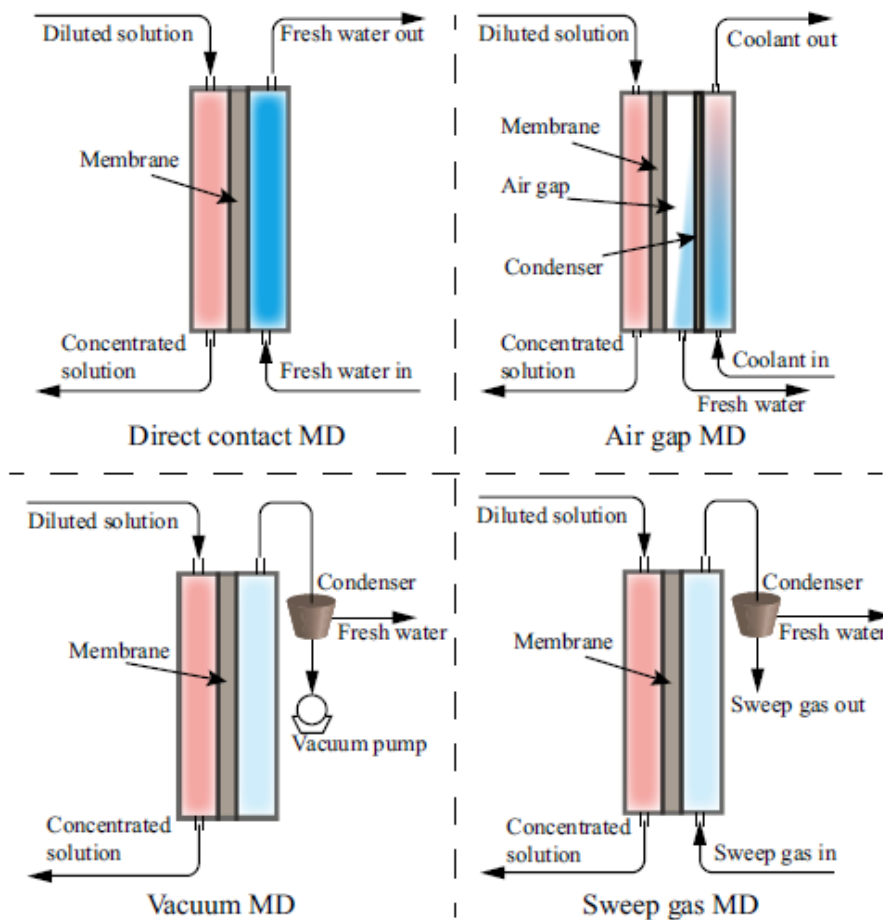


Fig.33: Schematic of various MD-LDEE configurations [128]

The low-temperature freshwater condenses the water vapour from the desiccant, and consequently, the desiccant is concentrated in direct contact type, as shown in Fig.33. However, the heat transfer between the water and desiccant through the membrane reduces the thermal efficiency of the MD-LDEE. Thus, an alternative design with an air gap between the coolant and desiccant was proposed. Even though the air gap decreased the heat transfer between the coolant and desiccant, it increased the resistance for the water vapour transfer. Consequently,

the vacuum and sweep gas-assisted configurations were developed to improve both the thermal efficiency and water vapour transfer rate [128]. However, they require an additional vacuum pump and fan, which increases the energy consumption of the LDAS. MD-LDEEs with direct contact and vacuum type configurations have mostly been used so far [134-136]. The performance comparison study by Zhou et al. [134] proved that the regeneration rate of the MD-LDEE is 4.5-6 times higher than that of the conventional PB-LDEE. The study also found that the vacuum assisted MD-LDEE can reduce the energy consumption of the LDAS by 10-37% [135]. The temperature and concentration polarizations are the inherent problems of the MD-LDEE [137, 138].

7.3 Number of streams

According to the number of streams, LDEEs are broadly classified as two, three and four fluid types, as shown in Fig.8. As the name indicates, the heat and mass transfer processes occur only between the desiccant and air in the two-fluid type, which is also referred to as adiabatic type (A-LDEE). The schematic of the A-LDEE for the dehumidification and regeneration processes is shown in Fig.34 (a) and (b), respectively. The heat of absorption generated during the dehumidification process raises the temperature of both air and desiccant which progressively declines the heat and mass transfer potentials of the A-LDEE. On the other hand, during the regeneration process, the heat transfer process between air and desiccant reduces the temperature of the desiccant. This, in turn, gradually reduces the mass transfer potential of A-LDEE. To mitigate the issue of the decrease in the potentials in both dehumidification and regeneration processes, A-LDEE is always designed with a higher contact area and higher desiccant flow rate. The latter increases the operating cost of LDAS and the probability of desiccant carryover in the A-LDEE [8, 46].

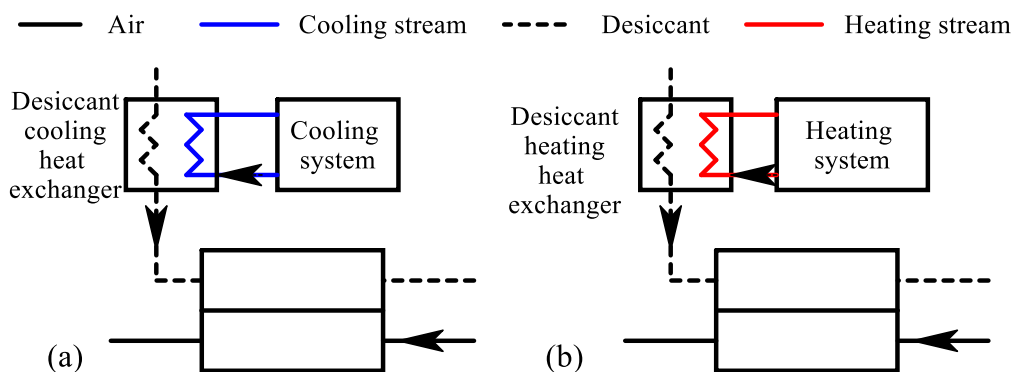


Fig.34: Schematic of A-LDEE for (a) dehumidification and (b) regeneration processes

The three-fluid type is also referred to as internally cooled or heated type (I-LDEE) since it has an additional hot or cold stream, as shown in Fig.35. The inlet temperature of the third fluid is lower and higher than that of the desiccant for the dehumidification and regeneration processes, respectively. During the dehumidification process, the additional cooling stream removes the heat of absorption, which maintains higher heat and mass transfer potentials in the I-LDEE. Similarly, during the regeneration process, the additional heating stream increases the temperature of the desiccant, which maintains higher heat and mass transfer potentials in the I-LDEE. PB-LDEE is the most researched ADLEE owing to its high heat and mass transfer performance. However, it is not suitable for the I-LDEE due to (i) difficulty in inserting the cooling or heating coil without damaging the fills and (ii) comparatively low contact area between the heating or cooling stream and desiccant [139]. Thus, most of the earlier works on direct contact I-LDEE were focused on the falling film type. The established heat exchanger configurations, namely pallet plate, plate-fin and tube-fin types, are widely used for falling film based I-LDEE [139]. In such types, the heating or cooling stream can be provided either in a separate channel, which is adjacent to the desiccant channel or in a tube placed in the desiccant channel [140, 141]. Liu et al. [139] compared the dehumidification performance of packed bed, parallel plate and tube-fin type I-LDEEs. The results revealed that the performance of tube-fin and packed bed was best and least among the selected configurations, respectively. To mitigate the corrosive issues of desiccant, Liu et al. [142] proposed a tube-fin type I-LDEE made up of the thermally conductive plastic material “polypropylene”. The proposed material was more conductive than conventional plastic material. The volumetric mass transfer coefficient for the dehumidification process in the proposed I-LDEE was comparable with that of I-LDEE made of copper or aluminium.

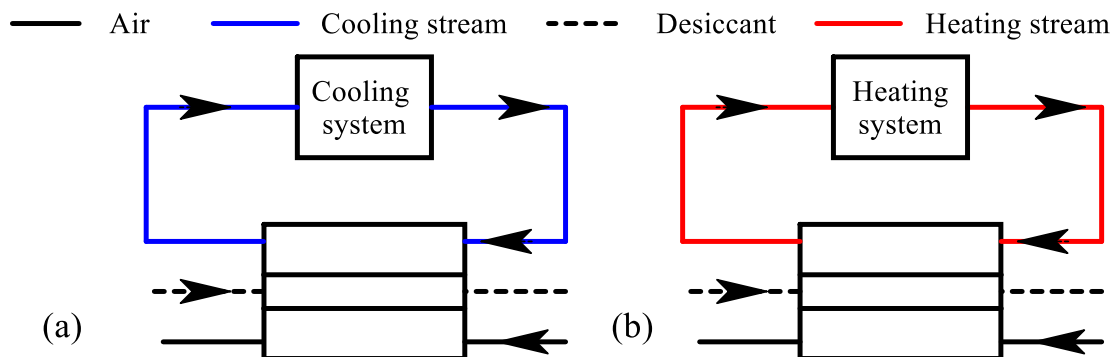


Fig.35: Schematic of I-LDEE for (a) dehumidification and (b) regeneration processes

The indirect contact LDEE was recently developed to mitigate the desiccant carryover issues. Therefore, there are limited studies on I-LDEE based on indirect contact type when compared to the direct contact type. Isetti et al. [108] introduced a hollow fiber type internally cooled LAMEE (I-LAMEE). Later, Abdel Salam et al. [50, 143] extensively studied the performance of flat plate type I-LAMEE for both dehumidification and regeneration processes. As expected, the performance of I-LAMEE was higher than that of adiabatic LAMEE (A-LAMEE).

Most of the earlier comparisons considered the same desiccant inlet temperature for both A-LDEE and I-LDEE. However, under actual field operating conditions, the desiccant is pre-cooled in a heat exchanger for the dehumidification process in the A-LDEE (Fig.34 (a)). In contrast, it is simultaneously cooled in the I-LDEE, as shown in Fig.35 (a). Therefore, the inlet temperature of desiccant in the A-LDEE is lower than that of I-LDEE for the dehumidification process. This operating condition was considered for the performance comparison of A-LAMEE and I-LAMEE by Gurubalan et al. [144]. Even with a higher desiccant inlet temperature, I-LAMEE outperforms A-LAMEE. Further, the study concluded the same result with a comparison considering an equal heat transfer area between the cooling water and desiccant. To achieve complete air conditioning, the temperature of the air is controlled using desiccant through the membrane in the I-LAMEE. This is not an energy-efficient process due to the low thermal conductivity of membrane and desiccant (when compared to water). To alleviate this issue, Gurubalan et al. [21] proposed a new arrangement for I-LAMEE in which separate cooling streams are provided for both air and desiccant, as shown in Fig.36. In the proposed arrangement, the humidity and temperature of air are controlled by desiccant and cooling water, respectively.

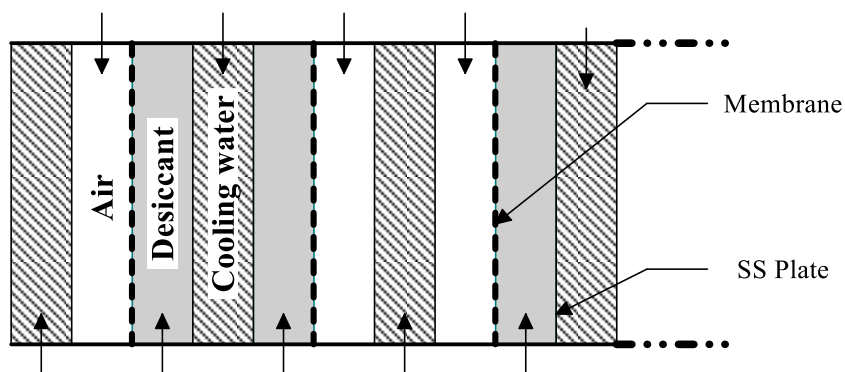


Fig.36: Schematic of I-LAMEE with separate cooling streams for both air and desiccant [21]

The I-LDEE types discussed so far utilize an additional stream for the simultaneous cooling or heating of the desiccant to improve their performance. However, Lun et al. [145] proposed a self-cooled desiccant for the I-LDEE. The author proposed a blend of LiCl and ethanol as a

mixed desiccant. During the dehumidification process, the ethanol evaporates by absorbing the heat of absorption. This maintains a lower desiccant temperature, and therefore improves the heat and mass transfer potentials in the I-LDEE. However, the diffusion of ethanol into the air is unacceptable in the view of IAQ. I-LDEE requires a lesser desiccant flow rate than A-LDEE due to its high heat and mass transfer potentials. This reduces the initial and operating costs of the LDAS. In addition, the probability of desiccant carryover is low in I-LDEE when compared to A-LDEE [109]. To summarize, the advantages of I-LDEE over the A-LDEE are (i) higher mass transfer performance (ii) lower operating (i.e., desiccant pumping) cost (iii) required lesser mass flow rate of desiccant for the given dehumidification load (iv) lesser desiccant storage (v) lesser probability of desiccant carryover and (vi) smaller size [146-148].

The four fluid LDEE is a modified I-LDEE (MI-LDEE) (Fig.37) and has so far been utilized only for the dehumidification process [149]. An additional secondary air stream is provided in the MI-LDEE to maintain the temperature of cooling water by evaporative cooling. It can be drawn separately from the ambient or bypassed from the conditioned air, as shown in Fig.38 [150].

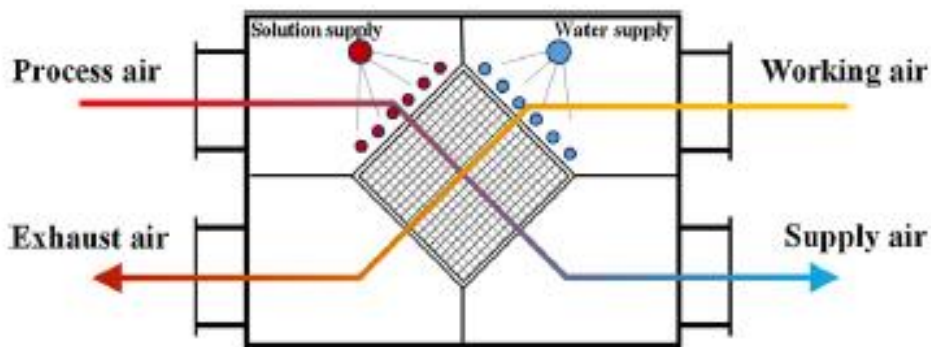
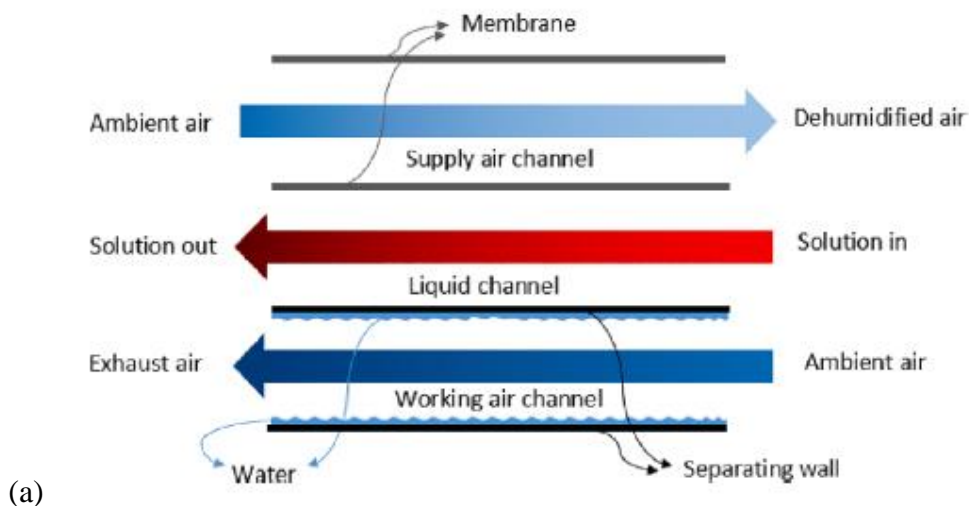


Fig.37: Schematic of MI-LDEE [112]



(a)

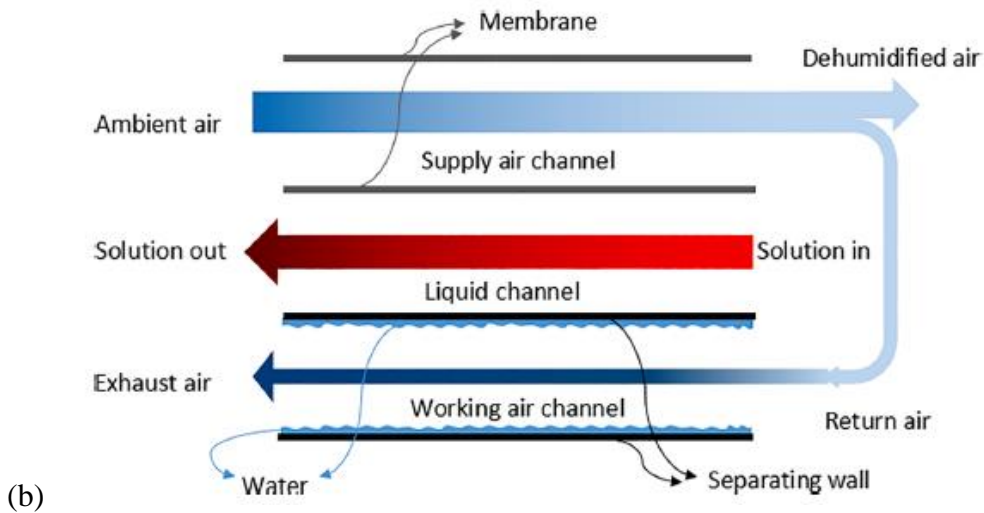


Fig.38: Schematic of MI-LDEE with (a) separate secondary air and (b) bypassed primary air [150]

7.4. Number of stages

The desiccant is pre-cooled in the A-LDEE, whereas it is simultaneously cooled in the I-LDEE for the dehumidification process, as discussed earlier. However, the increase in the desiccant temperature is inevitable in both A-LDEE and I-LDEE due to the heat of absorption released during the dehumidification process. The temperature rise of desiccant reduces the heat and mass transfer potentials in LDEEs. To mitigate this issue, the concept of multistage (Fig.39) is introduced. As shown in Fig.39, the desiccant is cooled separately in each stage. The irreversible losses in the multistage LDEE are lesser than that of single-stage LDEE because of maintaining a moderate mass transfer potential in each stage [12]. Consequently, the multistage design improves the performance of the LDAS. Kumar et al. [151] found that COP of LDAS with two and three-stage LDEEs was 67% and 116% higher than the single-stage, respectively. Even though the total mass flow rate of desiccant in multistage is higher than that of single-stage, the flow rate in each stage is low. Therefore, attention must be given to the distribution of desiccant in the multistage LDEE [12]. Similar to the dehumidification process, the regeneration process in the LDEE can be improved by introducing stages. Lowenstein et al. [152] presented a multi-effect LDEE (Fig.40) for the regeneration process. The working principle of such a LDEE and generator in the double-effect absorption refrigeration system is almost similar and independent of conditions of ambient air.

In general, the performance of the E-LDEE is lesser than that of the PB-LDEE [123]. Therefore, to improve the performance, Li et al. [153] studied the effect of staging in E-LDEE. It was numerically found that the two-stage E-LDEE could save more than 70% energy compared to

the single-stage E-LDEE. For higher solution concentration, the regeneration performance of MD-LDEE is significantly low even at a higher hot source temperature. To mitigate this, Datta et al. [154] presented a novel multi-stage configuration (Fig.41) to improve the performance of the MD-LDEE. Similarly, Chen et al. [155] developed an optimized multi-stage design (Fig.42) for the vacuum assisted MD-LDEE. It was numerically found that the energy consumption of the proposed MD-LDEE was 40-50% and 10-16% lesser than that of single-stage PB-LDEE and MD-LDEE, respectively. Most of the earlier work on multi-stage configurations was focussed on the A-LDEE. Recently, Cheng et al. [156] analyzed the effect of staging on the I-LDEE (Fig.43). It was found that the dehumidification efficiency of multi-stage I-LDEE was 7.3% higher than that of single-stage I-LDEE. Moreover, the optimum number of stages increased with an increase in the mass flow rate of air.

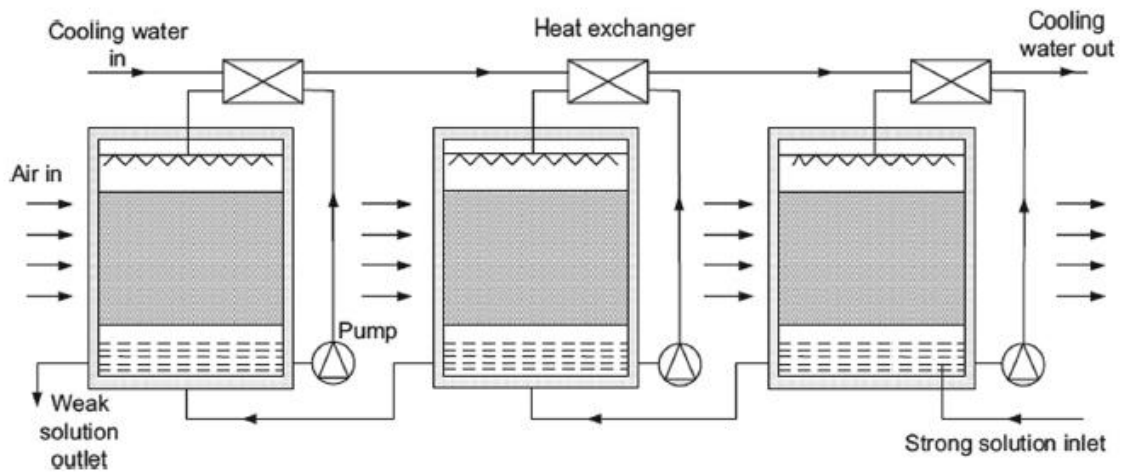


Fig.39: Schematic of multistage LDEE for dehumidification process [12]

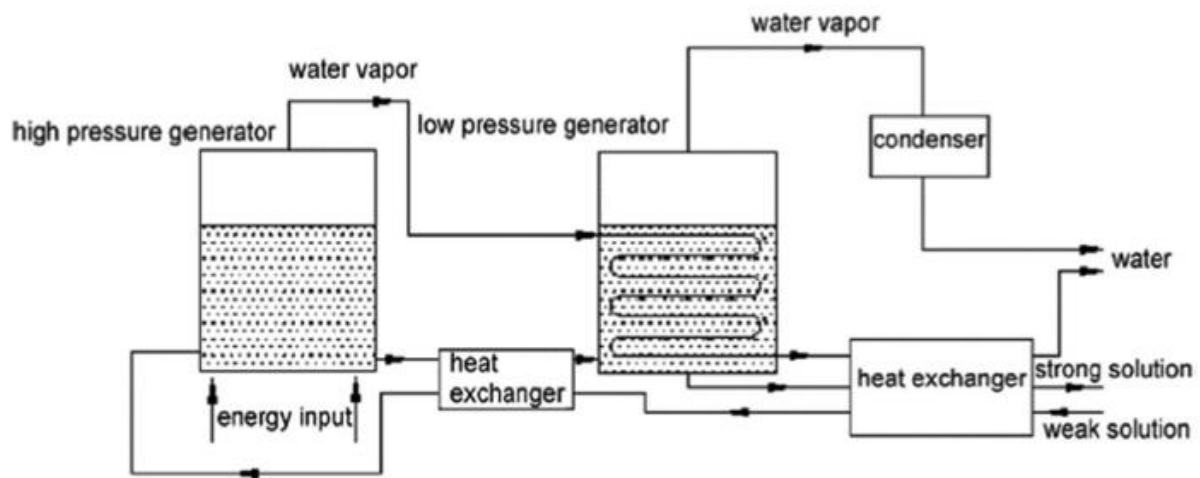


Fig.40: Schematic of multistage LDEE for regeneration process [152]

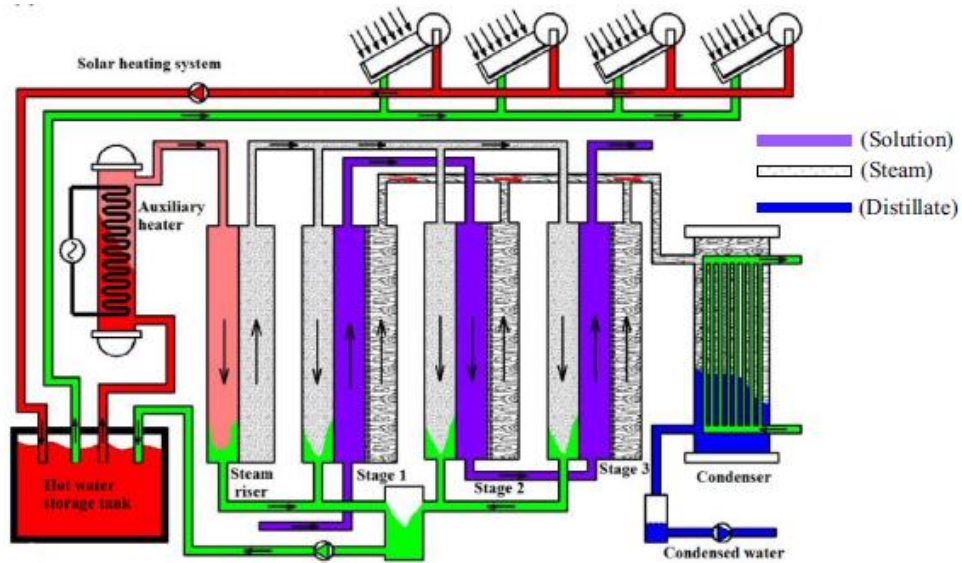


Fig.41: Schematic of multistage MD-LDEE for regeneration process [154]

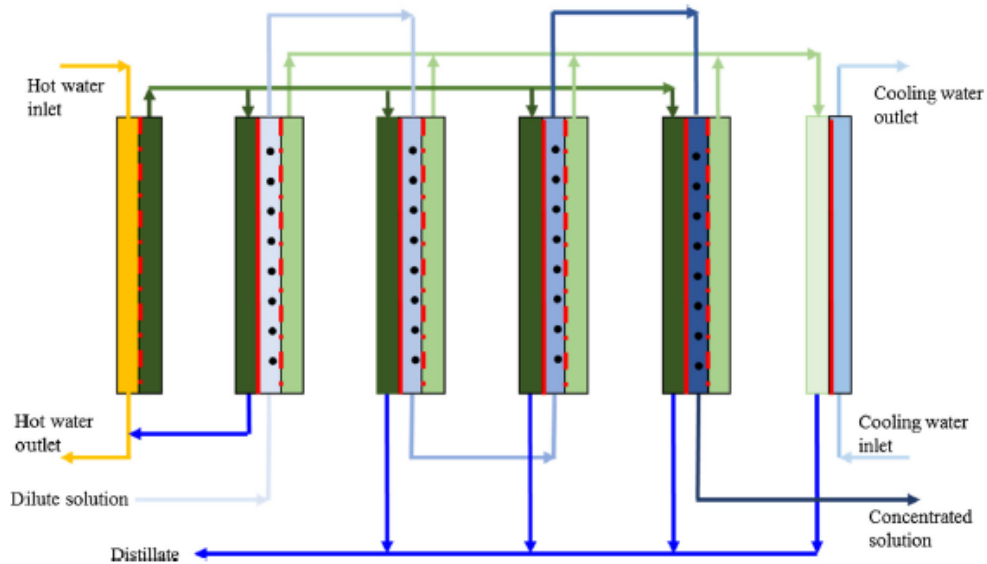


Fig.42: Schematic of the multistage vacuum-assisted MD-LDEE for regeneration process [155]

Xiong et al. [157, 158] proposed a LDAS with two-stage LDEE for both dehumidification and regeneration processes. In contrast to the conventional multi-stage LDEE, the air is dehumidified using CaCl_2 and LiBr in the first and second stages, respectively. As expected, COP of multistage LDAS was higher than that of single-stage LDAS. Also, employing different desiccants in each stage improved the energy storage capacity and reduced the initial cost of the LDAS. To minimize the effect of corrosion by the liquid desiccant, Zhang et al. [159] proposed an innovative multistage LDAS in which air was heated or cooled (instead of desiccant) between the stages, as shown in Fig.44.

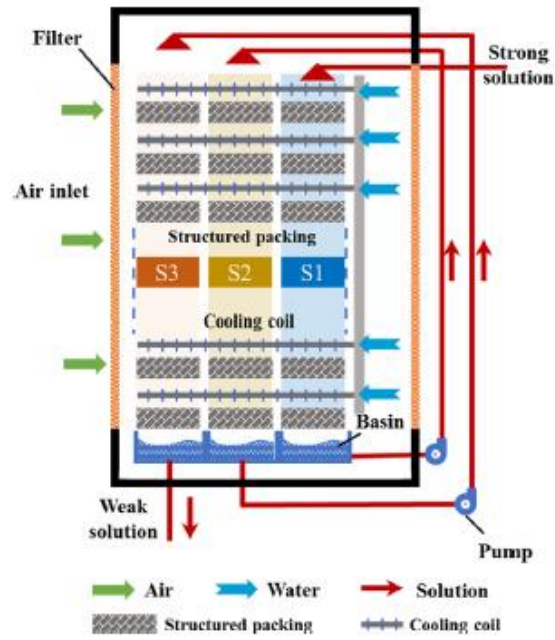


Fig.43: Schematic of multistage I-LDEE for dehumidification process [156]

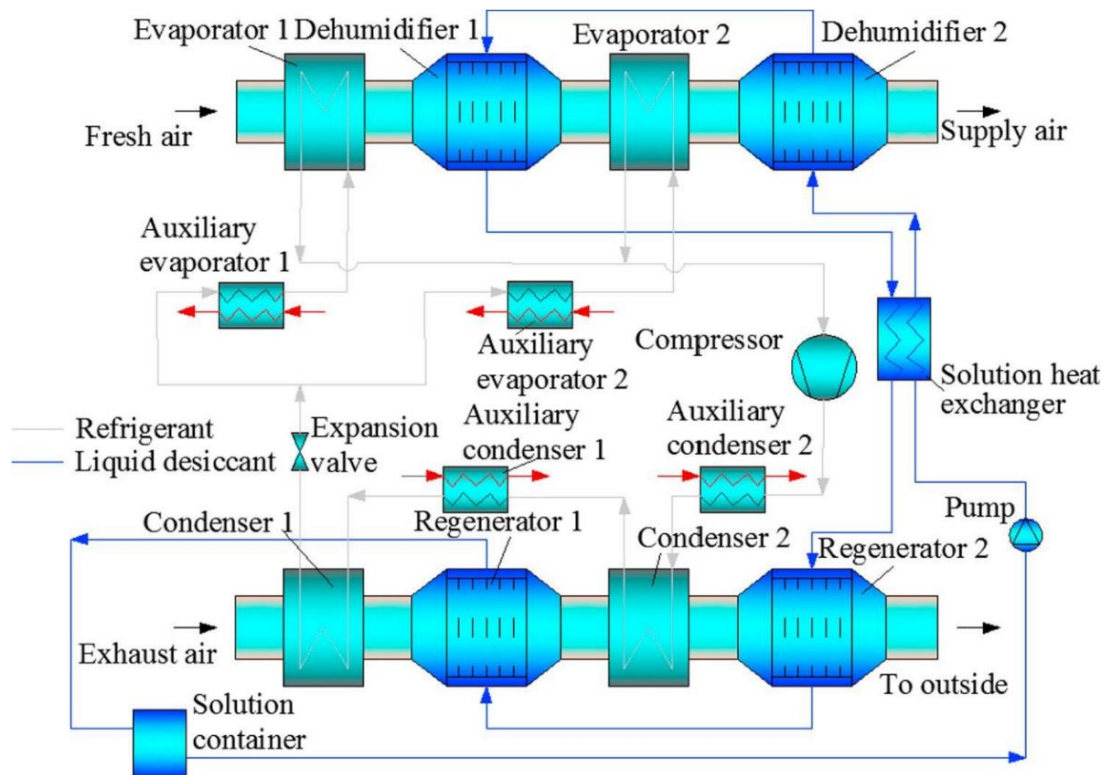


Fig.44: Schematic of LDAS with two-stage LDEE [159]

7.5 Flow configuration

Flow configuration plays a significant role in the design and performance of LDEE. The effect of various flow configurations on A-LDEE and I-LDEE are discussed as follows.

7.5.1 Flow configuration of A-LDEE

A-LDEEs were initially developed with three basic flow patterns, namely parallel, cross and counter, as shown in Fig.45. As expected, the performance of counterflow is the highest due to uniform heat and mass transfer potentials, and the crossflow is intermediate among the three flow patterns [160, 161]. However, there are a few exceptions, which are explained as follows. To reduce the effect of corrosion of liquid desiccant, Liu et al. [162] introduced a new design for LDEE in which air was heated instead of desiccant for the regeneration process. In this proposed design, the parallel flow showed better performance than the counterflow. However, the results revealed that the performance of LDEE with desiccant heating was higher than that of LDEE with air heating. For FF-LDEE, the theoretical study by Ali et al. [163] confirmed that the parallel flow performed better than the counterflow for the dehumidification process. Zhang et al. [164, 165] found that the performance of the hollow fiber A-LAMEE with crossflow was higher than that with counterflow.

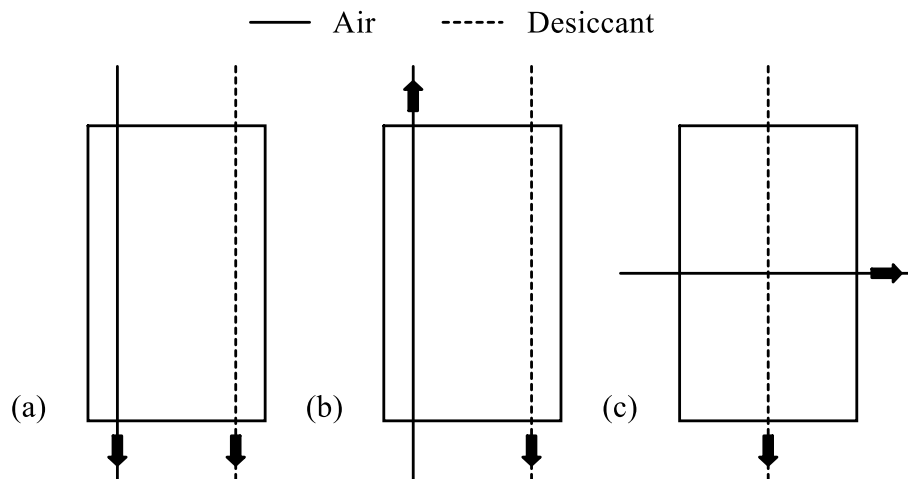


Fig.45: Schematic of (a) parallel flow (b) counterflow and (c) crossflow configurations

The header arrangements for parallel and counterflow configurations are not easy to install. Therefore, the crossflow is the most studied flow configuration in the A-LDEE [166]. In addition, the crossflow can potentially alleviate the desiccant carryover in the direct contact LDEE [167]. Even though the crossflow is preferred for LDEE due to its simple header design, its mass transfer performance is 10% lesser than that of the counterflow [168]. To mitigate this, Vali et al. [168, 169] proposed a counter-crossflow configuration (Fig.46 (a)) in which the header design is simpler, similar to crossflow. With equal contact area, the mass transfer performance of counter-cross flow configuration is better than that of crossflow but less than that of counterflow. The optimum aspect and entrance (desiccant inlet to outlet header length)

ratios should be less than 0.3 and 0.25, respectively [168]. Huang et al. [170] proposed a hexagonal-shaped LDEE as an alternative to the crossflow configuration (Fig. 46(b)). However, the performance of this LDEE was lesser than that of LDEE with crossflow [171]. For the given flow configuration, the desiccant can flow either from top to bottom or bottom to top. However, LAMEE with bottom to top desiccant flow has higher effectiveness when the heat capacity ratio between the desiccant and air is less than 5. This is because the effect of membrane deflection is minimum at a lower heat capacity (i.e., a lower desiccant flow rate) when the desiccant flows from bottom to top. However, the performance of the LAMEE is independent of desiccant flow direction at a higher heat capacity ratio (>5) [172].

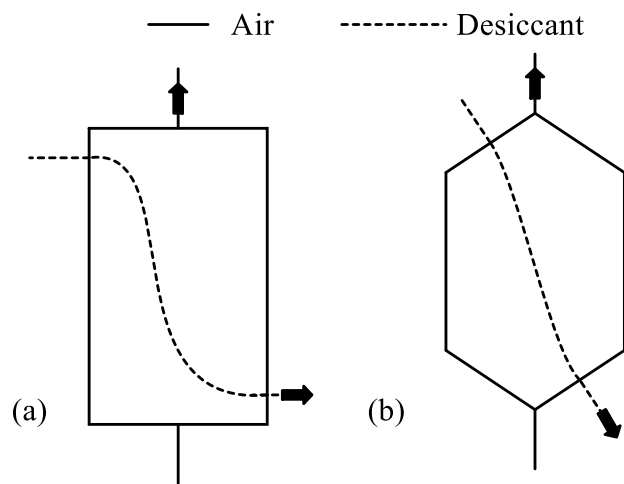


Fig.46: Schematic of LDEE with (a) counter-cross flow and (b) hexagonal shape

7.5.2 Flow configuration of I-LDEE

There are several flow configurations in I-LDEE due to its additional cooling or heating stream. In general, the desiccant flows from top to bottom (driven by gravity) in the direct contact LDEE. Accordingly, there are ten flow configurations that have been studied so far for I-LDEE [46]. Figure 47 shows these flow configurations [173]. Liu et al. [146] compared the dehumidification performance of six configurations (II-2.1, II-2.2, II-3, III-1, III-2, III-3) in the plate type I-LDEE. Among the selected configurations, I-LDEE with air and desiccant in counterflow arrangement (II-3 and III-3) had the highest performance. In addition, there was no significant difference in performance between the II-3 and III-3 configurations as well as between the remaining four configurations. Therefore, for dehumidification processes, I-LDEE has the flexibility of placing the headers for the cooling water. Liu et al. [173] reconfirmed that the dehumidification performance of III-3 configuration was the best among the ten configurations shown in Fig.47. However, this conclusion was valid only under any one of the

three operating conditions, namely (i) low desiccant and cooling water flow rates, (ii) low desiccant inlet temperature and (iii) a high desiccant inlet concentration. Therefore, the study recommended III-2 configuration due to evenly distributed heat and mass transfer potentials in I-LDEE [146]. Peng and Luo [174] compared six configurations (I-1, II-2.1, II-2.2, II-3, III-1, III-3) for the regeneration processes in the I-LDEE. The results revealed that the influences of flow configurations on the performance of the I-LDEE was insignificant. The above conclusions on the influence of flow configurations on I-LDEE are not valid if the refrigerant is used as a cooling or heating stream. This is because the temperature of the refrigerant is stable, and the direction of refrigerant flow is insignificant [46].

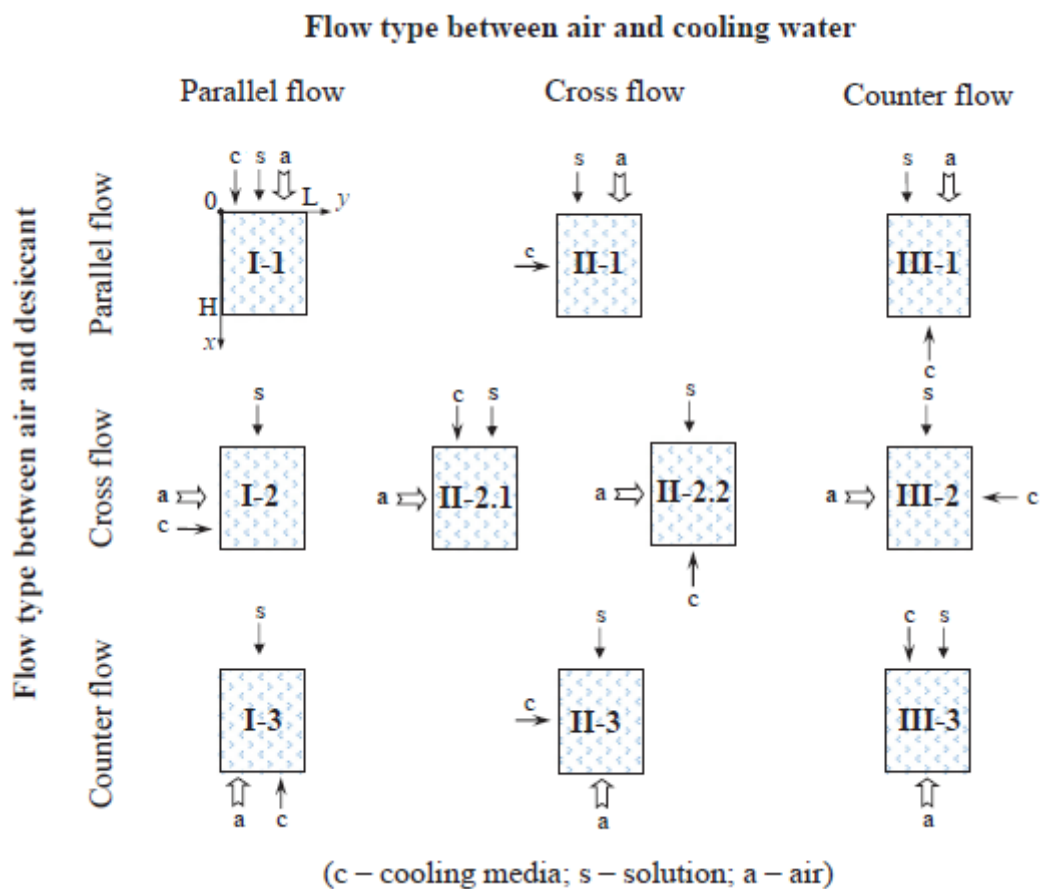


Fig.47: Flow configurations of three fluid LDEE [136]

Ali et al. [163] numerically compared the flow configurations of the I-LDEE with refrigerant as an additional stream. The results revealed that the parallel and counter flow showed better performance for the dehumidification and regeneration processes, respectively. As mentioned earlier in Section 7.3, Gurubalan et al. [21] proposed a new arrangement for I-LAMEE. The air and desiccant in the counterflow arrangement resulted in a better performance of the

I-LDEE [146, 173]. Therefore, the same arrangement was preferred in the proposed I-LAMEE. Hence, with respect to cooling water, the four possible configurations are (a) all counterflow (ACF) (b) cooling water and desiccant in counterflow (CWD) (c) cooling water and air in counterflow (CWA) and (d) all parallel flow (APF), as shown in Fig.48. The study experimentally compared these configurations for the dehumidification processes. Even though ACF configuration performed best, the authors recommended CWD configuration for the ease of header design.

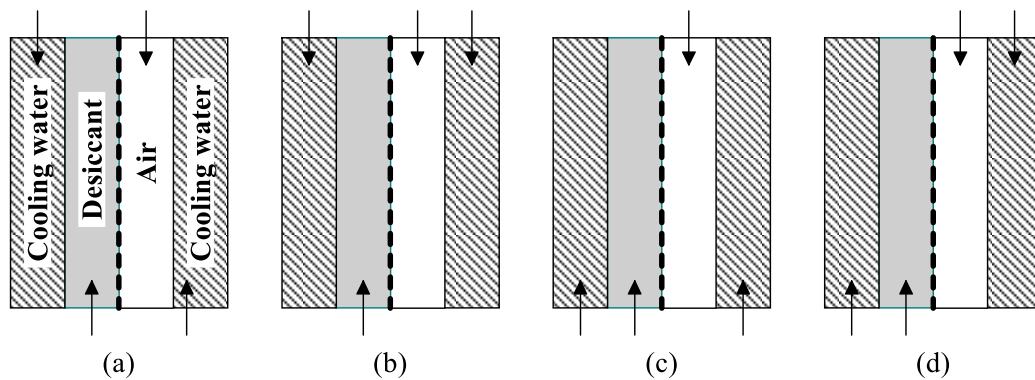


Fig.48: Schematic of (a) ACF (b) CWD (c) CWA and (d) APF flow configurations of I-LAMEE [21]

8. Mathematical Models

The working principle of LDEE for the application of dehumidification and regeneration processes is the same except for the direction of water vapor transfer, as mentioned earlier in Section 2. Therefore, the governing equations and modelling technique for these processes are the same. The commonly used models for the performance evaluation and control of LDEE are explained as follows [7].

The finite difference model is the most used modelling technique so far [7, 57, 175]. In the model, the governing equations consider the mass and energy balance of air and desiccant streams. Moreover, the heat and mass transfer coefficients are estimated for the constant heat flux and concentration boundary conditions, respectively [22, 176]. However, the actual boundary conditions are neither constant temperature nor constant concentration boundary conditions [177]. Hence, in the conjugate heat and mass transfer model, the naturally formed boundary conditions according to the air and desiccant flow conditions are considered. Therefore, the conjugate heat and mass transfer model is more accurate than the finite difference model [178].

Based on the performance at different operating conditions, various effectiveness correlations are available in literature for almost all the types of LDEEs [7, 57, 175]. Such correlations are utilized in the effectiveness-NTU model for the performance evaluation of LDEEs. This model needs less computational time than the finite difference and conjugate heat and mass transfer models [57, 175]. The prediction of the annual performance of the above discussed models of LDEE requires significant amount of time and computational efforts. On the other hand, the simplified model is most suitable for such analysis since it uses simple correlations to predict the performance of the LDEE. The correlations are developed based on the experimental performance of the LDEE. However, the correlations may not be appropriate for all operating conditions [7, 57, 175]. Hence, the simplified model can have a high estimation errors and computational time. To mitigate this, the artificial neural network model is used to simulate the performance of the LDEEs which is more accurate and faster than the other models in predicting the annual performance of LDEE [179].

The hybrid model is suitable for the real-time performance monitoring, control and optimization of the LDEE [180]. The model consists of two simple non-linear equations for the heat and mass transfer processes. Such equations are used to find the operating parameters to control and optimize the performance of the LDEE. The models explained so far are used to investigate only the steady state performance of the LDEE. Hence, Wang et al. [181] developed a detailed dynamic model to analyze the dynamic characteristics which influences the design of controllers and operating strategies of the LDEE. In the dynamic model, the parameters such as thermal mass of packing or membrane, air and desiccant held in LDEE are considered since these parameters delay the heat and mass transfer processes [181].

9. Conclusion

Liquid desiccant energy exchangers (LDEEs) are the performance influencing components of the liquid desiccant air conditioning system (LDAS), which is an energy-efficient and eco-friendly alternative to the conventional air conditioning system. The developments of LDEEs are critically reviewed in the present study. The characteristics, advantages, and disadvantages of LDEEs are summarized and presented in Appendix A. The salient conclusions from the present review are listed as follows.

- Direct contact LDEEs are extensively studied due to their high effectiveness, and simple structure and arrangement. However, the desiccant carryover issues restrict their application in the LDAS.

- Packed bed LDEE (PB-LDEE) is the most studied direct contact type. It not only has a higher mass transfer performance but also has a higher pressure drop in the airside. The recent developments in the packing material are promising in terms of improving the performance as well as reducing the pressure drop of air.
- Spray tower LDEE is more compact and simpler in construction than PB-LDEE. However, due to the fine sprayed droplets, the possibility of desiccant carryover is more predominant in spray tower LDEE.
- Falling film type is the most suitable configuration for the internally cooled or heated LDEEs, and its performance can be improved by utilizing surface modification, film inverting, and coating techniques.
- Solar collector based LDEEs are suitable only for the regeneration process. They simplify and reduce the initial and operating costs of LDAS due to the absence of a separate desiccant regeneration chamber.
- Pressurized LDEE is more suitable for the application where the air needs to be dried to a very low specific humidity (around 1 g/kg).
- Due to fine atomization of desiccant, the ultrasound-based LDEE not only requires a lower desiccant flow rate (40-75%) and regeneration temperature (around 4.5°C lower) but also consumes less energy (60% lower) than the PB-LDEE.
- Hypergravity, bubble absorption, and vacuum-based LDEEs are attractive options for LDAS. However, they have not yet been studied in detail thus far.
- Indirect contact LDEEs were developed to avoid the desiccant carryover with the air. However, their mass transfer performance is lower than that of most of the direct contact LDEEs.
- Membrane-based LDEE (LAMEE) is the most studied indirect contact type. Unlike the other types of indirect contact LDEEs, it can be used for both dehumidification and regeneration processes.
- Electrodialysis based LDEE (E-LDEE) works on electrical energy instead of thermal energy, and hence, it reduces the dependence of the LDAS on the availability of low-grade energy sources. However, the optimum concentration range of commonly used desiccants in E-LDEE is much lower when compared to their working concentration.
- Reverse osmosis based LDEE has been adopted from desalination applications. The operating pressure of the regeneration process is significantly higher than that of the desalination process.

- Membrane distillation based LDEE works on the principle of thermal distillation and membrane separation. Its desiccant regeneration rate is 4.5-6 times higher than that of PB-LDEE.
- An additional cooling or heating stream is provided in the internally cooled or heated LDEE (I-LDEE) to improve its efficiency for dehumidification and regeneration processes. The mass transfer performance of the I-LDEE is higher than that of the adiabatic LDEE (A-LDEE). Multi-staging is also an effective technique to improve the efficiency of the LDEEs.
- Counter-cross flow is the most suitable configuration for A-LDEE in terms of the performance and header design.
- For I-LDEE, the air and desiccant in the counterflow arrangement shows a better performance for the dehumidification process, whereas the influences of flow configurations are insignificant for the regeneration process.
- Halide salt-based desiccants are widely used in LDAS due to their attractive performance. However, they are more corrosive and costlier than glycol-based desiccants. Ionic liquids are currently considered promising desiccants due to their lower vapour pressure, lower regeneration temperature, and non-corrosiveness.

10. Suggested Topics for Future Research

There have been a number of research studies on LDEEs over the last two decades. However, their application is limited and not widely used in the field HVAC systems. To mitigate this problem, future research should prioritize the following topics.

- Practical problems of LDEEs: Cross contamination is the major issue in most of the direct contact LDEEs since it can deteriorate the indoor air quality of the air conditioning room and also corrodes the air handling equipment. Similarly, the leakage and blockage (due to crystallization of desiccant) of the membrane are the key problems in the indirect contact LDEEs. Due to these practical problems, LDEEs are not widely used in the air handling systems. On the other hand, most of the available literature on LDEEs are focussed only on performance evaluation and hence, the future studies should have a focus on these practical problems of LDEEs.
- Long term performance study in the practical systems: Most of LDEEs research are still theoretical or laboratory-scale experiments rather than practical systems. Hence, more research should be directed towards the performance study of LDEEs on the practical

systems (i.e., field study). In addition, the long-term performance data from the field study is essential to identify the effects of scaling, fouling and ageing of the contact materials. Moreover, the long-term performance data is vital to assess the maintenance cost which is useful to analyze the economic feasibility of LDEEs in the practical systems.

- Noncorrosive and inexpensive solution: Most of the conventional desiccants are corrosive. On the other hand, the alternatives are costlier and lesser efficient than the conventional desiccants. Hence, there is a need for an efficient, inexpensive and non-corrosive desiccant or additives, which can nullify the corrosive nature of conventional desiccants without altering the other properties.
- Compatible material for efficient heat and mass transfer: Contact material between the air and desiccant in LDEEs should withstand the corrosive nature of desiccant and also have less heat and mass transfer resistance.
- Generalized design and performance control methodology: Design methodologies are available for the solid desiccant-based energy exchangers [182]. Similar design methodology is essential for HVAC designers and engineers to develop LDEEs for different applications. Moreover, the studies on the control variables are still theoretical or small-scale experiments and thus, the future researches should develop a control methodology based on the practical experiments.

Based on the current review, the proposed specific suggestions for further research on LDEEs are listed below.

- Performance characterization of LDAS with desiccant based latent thermal energy storage.
- Performance analysis of LDAS with bubble absorption LDEEs.
- Performance of PB-LDEE with innovative next generation randomly packing fills.
- Effect of various surface modification techniques (e.g., scratched surfaces, micro-finned tubes, corrugated plates) on the performance of FF-LDEE.
- Performance analysis of the internally cooled or heated based hollow fiber LAMEE.
- Performance analysis of osmotically assisted reverse osmosis LDEE.
- Developing desiccant based performance parameters for the regeneration process in I-LDEE.
- Performance analysis of of spray tower, hypergravity, bubble absorption based I-LDEE.

- Influence of flow configuration on the performance of I-LAMEE and membrane distillation LDEE.
- Comparison between the series and parallel flow configurations of the multi-stage LDEE.
- Comprehensive comparison of halide salt type, glycol type, weak organic acid type and ionic liquid type desiccants based on the marking criteria of Studak and Peterson [29].

Acknowledgements

This research did not receive any specific grant from funding agencies in the public, commercial, or not-for-profit sectors.

References

- [1]. “BP energy Outlook”, <https://www.bp.com/content/dam/bp/business-sites/en/global/corporate/pdfs/energy-economics/energy-outlook/bp-energy-outlook-2019.pdf> [accessed 21st March 2020].
- [2]. “The future of cooling opportunities for energy efficient air conditioning by International Energy Agency”, <https://www.iea.org/reports/the-future-of-cooling> [accessed 21st March 2020].
- [3]. “Alternatives to Vapor-Compression HVAC Technology”, ASHRAE Journal Article, https://www.ashrae.org/File%20Library/docLib/.../2014Oct012-023_Goetzler.pdf [accessed 21st March 2020]
- [4]. Gurubalan A, Maiya MP, Tiwari S. Performance characterization of a novel membrane-based liquid desiccant air conditioning system. *Int J Refrig* 2020;120. <https://doi.org/10.1016/j.ijrefrig.2020.09.007>.
- [5]. Abdel-Salam MRH, Ge G, Fauchoux M, Besant RW, Simonson CJ. State-of-the-art in liquid-to-air membrane energy exchangers (LAMEEs): A comprehensive review. *Renew Sustain Energy Rev* 2014;39:700–28. <https://doi.org/https://doi.org/10.1016/j.rser.2014.07.022>.
- [6]. Abas N, Kalair AR, Khan N, Haider A, Saleem Z, Saleem MS. Natural and synthetic refrigerants, global warming: A review. *Renew Sustain Energy Rev* 2018;90:557–69. <https://doi.org/https://doi.org/10.1016/j.rser.2018.03.099>.
- [7]. Gurubalan A, Maiya MP, Geoghegan PJ. A comprehensive review of liquid desiccant air conditioning system. *Appl Energy* 2019;254. <https://doi.org/10.1016/j.apenergy.2019.113673>.
- [8]. Rafique MM, Gandhidasan P, Bahaidarah HMS. Liquid desiccant materials and dehumidifiers – A review. *Renew Sustain Energy Rev* 2016;56:179–95. <https://doi.org/https://doi.org/10.1016/j.rser.2015.11.061>.
- [9]. Sahlot M, Riffat SB. Desiccant cooling systems: a review. *Int J Low-Carbon Technol* 2016;11:489–505. <https://doi.org/10.1093/ijlct/ctv032>.
- [10]. Abdel-salam AH, Simonson CJ. State-of-the-art in liquid desiccant air conditioning equipment and systems. *Renew Sustain Energy Rev* 2016;58:1152–83. <https://doi.org/10.1016/j.rser.2015.12.042>.

- [11]. Abdel-Salam AH, Ge G, Simonson CJ. Performance analysis of a membrane liquid desiccant air-conditioning system. *Energy Build* 2013;62:559–69. <https://doi.org/https://doi.org/10.1016/j.enbuild.2013.03.028>.
- [12]. Mei L, Dai YJ. A technical review on use of liquid-desiccant dehumidification for air-conditioning application. *Renew Sustain Energy Rev* 2008;12:662–89. <https://doi.org/https://doi.org/10.1016/j.rser.2006.10.006>.
- [13]. Gurubalan A, Maiya MP, Tiwari S. Performance characterization of membrane dehumidifier with desiccants in flat-plate arrangement. *Energy Build* 2017;156:151–62. <https://doi.org/https://doi.org/10.1016/j.enbuild.2017.09.040>.
- [14]. Alizadeh S. Performance of a solar liquid desiccant air conditioner – An experimental and theoretical approach. *Sol Energy* 2008;82:563–72. <https://doi.org/https://doi.org/10.1016/j.solener.2007.10.009>.
- [15]. Yamaguchi S, Jeong J, Saito K, Miyauchi H, Harada M. Hybrid liquid desiccant air-conditioning system: Experiments and simulations. *Appl Therm Eng* 2011;31:3741–7. <https://doi.org/https://doi.org/10.1016/j.applthermaleng.2011.04.009>.
- [16]. Zhao K, Liu X-H, Zhang T, Jiang Y. Performance of temperature and humidity independent control air-conditioning system in an office building. *Energy Build* 2011;43:1895–903. <https://doi.org/https://doi.org/10.1016/j.enbuild.2011.03.041>.
- [17]. Bassuoni MM. Experimental performance study of a proposed desiccant based air conditioning system. *J Adv Res* 2014;5:87–95. <https://doi.org/https://doi.org/10.1016/j.jare.2012.12.002>.
- [18]. Longo GA, Gasparella A. Three years experimental comparative analysis of a desiccant based air conditioning system for a flower greenhouse: Assessment of different desiccants. *Appl Therm Eng* 2015;78:584–90. <https://doi.org/https://doi.org/10.1016/j.applthermaleng.2014.12.005>.
- [19]. Guan B, Zhang T, Liu X. On-site performance investigation of liquid-desiccant air-conditioning system applied in laboratory rodent room: A comparative study. *Energy Build* 2021;232:110664. <https://doi.org/https://doi.org/10.1016/j.enbuild.2020.110664>.
- [20]. Ge G, Ghadiri Moghaddam D, Abdel-Salam AH, Besant RW, Simonson CJ. Comparison of experimental data and a model for heat and mass transfer performance of a liquid-to-air membrane energy exchanger (LAMEE) when used for air dehumidification and salt solution regeneration. *Int J Heat Mass Transf* 2014;68:119–31. <https://doi.org/https://doi.org/10.1016/j.ijheatmasstransfer.2013.09.016>.
- [21]. Gurubalan A, Maiya MP, Tiwari S. Experiments on a novel membrane-based liquid desiccant dehumidifier for hybrid air conditioner. *Int J Refrig* 2019;108. <https://doi.org/10.1016/j.ijrefrig.2019.09.004>.
- [22]. Ghadiri Moghaddam D, Oghabi A, Ge G, Besant RW, Simonson CJ. Numerical model of a small-scale liquid-to-air membrane energy exchanger: Parametric study of membrane resistance and air side convective heat transfer coefficient. *Appl Therm Eng* 2013;61:245–58. <https://doi.org/https://doi.org/10.1016/j.applthermaleng.2013.07.017>.
- [23]. Lowenstein, A. Review of liquid desiccant technology for HVAC applications. *HVAC&R Res.* 2008;14:22. <http://dx.doi.org/10.1080/10789669.2008.10391042>
- [24]. F.M. Gómez-Castro, D. Schneider, T. Päßler, U. Eicker, Review of indirect and direct solar thermal regeneration for liquid desiccant systems, *Renew Sustain Energy Rev*, 82 (2018), pp. 545-575. <https://doi.org/10.1016/j.rser.2017.09.053>
- [25]. Luo Y, Shao S, Qin F, Tian C, Yang H. Investigation on feasibility of ionic liquids used in solar liquid desiccant air conditioning system. *Sol Energy* 2012;86:2718–24. <https://doi.org/https://doi.org/10.1016/j.solener.2012.06.008>.

- [26]. N. Enteria, H. Yoshino, A. Mochida, Review of the advances in open-cycle absorption air-conditioning systems, *Renew. Sustain. Energy Rev.*, 28 (2013), pp. 265-289. <https://doi.org/10.1016/j.rser.2013.07.012>
- [27]. X. Chen, S. Riffat, B. Hongyu, X. Zheng, D. Reay, Recent progress in liquid desiccant dehumidification and air-conditioning: a review, *Energy Built Environ.*, 1 (2020), pp. 106-130. <https://doi.org/10.1016/j.enbenv.2019.09.001>
- [28]. Giampieri A, Ma Z, Smallbone A, Roskilly AP. Thermodynamics and economics of liquid desiccants for heating, ventilation and air-conditioning – an overview. *Appl Energy* 2018;220:455–79. <https://doi.org/10.1016/j.apenergy.2018.03.112>
- [29]. Studak JW, Peterson JL. A preliminary evaluation of alternative liquid desiccants for a hybrid desiccant air conditioner. Atlanta, GA: Desiccant cooling and dehumidification, ASHARE; 1992.
- [30]. Qi R, Dong C, Zhang L-Z. A review of liquid desiccant air dehumidification: From system to material manipulations. *Energy Build* 2020;215:109897. <https://doi.org/https://doi.org/10.1016/j.enbuild.2020.109897>.
- [31]. Ali A, Vafai K, Khaled A-RA. Analysis of heat and mass transfer between air and falling film in a cross flow configuration. *Int J Heat Mass Transf* 2004;47:743–55. <https://doi.org/https://doi.org/10.1016/j.ijheatmasstransfer.2003.07.017>.
- [32]. Ali A, Vafai K. An investigation of heat and mass transfer between air and desiccant film in an inclined parallel and counter flow channels. *Int J Heat Mass Transf* 2004;47:1745–60. <https://doi.org/https://doi.org/10.1016/j.ijheatmasstransfer.2003.10.008>.
- [33]. Kang YT, Kim HJ, Lee K II. Heat and mass transfer enhancement of binary nanofluids for H₂O/LiBr falling film absorption process. *Int J Refrig* 2008;31:850–6. <https://doi.org/https://doi.org/10.1016/j.ijrefrig.2007.10.008>.
- [34]. Wu WD, Pang CW, Sheng W, Cheng SX, Wu RY. Enhancement on NH₃/H₂O bubble absorption in binary nanofluids by mono nano Ag. *CIESC J.* 2010;61(5):1112–1117.
- [35]. Yang L, Du K, Niu XF, Cheng B, Jiang YF. Experimental study on enhancement of ammonia–water falling film absorption by adding nano-particles. *Int J Refrig* 2011;34:640–7. <https://doi.org/https://doi.org/10.1016/j.ijrefrig.2010.12.017>.
- [36]. Wen T, Lu L, Dong C, Luo Y. Investigation on the regeneration performance of liquid desiccant by adding surfactant PVP-K30. *Int J Heat Mass Transf* 2018;123:445–54. <https://doi.org/https://doi.org/10.1016/j.ijheatmasstransfer.2018.03.005>.
- [37]. Cihan E, Kavasogullari B, Demir H. Enhancement of performance of open liquid desiccant system with surface additive. *Renew Energy* 2017;114:1101–12. <https://doi.org/https://doi.org/10.1016/j.renene.2017.08.002>.
- [38]. Kang BH, Kim KH, Lee D-Y. Fluid flow and heat transfer on a falling liquid film with surfactant from a heated vertical surface. *J Mech Sci Technol* 2007;21:1807. <https://doi.org/10.1007/BF03177436>.
- [39]. Rivera W, Cerezo J. Experimental study of the use of additives in the performance of a single-stage heat transformer operating with water–lithium bromide. *Int J Energy Res* 2005;29:121–30. <https://doi.org/https://doi.org/10.1002/er.1045>.
- [40]. Fu Lin SJ, Shigang Z. Experimental study on vertical vapor absorption into LiBr solution with and without additive. *Appl Therm Eng* 2011;31:2850–4. <https://doi.org/https://doi.org/10.1016/j.applthermaleng.2011.05.010>.
- [41]. Wen T, Lu L, Dong C, Luo Y. Investigation on the regeneration performance of liquid desiccant by adding surfactant PVP-K30. *Int J Heat Mass Transf* 2018;123:445–54. <https://doi.org/https://doi.org/10.1016/j.ijheatmasstransfer.2018.03.005>.
- [42]. Wen T, Lu L, Nie Y, Zhong H. Development and investigation on the dehumidification and corrosion resistance performance of a new mixed liquid

- desiccant. *Int J Heat Mass Transf* 2019;130:72–82.
<https://doi.org/https://doi.org/10.1016/j.ijheatmasstransfer.2018.10.066>.
- [43]. Conde MR. Properties of aqueous solutions of lithium and calcium chlorides: Formulations for use in air conditioning equipment design. *Int J Therm Sci* 2004;43:367–82. <https://doi.org/10.1016/j.ijthermalsci.2003.09.003>.
- [44]. Gandhidasan P. A simplified model for air dehumidification with liquid desiccant. *Sol Energy* 2004;76:409–16. <https://doi.org/https://doi.org/10.1016/j.solener.2003.10.001>.
- [45]. Fumo N, Goswami DY. Study of an aqueous lithium chloride desiccant system: air dehumidification and desiccant regeneration. *Sol Energy* 2002;72:351–61. [https://doi.org/https://doi.org/10.1016/S0038-092X\(02\)00013-0](https://doi.org/https://doi.org/10.1016/S0038-092X(02)00013-0).
- [46]. Ren H, Ma Z, Liu J, Gong X, Li W. A review of heat and mass transfer improvement techniques for dehumidifiers and regenerators of liquid desiccant cooling systems. *Appl Therm Eng* 2019;162:114271. <https://doi.org/https://doi.org/10.1016/j.applthermaleng.2019.114271>.
- [47]. Simonson CJ, Besant RW. Energy wheel effectiveness: part I—development of dimensionless groups. *Int J Heat Mass Transf* 1999;42:2161–70. [https://doi.org/https://doi.org/10.1016/S0017-9310\(98\)00325-1](https://doi.org/https://doi.org/10.1016/S0017-9310(98)00325-1).
- [48]. Ge G, Abdel-Salam MRH, Besant RW, Simonson CJ. Research and applications of liquid-to-air membrane energy exchangers in building HVAC systems at University of Saskatchewan: A review. *Renew Sustain Energy Rev* 2013;26:464–79. <https://doi.org/https://doi.org/10.1016/j.rser.2013.04.022>.
- [49]. Saman WY, Alizadeh S. An experimental study of a cross-flow type plate heat exchanger for dehumidification/cooling. *Sol Energy* 2002;73:59–71. [https://doi.org/https://doi.org/10.1016/S0038-092X\(01\)00078-0](https://doi.org/https://doi.org/10.1016/S0038-092X(01)00078-0).
- [50]. Abdel-Salam MRH, Besant RW, Simonson CJ. Design and testing of a novel 3-fluid liquid-to-air membrane energy exchanger (3-fluid LAMEE). *Int J Heat Mass Transf* 2016;92:312–29. <https://doi.org/https://doi.org/10.1016/j.ijheatmasstransfer.2015.08.075>.
- [51]. Kessling W, Laevemann E, Peltzer M. Energy storage in open cycle liquid desiccant cooling systems. *Int J Refrig* 1998;21:150–6. [https://doi.org/https://doi.org/10.1016/S0140-7007\(97\)00045-5](https://doi.org/https://doi.org/10.1016/S0140-7007(97)00045-5).
- [52]. Bai H, Zhu J, Chen Z, Chu J, Liu Y. Performance evaluation of a membrane-based flat-plate heat and mass exchanger used for liquid desiccant regeneration. *Appl Therm Eng* 2018;139:569–84. <https://doi.org/https://doi.org/10.1016/j.applthermaleng.2018.05.011>.
- [53]. Yang Z, Lian Z, Li X, Zhang K. Concept of dehumidification perfectness and its potential applications. *Energy* 2015;91:176–91. <https://doi.org/https://doi.org/10.1016/j.energy.2015.08.036>.
- [54]. Abdel-Salam MRH, Besant RW, Simonson CJ. Performance Definitions for Three-Fluid Heat and Moisture Exchangers. *J Heat Transfer* 2016;139. <https://doi.org/10.1115/1.4034756>.
- [55]. Ghadiri Moghaddam D, Besant RW, Simonson CJ. Solution-side effectiveness for a liquid-to-air membrane energy exchanger used as a dehumidifier/regenerator. *Appl Energy* 2014;113:872–82. <https://doi.org/https://doi.org/10.1016/j.apenergy.2013.08.037>.
- [56]. Fekadu G, Subudhi S. Renewable energy for liquid desiccants air conditioning system: A review. *Renew Sustain Energy Rev* 2018;93:364–79. <https://doi.org/https://doi.org/10.1016/j.rser.2018.05.016>.
- [57]. Bai H, Zhu J, Chen Z, Chu J. State-of-art in modelling methods of membrane-based liquid desiccant heat and mass exchanger: A comprehensive review. *Int J Heat Mass*

- Transf 2018;125:445–70.
<https://doi.org/https://doi.org/10.1016/j.ijheatmasstransfer.2018.04.100>.
- [58]. Kamali H, Ge G, Besant RW, Simonson CJ. Extension of the Concepts of Heat Capacity Rate Ratio and Effectiveness-Number of Transfer Units Model to the Coupled Heat and Moisture Exchange in Liquid-to-Air Membrane Energy Exchangers. *J Heat Transfer* 2016;138:1–12. <https://doi.org/10.1115/1.4033418>.
- [59]. ASHRAE Handbook Fundamentals 2009, Climatic Design Information. Atlanta, USA: American Society of Heating, Refrigerating and Air-Conditioning Engineers; 2009.
- [60]. Gurubalan A, Tiwari S, Maiya MP. Performance comparison of direct contact-packed bed and indirect contact-membrane dehumidifiers. In: Proceedings of the 24th National and 2nd International ISHMT-ASTFE Heat and Mass Transfer Conference (IHMTTC-2017), Pg. 201-209. <https://doi.org/10.1615/IHMTTC-2017.280>
- [61]. Marisa Fernandes Mendes (2011). HETP Evaluation of Structured and Randomic Packing Distillation Column, *Mass Transfer in Chemical Engineering Processes*, Intech Open. , DOI: 10.5772/19671. Available at <https://www.intechopen.com/books/mass-transfer-in-chemical-engineering-processes/hetp-evaluation-of-structured-and-randomic-packing-distillation-column> [last accessed 21st March 2020].
- [62]. Gavin Towler and Ray Sinnott (2012), *Chemical Engineering Design: Principles, Practice and Economics of Plant and Process Design*, 2nd edition, Elsevier.
- [63]. Arachchige USPR, Melaaen MC. Selection of packing material for gas absorption. *Eur J Sci Res* 2012;87:117–26.
- [64]. Metal Random Packing Cascade Mini Ring for Distillation Column. Available at https://www.alibaba.com/product-detail/Metal-Random-Packing-Cascade-Mini-Ring_60566540527.html [last accessed 21st March 2020].
- [65]. Longo GA, Gasparella A. Experimental Analysis on Chemical Dehumidification of Air in a Packed Column by Hygroscopic Salt Solution: Comparison between Structured and Random Packings. *HVAC&R Res* 2006;12:713–29. <https://doi.org/10.1080/10789669.2006.10391203>.
- [66]. Random packing - From competitive products to advanced solutions by Sulzer. Available at https://www.sulzer.com/-/media/files/products/separation-technology/distillation-and-absorption/brochures/random_packing.ashx?la=en [last accessed 21st March 2020].
- [67]. Warnakulasuriya FSK, Worek WM. Adiabatic water absorption properties of an aqueous absorbent at very low pressures in a spray absorber. *Int J Heat Mass Transf* 2006;49:1592–602. <https://doi.org/https://doi.org/10.1016/j.ijheatmasstransfer.2005.11.003>.
- [68]. Chung TW, Wu H. Mass Transfer Correlation for Dehumidification of Air in a Packed Absorber with an Inverse U-Shaped Tunnel. *Sep Sci Technol* 2000;35:1503–15. <https://doi.org/10.1081/SS-100100238>.
- [69]. Yin Y, Qian J, Zhang X. Recent advancements in liquid desiccant dehumidification technology. *Renew Sustain Energy Rev* 2014;31:38–52. <https://doi.org/https://doi.org/10.1016/j.rser.2013.11.021>.
- [70]. Kumar R, Dhar PL, Jain S. Development of new wire mesh packings for improving the performance of zero carryover spray tower. *Energy* 2011;36:1362–74. <https://doi.org/https://doi.org/10.1016/j.energy.2010.09.040>.
- [71]. Ibarra-Bahena J, Romero RJ. Performance of Different Experimental Absorber Designs in Absorption Heat Pump Cycle Technologies: A Review. *Energies* 2014;7. <https://doi.org/10.3390/en7020751>.

- [72]. Feyka S, Vafai K. An Investigation of a Falling Film Desiccant Dehumidification/Regeneration Cooling System. *Heat Transf Eng* 2007;28:163–72. <https://doi.org/10.1080/01457630601023666>.
- [73]. Jain S, Dhar PL, Kaushik SC. Experimental studies on the dehumidifier and regenerator of a liquid desiccant cooling system. *Appl Therm Eng* 2000;20:253–67. [https://doi.org/https://doi.org/10.1016/S1359-4311\(99\)00030-7](https://doi.org/https://doi.org/10.1016/S1359-4311(99)00030-7).
- [74]. Wen T, Lu L, Dong C, Luo Y. Development and experimental study of a novel plate dehumidifier made of anodized aluminum. *Energy* 2018;144:169–77. <https://doi.org/https://doi.org/10.1016/j.energy.2017.12.020>.
- [75]. Dong C, Lu L. Enhancing the dehumidification efficiency of solar-assisted liquid desiccant air dehumidifiers using nanoscale TiO₂ super-hydrophilic coating. *Energy Procedia* 2019;158:5765–9. <https://doi.org/https://doi.org/10.1016/j.egypro.2019.01.554>.
- [76]. Wen T, Luo Y, Lu L, He W. Enhancing the falling film dehumidification performance from the prospective of CFD simulation. *Int J Heat Mass Transf* 2020;151:119459. <https://doi.org/https://doi.org/10.1016/j.ijheatmasstransfer.2020.119459>.
- [77]. Raisul Islam M, Wijesundera NE, Ho JC. Performance study of a falling-film absorber with a film-inverting configuration. *Int J Refrig* 2003;26:909–17. [https://doi.org/https://doi.org/10.1016/S0140-7007\(03\)00078-1](https://doi.org/https://doi.org/10.1016/S0140-7007(03)00078-1).
- [78]. Amaris C, Vallès M, Bourouis M. Vapour absorption enhancement using passive techniques for absorption cooling/heating technologies: A review. *Appl Energy* 2018;231:826–53. <https://doi.org/https://doi.org/10.1016/j.apenergy.2018.09.071>.
- [79]. Peng D, Zhang X. An analytical model for coupled heat and mass transfer processes in solar collector/regenerator using liquid desiccant. *Appl Energy* 2011;88:2436–44. <https://doi.org/https://doi.org/10.1016/j.apenergy.2011.01.027>.
- [80]. Haim I, Grossman G, Shavit A. Simulation and analysis of open cycle absorption systems for solar cooling. *Sol Energy* 1992;49:515–34. [https://doi.org/https://doi.org/10.1016/0038-092X\(92\)90160-C](https://doi.org/https://doi.org/10.1016/0038-092X(92)90160-C).
- [81]. Kakabaev A. Absorption solar regeneration unit with open regeneration of solution. *Appl Sol Energy* 1976;5:69–72.
- [82]. Gandhidasan P, Al-Farayedhi AA. Solar regeneration of liquid desiccants suitable for humid climates. *Energy* 1994;19:831–6. [https://doi.org/https://doi.org/10.1016/0360-5442\(94\)90035-3](https://doi.org/https://doi.org/10.1016/0360-5442(94)90035-3).
- [83]. Nelson DJ, Wood BD. Evaporation Rate Model for a Natural Convection Glazed Collector/Regenerator. *J Sol Energy Eng* 1990;112:51–7. <https://doi.org/10.1115/1.2930759>.
- [84]. Yang R, Wang PL. Experimental Study of a Forced Convection Solar Collector/Regenerator for Open-Cycle Absorption Cooling. *J Sol Energy Eng* 1994;116:194–9. <https://doi.org/10.1115/1.2930081>.
- [85]. Yang R, Wang PL. Experimental Study for a Double-Glazed Forced-Flow Solar Collector/Regenerator. *J Sol Energy Eng* 1998;120:253–9. <https://doi.org/10.1115/1.2888128>.
- [86]. Yang R, Wang P-L. A Simulation Study of Performance Evaluation of Single-Glazed and Double-Glazed Collectors/Regenerators for an Open-Cycle Absorption Solar Cooling System. *Sol Energy* 2001;71:263–8. [https://doi.org/https://doi.org/10.1016/S0038-092X\(01\)00047-0](https://doi.org/https://doi.org/10.1016/S0038-092X(01)00047-0).
- [87]. Singh PL. Silk cocoon drying in forced convection type solar dryer. *Appl Energy* 2011;88:1720–6. <https://doi.org/https://doi.org/10.1016/j.apenergy.2010.11.016>.
- [88]. Tuğrul Oğulata R. Utilization of waste-heat recovery in textile drying. *Appl Energy* 2004;79:41–9. <https://doi.org/https://doi.org/10.1016/j.apenergy.2003.12.002>.

- [89]. Yin Y, Zheng B, Yang C, Zhang X. A proposed compressed air drying method using pressurized liquid desiccant and experimental verification. *Appl Energy* 2015;141:80–9. <https://doi.org/https://doi.org/10.1016/j.apenergy.2014.12.015>.
- [90]. Wang L, Lian ZW. Improvement of conventional liquid desiccant dehumidification technology. *Journal of Southeast University* 2010;26:212–216.
- [91]. Yao Y, Li W, Hu Y. Modeling and performance investigation on the counter-flow ultrasonic atomization liquid desiccant regenerator. *Appl Therm Eng* 2020;165:114573. <https://doi.org/https://doi.org/10.1016/j.applthermaleng.2019.114573>.
- [92]. Yang Z, Lin B, Zhang K, Lian Z. Experimental study on mass transfer performances of the ultrasonic atomization liquid desiccant dehumidification system. *Energy Build* 2015;93:126–36. <https://doi.org/https://doi.org/10.1016/j.enbuild.2015.02.035>.
- [93]. Yang Z, Zhang K, Hwang Y, Lian Z. Performance investigation on the ultrasonic atomization liquid desiccant regeneration system. *Appl Energy* 2016;171:12–25. <https://doi.org/https://doi.org/10.1016/j.apenergy.2016.03.008>.
- [94]. Bian Z, Yang ZL, Lian ZW. Experimental study of ultrasound atomization dehumidifying system with liquid desiccant. *Journal of Shanghai Jiaotong University* 2012;46:1604–1608.
- [95]. Gu Y, Zhang X. Performance investigation on the liquid desiccant regeneration using rotating packed bed. *Int J Refrig* 2020;109:45–54. <https://doi.org/https://doi.org/10.1016/j.ijrefrig.2019.09.017>.
- [96]. C. Ramshaw, R. Mallinson. Mass Transfer Process, US Patent, US4283255A, 1981. <https://patents.google.com/patent/US4283255A/en>
- [97]. Tan CS, Chen JE. Absorption of carbon dioxide with piperazine and its mixtures in a rotating packed bed. *Sep Purif Technol* 2006;49:174–80. <https://doi.org/https://doi.org/10.1016/j.seppur.2005.10.001>.
- [98]. Cheng H-H, Tan C-S. Reduction of CO₂ concentration in a zinc/air battery by absorption in a rotating packed bed. *J Power Sources* 2006;162:1431–6. <https://doi.org/https://doi.org/10.1016/j.jpowsour.2006.07.046>.
- [99]. Jassim MS, Rochelle G, Eimer D, Ramshaw C. Carbon Dioxide Absorption and Desorption in Aqueous Monoethanolamine Solutions in a Rotating Packed Bed. *Ind Eng Chem Res* 2007;46:2823–33. <https://doi.org/10.1021/ie051104r>.
- [100]. Gu Y, Zhang X. A proposed hyper-gravity liquid desiccant dehumidification system and experimental verification. *Appl Therm Eng* 2019;159:113871. <https://doi.org/https://doi.org/10.1016/j.applthermaleng.2019.113871>.
- [101]. Saurabh, Murthy DS. Analysis and optimization of thermal characteristics in a rotating packed bed. *Appl Therm Eng* 2020;165:114533. <https://doi.org/https://doi.org/10.1016/j.applthermaleng.2019.114533>.
- [102]. Yon HR, Cai W, Wang Y, Shen S. Performance investigation on a novel liquid desiccant regeneration system operating in vacuum condition. *Appl Energy* 2018;211:249–58. <https://doi.org/https://doi.org/10.1016/j.apenergy.2017.10.124>.
- [103]. Gao WZ, Shi YZ, Zhang XL, Anderson K. Experimental investigation on a new method of regenerating dehumidification solution–release solution droplet into vacuum. *Appl Therm Eng* 2013;59:14–20. <https://doi.org/https://doi.org/10.1016/j.applthermaleng.2013.05.011>.
- [104]. Yon HR, Cai W, Wang Y, Wang X, Shen S. Dynamic model for a novel liquid desiccant regeneration system operating in vacuum condition. *Energy Build* 2018;167:69–78. <https://doi.org/https://doi.org/10.1016/j.enbuild.2018.02.024>.

- [105]. Kabeel AE. Dehumidification and humidification process of desiccant solution by air injection. *Energy* 2010;35:5192–201.
<https://doi.org/https://doi.org/10.1016/j.energy.2010.07.047>.
- [106]. Kasamsetty S, Raphael B. Performance evaluation of a high-influx, bubble dehumidifier. *Energy Build* 2018;173:291–301.
<https://doi.org/https://doi.org/10.1016/j.enbuild.2018.05.047>.
- [107]. Wu X, Xu S, Jiang M. Development of bubble absorption refrigeration technology: A review. *Renew Sustain Energy Rev* 2018;82:3468–82.
<https://doi.org/https://doi.org/10.1016/j.rser.2017.10.109>.
- [108]. Isetti C, Nannei E, Orlandini B. Three-fluid membrane contactors for improving the energy efficiency of refrigeration and air-handling systems. *Int J Ambient Energy* 2013;34:181–94. <https://doi.org/10.1080/01430750.2012.755905>.
- [109]. Ge G, Abdel-Salam AH, Abdel-Salam MRH, Besant RW, Simonson CJ. Heat and mass transfer performance comparison between a direct-contact liquid desiccant packed bed and a liquid-to-air membrane energy exchanger for air dehumidification. *Sci Technol Built Environ* 2017;23:2–15.
<https://doi.org/10.1080/23744731.2016.1203712>.
- [110]. Yang B, Yuan W, Gao F, Guo B. A review of membrane-based air dehumidification. *Indoor Built Environ* 2013;24:11–26. <https://doi.org/10.1177/1420326X13500294>.
- [111]. Metz SJ, van de Ven WJC, Potreck J, Mulder MH V, Wessling M. Transport of water vapor and inert gas mixtures through highly selective and highly permeable polymer membranes. *J Memb Sci* 2005;251:29–41.
<https://doi.org/https://doi.org/10.1016/j.memsci.2004.08.036>.
- [112]. Pei L, Zhou J, Zhang L. Preparation and properties of Ag-coated activated carbon nanocomposites for indoor air quality control. *Build Environ* 2013;63:108–13.
<https://doi.org/https://doi.org/10.1016/j.buildenv.2013.02.010>.
- [113]. Abdel-Salam MRH, Besant RW, Simonson CJ. Sensitivity of the performance of a flat-plate liquid-to-air membrane energy exchanger (LAMEE) to the air and solution channel widths and flow maldistribution. *Int J Heat Mass Transf* 2015;84:1082–100.
<https://doi.org/10.1016/j.ijheatmasstransfer.2015.01.042>.
- [114]. Larson MD, Simonson CJ, Besant RW, Gibson PW. The elastic and moisture transfer properties of polyethylene and polypropylene membranes for use in liquid-to-air energy exchangers. *J Memb Sci* 2007;302:136–49.
<https://doi.org/https://doi.org/10.1016/j.memsci.2007.06.050>.
- [115]. Ge G, Mahmood GI, Moghaddam DG, Simonson CJ, Besant RW, Hanson S, et al. Material properties and measurements for semi-permeable membranes used in energy exchangers. *J Memb Sci* 2014;453:328–36.
<https://doi.org/https://doi.org/10.1016/j.memsci.2013.11.013>.
- [116]. Mansourizadeh A, Ismail AF. Hollow fiber gas–liquid membrane contactors for acid gas capture: A review. *J Hazard Mater* 2009;171:38–53.
<https://doi.org/https://doi.org/10.1016/j.jhazmat.2009.06.026>.
- [117]. Zhang L-Z, Huang S-M, Zhang W-B. Turbulent heat and mass transfer across a hollow fiber membrane bundle considering interactions between neighboring fibers. *Int J Heat Mass Transf* 2013;64:162–72.
<https://doi.org/https://doi.org/10.1016/j.ijheatmasstransfer.2013.04.035>.
- [118]. Huang S-M, Qiu D, Wu Z, Yang M, Zeng S, Chen Y. Fluid flow and heat transfer across a curved hollow fiber membrane tube bank (CHFMTB): Effects of the tube deformations. *Int J Heat Mass Transf* 2018;116:471–83.
<https://doi.org/https://doi.org/10.1016/j.ijheatmasstransfer.2017.09.041>.

- [119]. Back JO, Brandstätter R, Spruck M, Koch M, Penner S, Rupprich M. Parameter Screening of PVDF/PVP Multi-Channel Capillary Membranes. *Polymers (Basel)* 2019;11:463. <https://doi.org/10.3390/polym11030463>.
- [120]. Bettahalli NMS, Lefers R, Fedoroff N, Leiknes T, Nunes SP. Triple-bore hollow fiber membrane contactor for liquid desiccant based air dehumidification. *J Memb Sci* 2016;514:135–42. <https://doi.org/https://doi.org/10.1016/j.memsci.2016.04.059>.
- [121]. Li Z-X, Zhang L-Z. Flow maldistribution and performance deteriorations in a counter flow hollow fiber membrane module for air humidification/dehumidification. *Int J Heat Mass Transf* 2014;74:421–30. <https://doi.org/https://doi.org/10.1016/j.ijheatmasstransfer.2014.03.047>.
- [122]. Gurubalan A, Geoghegan PJ, Maiya MP, Simonson CJ. Performance improvement of mass transfer through membrane using ultrasound for hvac application. *ASME 2020 Heat Transf. Summer Conf. HT 2020, collocated with ASME 2020 Fluids Eng. Div. Summer Meet. ASME 2020 18th Int. Conf. Nanochannels, Microchannels, Minichannels, 2020*. <https://doi.org/10.1115/HT2020-9058>.
- [123]. Li X-W, Zhang X-S. Photovoltaic–electrodialysis regeneration method for liquid desiccant cooling system. *Sol Energy* 2009;83:2195–204. <https://doi.org/https://doi.org/10.1016/j.solener.2009.09.001>.
- [124]. Lee H-J, Sarfert F, Strathmann H, Moon S-H. Designing of an electrodialysis desalination plant. *Desalination* 2002;142:267–86. [https://doi.org/https://doi.org/10.1016/S0011-9164\(02\)00208-4](https://doi.org/https://doi.org/10.1016/S0011-9164(02)00208-4).
- [125]. Al-Jubainawi A, Ma Z, Guo Y, Nghiem LD, Cooper P, Li W. Factors governing mass transfer during membrane electrodialysis regeneration of LiCl solution for liquid desiccant dehumidification systems. *Sustain Cities Soc* 2017;28:30–41. <https://doi.org/https://doi.org/10.1016/j.scs.2016.08.021>.
- [126]. Guo Y, Ma Z, Al-Jubainawi A, Cooper P, Nghiem LD. Using electrodialysis for regeneration of aqueous lithium chloride solution in liquid desiccant air conditioning systems. *Energy Build* 2016;116:285–95. <https://doi.org/https://doi.org/10.1016/j.enbuild.2016.01.014>.
- [127]. Al-Farayedhi AA, Gandhidasan P, Younus Ahmed S. Regeneration of liquid desiccants using membrane technology. *Energy Convers Manag* 1999;40:1405–11. [https://doi.org/https://doi.org/10.1016/S0196-8904\(99\)00036-9](https://doi.org/https://doi.org/10.1016/S0196-8904(99)00036-9).
- [128]. Duong HC, Ansari AJ, Nghiem LD, Cao HT, Vu TD, Nguyen TP. Membrane Processes for the Regeneration of Liquid Desiccant Solution for Air Conditioning. *Curr Pollut Reports* 2019;5:308–18. <https://doi.org/10.1007/s40726-019-00120-9>.
- [129]. Peñate B, García-Rodríguez L. Current trends and future prospects in the design of seawater reverse osmosis desalination technology. *Desalination* 2012;284:1–8. <https://doi.org/https://doi.org/10.1016/j.desal.2011.09.010>.
- [130]. Pang R, Zhang K. Fabrication of hydrophobic fluorinated silica-polyamide thin film nanocomposite reverse osmosis membranes with dramatically improved salt rejection. *J Colloid Interface Sci* 2018;510:127–32. <https://doi.org/https://doi.org/10.1016/j.jcis.2017.09.062>.
- [131]. Fujioka T, Ishida KP, Shintani T, Kodamatani H. High rejection reverse osmosis membrane for removal of N-nitrosamines and their precursors. *Water Res* 2018;131:45–51. <https://doi.org/https://doi.org/10.1016/j.watres.2017.12.025>.
- [132]. Peters CD, Hankins NP. Osmotically assisted reverse osmosis (OARO): Five approaches to dewatering saline brines using pressure-driven membrane processes. *Desalination* 2019;458:1–13. <https://doi.org/https://doi.org/10.1016/j.desal.2019.01.025>.

- [133]. Wang P, Chung T-S. Recent advances in membrane distillation processes: Membrane development, configuration design and application exploring. *J Memb Sci* 2015;474:39–56. <https://doi.org/https://doi.org/10.1016/j.memsci.2014.09.016>.
- [134]. Zhou J, Zhang X, Su W, Sun B. Performance analysis of vacuum membrane distillation regenerator in liquid desiccant air conditioning system. *Int J Refrig* 2019;102:112–21. <https://doi.org/https://doi.org/10.1016/j.ijrefrig.2019.03.017>.
- [135]. Zhou J, Zhang X, Sun B, Su W. Performance analysis of solar vacuum membrane distillation regeneration. *Appl Therm Eng* 2018;144:571–82. <https://doi.org/https://doi.org/10.1016/j.applthermaleng.2018.08.052>.
- [136]. Lefers R, Bettahalli NMS, Fedoroff N, Nunes SP, Leiknes T. Vacuum membrane distillation of liquid desiccants utilizing hollow fiber membranes. *Sep Purif Technol* 2018;199:57–63. <https://doi.org/https://doi.org/10.1016/j.seppur.2018.01.042>.
- [137]. Duong HC, Hai FI, Al-Jubainawi A, Ma Z, He T, Nghiem LD. Liquid desiccant lithium chloride regeneration by membrane distillation for air conditioning. *Sep Purif Technol* 2017;177:121–8. <https://doi.org/https://doi.org/10.1016/j.seppur.2016.12.031>.
- [138]. Duong HC, Álvarez IRC, Nguyen T V, Nghiem LD. Membrane distillation to regenerate different liquid desiccant solutions for air conditioning. *Desalination* 2018;443:137–42. <https://doi.org/https://doi.org/10.1016/j.desal.2018.05.023>.
- [139]. Liu J, Liu X, Zhang T. Performance comparison of three typical types of internally-cooled liquid desiccant dehumidifiers. *Build Environ* 2016;103:134–45. <https://doi.org/https://doi.org/10.1016/j.buildenv.2016.04.006>.
- [140]. Yoon J-I, Phan T-T, Moon C-G, Bansal P. Numerical study on heat and mass transfer characteristic of plate absorber. *Appl Therm Eng* 2005;25:2219–35. <https://doi.org/https://doi.org/10.1016/j.applthermaleng.2005.01.004>.
- [141]. Yin Y, Zhang X, Wang G, Luo L. Experimental study on a new internally cooled/heated dehumidifier/regenerator of liquid desiccant systems. *Int J Refrig* 2008;31:857–66. <https://doi.org/https://doi.org/10.1016/j.ijrefrig.2007.10.004>.
- [142]. Liu J, Zhang T, Liu X, Jiang J. Experimental analysis of an internally-cooled / heated liquid desiccant dehumidifier / regenerator made of thermally conductive plastic. *Energy Build* 2015;99:75–86. <https://doi.org/10.1016/j.enbuild.2015.04.023>.
- [143]. Abdel-Salam MRH, Besant RW, Simonson CJ. Performance testing of a novel 3-fluid liquid-to-air membrane energy exchanger (3-fluid LAMEE) under desiccant solution regeneration operating conditions. *Int J Heat Mass Transf* 2016;95:773–86. <https://doi.org/https://doi.org/10.1016/j.ijheatmasstransfer.2015.10.065>.
- [144]. Annadurai G, Tiwari S, Maiya MP. Experimental performance comparison of adiabatic and internally-cooled membrane dehumidifiers. *Int J Low-Carbon Technol* 2018;13:240–9. <https://doi.org/10.1093/ijlct/cty020>.
- [145]. Lun W, Li K, Liu B, Zhang H, Yang Y, Yang C. Experimental analysis of a novel internally-cooled dehumidifier with self-cooled liquid desiccant. *Build Environ* 2018;141:117–26. <https://doi.org/https://doi.org/10.1016/j.buildenv.2018.05.055>.
- [146]. Liu XH, Chang XM, Xia JJ, Jiang Y. Performance analysis on the internally cooled dehumidifier using liquid desiccant 2009;44:299–308. <https://doi.org/10.1016/j.buildenv.2008.03.009>.
- [147]. Gao WZ, Shi YR, Cheng YP, Sun WZ. Experimental study on partially internally cooled dehumidification in liquid desiccant air conditioning system. *Energy Build* 2013;61:202–9. <https://doi.org/10.1016/j.enbuild.2013.02.034>.
- [148]. Yin Y, Zhang X. Comparative study on internally heated and adiabatic regenerators in liquid desiccant air conditioning system. *Build Environ* 2010;45:1799–807. <https://doi.org/https://doi.org/10.1016/j.buildenv.2010.02.008>.

- [149]. Park J-Y, Kim B-J, Yoon S-Y, Byon Y-S, Jeong J-W. Experimental analysis of dehumidification performance of an evaporative cooling-assisted internally cooled liquid desiccant dehumidifier. *Appl Energy* 2019;235:177–85. <https://doi.org/https://doi.org/10.1016/j.apenergy.2018.10.101>.
- [150]. Jafarian H, Sayyaadi H, Torabi F. Numerical modeling and comparative study of different membrane-based liquid desiccant dehumidifiers. *Energy Convers Manag* 2019;184:735–47. <https://doi.org/https://doi.org/10.1016/j.enconman.2019.01.099>.
- [151]. Kumar R, Dhar PL, Jain S, Asati AK. Multi absorber standalone liquid desiccant air conditioning systems for higher performance. *Sol Energy* 2009;83:761–72. <https://doi.org/10.1016/j.solener.2008.11.010>
- [152]. Lowenstein A, Novosel D. Seasonal performance of a liquid-desiccant air conditioner. *ASHRAE Trans* 1995;101(1):679–85.
- [153]. Li X-W, Zhang X-S, Quan S. Single-stage and double-stage photovoltaic driven regeneration for liquid desiccant cooling system. *Appl Energy* 2011;88:4908–17. <https://doi.org/https://doi.org/10.1016/j.apenergy.2011.06.052>.
- [154]. Datta N, Chakraborty A, Ali SM, Choo FH. Experimental investigation of multi-effect regenerator for desiccant dehumidifier: Effects of various regeneration temperatures and solution flow rates on system performances. *Int J Refrig* 2017;76:7–18. <https://doi.org/https://doi.org/10.1016/j.ijrefrig.2017.01.019>.
- [155]. Chen Q, Kum Ja M, Li Y, Chua KJ. Thermodynamic optimization of a vacuum multi-effect membrane distillation system for liquid desiccant regeneration. *Appl Energy* 2018;230:960–73. <https://doi.org/https://doi.org/10.1016/j.apenergy.2018.09.072>.
- [156]. Cheng X, Rong Y, Zhou X, Gu C, Zhi X, Qiu L, et al. Performance analysis of a multistage internal circulation liquid desiccant dehumidifier. *Appl Therm Eng* 2020;172:115163. <https://doi.org/https://doi.org/10.1016/j.applthermaleng.2020.115163>.
- [157]. Xiong ZQ, Dai YJ, Wang RZ. Investigation on a two-stage solar liquid-desiccant (LiBr) dehumidification system assisted by CaCl₂ solution. *Appl Therm Eng* 2009;29:1209–15. <https://doi.org/https://doi.org/10.1016/j.applthermaleng.2008.06.020>.
- [158]. Xiong ZQ, Dai YJ, Wang RZ. Development of a novel two-stage liquid desiccant dehumidification system assisted by CaCl₂ solution using exergy analysis method. *Appl Energy* 2010;87:1495–504. <https://doi.org/https://doi.org/10.1016/j.apenergy.2009.08.048>.
- [159]. Zhang N, Yin S-Y, Zhang L-Z. Performance study of a heat pump driven and hollow fiber membrane-based two-stage liquid desiccant air dehumidification system. *Appl Energy* 2016;179:727–37. <https://doi.org/https://doi.org/10.1016/j.apenergy.2016.07.037>.
- [160]. Liu XH, Jiang Y. Coupled heat and mass transfer characteristic in packed bed dehumidifier/regenerator using liquid desiccant. *Energy Convers Manag* 2008;49:1357–66. <https://doi.org/https://doi.org/10.1016/j.enconman.2008.01.009>.
- [161]. Liu XH, Jiang Y, Chang XM, Yi XQ. Experimental investigation of the heat and mass transfer between air and liquid desiccant in a cross-flow regenerator. *Renew Energy* 2007;32:1623–36. <https://doi.org/https://doi.org/10.1016/j.renene.2006.07.002>.
- [162]. Liu XH, Jiang Y, Yi XQ. Effect of regeneration mode on the performance of liquid desiccant packed bed regenerator. *Renew Energy* 2009;34:209–16. <https://doi.org/https://doi.org/10.1016/j.renene.2008.03.003>.
- [163]. Ali A, Vafai K, Khaled A-RA. Comparative study between parallel and counter flow configurations between air and falling film desiccant in the presence of nanoparticle

- suspensions. *Int J Energy Res* 2003;27:725–45.
<https://doi.org/https://doi.org/10.1002/er.908>.
- [164]. Zhang N, Zhang L-Z, Xu J-C. A heat pump driven and hollow fiber membrane-based liquid desiccant air dehumidification system: A transient performance study. *Int J Refrig* 2016;67:143–56. <https://doi.org/https://doi.org/10.1016/j.ijrefrig.2016.01.001>.
- [165]. Zhang N, Yin S-Y, Li M. Model-based optimization for a heat pump driven and hollow fiber membrane hybrid two-stage liquid desiccant air dehumidification system. *Appl Energy* 2018;228:12–20.
<https://doi.org/https://doi.org/10.1016/j.apenergy.2018.06.058>.
- [166]. Moon CG, Bansal PK, Jain S. New mass transfer performance data of a cross-flow liquid desiccant dehumidification system. *Int J Refrig* 2009;32:524–33.
<https://doi.org/https://doi.org/10.1016/j.ijrefrig.2008.06.011>.
- [167]. Cho H-J, Cheon S-Y, Jeong J-W. Experimental analysis of dehumidification performance of counter and cross-flow liquid desiccant dehumidifiers. *Appl Therm Eng* 2019;150:210–23.
<https://doi.org/https://doi.org/10.1016/j.applthermaleng.2019.01.006>.
- [168]. Vali A, Simonson CJ, Besant RW, Mahmood G. Numerical model and effectiveness correlations for a run-around heat recovery system with combined counter and cross flow exchangers. *Int J Heat Mass Transf* 2009;52:5827–40.
<https://doi.org/https://doi.org/10.1016/j.ijheatmasstransfer.2009.07.020>.
- [169]. Vali A, Ge G, Besant RW, Simonson CJ. Numerical modeling of fluid flow and coupled heat and mass transfer in a counter-cross-flow parallel-plate liquid-to-air membrane energy exchanger. *Int J Heat Mass Transf* 2015;89:1258–76.
<https://doi.org/https://doi.org/10.1016/j.ijheatmasstransfer.2015.06.043>.
- [170]. Huang S-M, Qiu D, Huang W, Yang M, Xiao H. Laminar flow and heat transfer in a quasi-counter flow parallel-plate membrane channel in the solution side with cooling tubes. *Int J Heat Mass Transf* 2017;105:769–80.
<https://doi.org/https://doi.org/10.1016/j.ijheatmasstransfer.2016.10.047>.
- [171]. Huang S-M, Yang M, Yang X. Performance analysis of a quasi-counter flow parallel-plate membrane contactor used for liquid desiccant air dehumidification. *Appl Therm Eng* 2014;63:323–32.
<https://doi.org/https://doi.org/10.1016/j.applthermaleng.2013.11.027>.
- [172]. Mahmud K, Mahmood GI, Simonson CJ, Besant RW. Performance testing of a counter-cross-flow run-around membrane energy exchanger (RAMEE) system for HVAC applications. *Energy Build* 2010;42:1139–47.
<https://doi.org/10.1016/j.enbuild.2010.02.005>.
- [173]. Liu J, Liu X, Zhang T. Performance comparison and exergy analysis of different flow types in internally-cooled liquid desiccant dehumidifiers (ICDs). *Appl Therm Eng* 2018;142:278–91.
<https://doi.org/https://doi.org/10.1016/j.applthermaleng.2018.07.006>.
- [174]. Peng D, Luo D. Modeling and parametrical analysis on internally-heated liquid desiccant regenerator in liquid desiccant air conditioning. *Energy* 2017;141:461–71.
<https://doi.org/https://doi.org/10.1016/j.energy.2017.09.106>.
- [175]. Luo Y, Yang H, Lu L, Qi R. A review of the mathematical models for predicting the heat and mass transfer process in the liquid desiccant dehumidifier. *Renew Sustain Energy Rev* 2014;31:587–99.
<https://doi.org/https://doi.org/10.1016/j.rser.2013.12.009>.
- [176]. Koronaki IP, Christodoulaki RI, Papaefthimiou VD, Rogdakis ED. Thermodynamic analysis of a counter flow adiabatic dehumidifier with different liquid desiccant

- materials. *Appl Therm Eng* 2013;50:361–73.
<https://doi.org/10.1016/j.applthermaleng.2012.06.043>
- [177]. Zhang L-Z. Heat and mass transfer in a randomly packed hollow fiber membrane module: A fractal model approach. *Int J Heat Mass Transf* 2011;54:2921–31.
<https://doi.org/https://doi.org/10.1016/j.ijheatmasstransfer.2011.03.005>.
- [178]. Zhang L-Z, Huang S-M, Chi J-H, Pei L-X. Conjugate heat and mass transfer in a hollow fiber membrane module for liquid desiccant air dehumidification: A free surface model approach. *Int J Heat Mass Transf* 2012;55:3789–99.
<https://doi.org/https://doi.org/10.1016/j.ijheatmasstransfer.2012.03.034>.
- [179]. Zendejboudi A, Tatar A, Li X. A comparative study and prediction of the liquid desiccant dehumidifiers using intelligent models. *Renew Energy* 2017;114:1023–35.
<https://doi:10.1016/j.renene.2017.07.078>
- [180]. Wang X, Cai W, Lu J, Sun Y, Zhao L. Model-based optimization strategy of chiller driven liquid desiccant dehumidifier with genetic algorithm. *Energy* 2015;82:939–48.
<https://doi:10.1016/j.energy.2015.01.103>
- [181]. Wang L, Xiao F, Niu X, Gao D. A dynamic dehumidifier model for simulations and control of liquid desiccant hybrid air conditioning systems. *Energy Build* 2017;140:418–29. <https://doi:10.1016/j.enbuild.2017.01.073>
- [182]. Jagirdar M, Lee PS, Padding JT. Performance of an internally cooled and heated desiccant-coated heat and mass exchanger: Effectiveness criteria and design methodology. *Appl Therm Eng* 2021;188:116593.
<https://doi.org/https://doi.org/10.1016/j.applthermaleng.2021.116593>.

Table-A.1: Summary of direct contact liquid desiccant energy exchangers (LDEEs)

Type of LDEE	Characteristics	Process	Advantage	Disadvantage
1. Packed bed LDEE (PB-LDEE)	Packing materials improve the contact area between air and desiccant	Dehumidification and Regeneration	Comparatively higher heat and mass transfer performance	<ul style="list-style-type: none"> • Comparatively higher pressure drop for air • To improve the wetting, either coating or higher desiccant flow rate is required. • Desiccant carryover
2. Spray tower LDEE	Desiccant is sprayed to improve the contact area between air and desiccant	Dehumidification and Regeneration	<p>When compared to PB-LDEE</p> <ul style="list-style-type: none"> • Simpler construction • Lesser initial and operating costs • More compactness • Lesser pressure drop of air 	Desiccant carryover (in regular tower design)
3. Falling film LDEE	Desiccant flows by gravity as a continuous thin film over the surface of tubes or plates	Dehumidification and Regeneration	<ul style="list-style-type: none"> • Most suitable configuration for internally cooled or heated LDEE (I-LDEE) • Pressure drop of air is lesser than that in PB-LDEE 	<ul style="list-style-type: none"> • Desiccant carryover • Higher initial cost • Difficult to maintain the required film thickness throughout LDEE
4. Solar collector based LDEE	Combines the effects of photothermal transformation and regeneration of the desiccant	Regeneration	<ul style="list-style-type: none"> • More efficient in terms of solar utilization ratio • Simpler construction • Lesser initial and operating costs 	Performance critically depends on climatic conditions
5. Pressurized LDEE	Pressure of air is increased to improve the mass transfer driving potential	Dehumidification	Most suitable for the application where air is required at a very low specific humidity ($<1 \text{ g}_w/\text{kg}_{da}$)	<ul style="list-style-type: none"> • Energy consumption of liquid desiccant air conditioning system (LDAS) would increase due to the compressor • Desiccant carryover • Higher initial and operating costs

Table-A.1: Summary of direct contact LDEEs (Cont.)

Type of LDEE	Characteristics	Process	Advantage	Disadvantage
6. Ultrasound based LDEE	It employs an ultrasound transducer which convert the desiccant into finely atomized ($\approx 50 \mu\text{m}$ diameter) droplets to improve the contact area between air and desiccant	Dehumidification and Regeneration	When compared to PB-LDEE, it requires <ul style="list-style-type: none"> • Lower desiccant flow rate (40-75%) • Lesser desiccant regeneration temperature ($\approx 4.5^\circ\text{C}$) • Lesser energy (60%) 	Desiccant carryover
7. Hypergravity LDEE	It employs a rotating packed bed which convert the desiccant into thin films and fine droplets to improve the contact area between air and desiccant	Dehumidification and Regeneration	<ul style="list-style-type: none"> • Higher heat and mass transfer performance than PB-LDEE • Self cleaning mechanism due to rotation No desiccant carryover	<ul style="list-style-type: none"> • Energy consumption of LDAS would increase due to the motor • Higher initial and operating costs
8. Vacuum LDEE	Required regeneration temperature of desiccant is reduced by introducing vacuum condition inside LDEE	Regeneration	<ul style="list-style-type: none"> • Lesser desiccant regeneration temperature • No need of regenerative air No desiccant carryover	<ul style="list-style-type: none"> • Energy consumption of LDAS would increase due to the vacuum pump • Higher initial and operating costs
9. Bubble absorption LDEE	Air is injected into the liquid desiccant storage tank instead of being passed over the surface of flowing desiccant	Dehumidification and Regeneration	Higher heat and mass transfer performance than PB-LDEE	<ul style="list-style-type: none"> • More fan power is required • Desiccant carryover

Table-A.2: Summary of indirect contact LDEEs

Type of LDEE	Characteristics	Process	Advantage	Disadvantage
1. Membrane-based LDEE	An intermediate membrane is introduced between the air and desiccant to avoid direct contact	Dehumidification and Regeneration	<ul style="list-style-type: none"> No desiccant carryover Lesser pressure drop of air and transient response delay time than PB-LDEE 	Under same contact area, the heat and mass transfer performance are lesser than that of PB-LDEE
2. Electrodialysis based LDEE	Works based on electrochemical membrane separation method which is the transport of ions through selective membranes under the influence of an electrical field	Regeneration	<ul style="list-style-type: none"> No desiccant carryover No need of regenerative air Works on electrical energy instead of thermal energy 	Optimum concentration range of commonly used desiccants is much lower when compared to its working concentration
3. Reverse osmosis LDEE	Works based on reverse osmosis method in which the pressure is applied to transfer the solvent through the membrane	Regeneration	<ul style="list-style-type: none"> No desiccant carryover No need of regenerative air Works on pressure energy instead of thermal energy 	<ul style="list-style-type: none"> Requires a very high working pressure (>100 bar) Energy consumption of LDAS would increase due to the pump Higher initial and operating costs
4. Membrane distillation LDEE	Combines the effects of on thermal distillation and membrane separation	Regeneration	<ul style="list-style-type: none"> No desiccant carryover No need of regenerative air 	<ul style="list-style-type: none"> Temperature and concentration polarizations